

KLAIPĒDA UNIVERSITY
COASTAL RESEARCH AND PLANNING INSTITUTE

DIANA VAIČIŪTĒ

**DISTRIBUTION PATTERNS OF OPTICALLY ACTIVE
COMPONENTS AND PHYTOPLANKTON IN THE ESTUARINE
PLUME IN THE SOUTH EASTERN BALTIC SEA**

Doctoral dissertation

Biomedical sciences, ecology and environmental sciences (03B),
hydrobiology, marine biology, aquatic ecology, limnology (B260)

Klaipėda, 2012

Dissertation prepared 2007–2011 at Klaipėda University, Coastal Research and Planning Institute

Supervisor:

dr. Renata Pilkaitytė (Klaipėda University; Biomedical Sciences, Ecology and Environmental Sciences – 03B)

Research advisors:

doc. dr. Darius Daunys (Klaipėda University; Biomedical Sciences, Ecology and Environmental Sciences – 03B)

doc. dr. Zita Rasuolė Gasiūnaitė (Klaipėda University; Biomedical Sciences, Ecology and Environmental Sciences – 03)

TABLE OF CONTENTS

INTRODUCTION5

1. LITERATURE REVIEW15

1.1. Riverine fronts and their role in shaping environment characteristics15

1.2. River fronts in the Baltic Sea region19

1.3. Investigation of Nemunas River plume in the Lithuanian Baltic Sea coastal waters21

1.4. Water optics and Remote Sensing.....24

1.4.1. Optical Remote Sensing24

1.4.2. Optical properties of water basins29

1.4.3. Optically active components30

1.5. Optical Remote Sensing in the Baltic Sea region and in the Lithuanian waters.....32

2. DESCRIPTION OF THE STUDY AREA34

2.1. Geolocation.....34

2.2. Local hydrometeorological conditions and hydrodynamics34

2.3. Hydrophysics and hydrochemistry36

3. MATERIAL AND METHODS38

3.1. Validation of satellite data38

3.2. Analysis of the plume area43

3.3. Analysis of samples.....45

3.4. Measurement of environmental parameters47

3.5. Long-term data and satellite images48

3.6. Statistical analysis.....48

4. RESULTS49

4.1. Validation of satellite remote sensing technique49

4.1.1. Validation of chlorophyll *a* concentration.....49

4.1.2. Validation of dissolved coloured organic matter (CDOM) absorption.....53

4.1.3. Validation of total suspended matter TSM concentration...55

4.2. Delineation of the plume58

4.2.1. Identification of the plume by salinity threshold58

4.2.2. Delineation of the plume by the optically active components.....	59
4.2.3. Spatio-temporal variability of the plume	60
4.3. The role of the plume for spatial variability of the optical water properties and phytoplankton	65
4.3.1. Optical water properties	65
4.3.2. Phytoplankton biomass and community structure.....	66
5. DISCUSSION	75
5.1. Validation: different algorithms and effect of environmental conditions.....	75
5.2. Indicators of dynamically active hydrofront.....	81
5.3. Phytoplankton communities in the plume and coastal waters	84
5.4. Remote sensing application in the assessment of the plume area	89
5.5. Remote sensing application for water quality assessment	92
6. CONCLUSIONS	99
7. REFERENCE.....	100

INTRODUCTION

Relevance of the problem. The Baltic Sea represents the world's largest brackish-water sea area (382 000 km²) influenced by a limited inflow of marine, fully saline water from the North Sea and a high input of fresh water from the many rivers flowing into the enclosed basin. Although the Baltic Sea is considered as one of the biggest “estuary” in the world, there are five main estuaries landscaped by the big rivers entering the sea – Neva, Vistula, Nemunas, Daugava and Oder. Great scientific interest to these hydrodynamically and ecologically unique environments continues over the decades, where attempts to understand the physical forcing of the plume and model its development under hydrometeorological conditions with the emphasis to the transportation of dissolved and particulate materials (e.g. Geyer, 1986; Dagg et al., 2004). The other studies focus on changes of physical-chemical characteristics in the plume waters (e.g. Geyer et al., 1991), whereas the one assesses the effects of plume water on marine organisms: mainly plankton (e.g. Telesh, 2004; Korshenko, 1991; Kononen et al., 1996; Moisander et al., 1997; Olenina, 1997; 2004), fishes (e.g. Connolly et al., 2009) and distribution of benthic vegetation.

The plume waters according to Water Framework Directive (WFD) and Marine Strategy Framework Directive (MSFD) are termed transitional waters. However, there are no one general consensus how to delineate them and therefore European Union (EU) Member States (MS) used different approaches (e.g. Daunys et al., 2007). According to WFD the ecological status of transitional waters is being assessed by carrying out national monitoring in each country. Although the monitoring programs follow the common guidelines and recommendations by HELCOM (Helsinki Commission), there are huge differences in the monitoring methods: sampling frequency, measured parameters, investigation methods. Therefore the assessment of the water quality becomes a difficult task over the entire Baltic Sea region. Moreover, only few countries (e.g. Finland and

Sweden) next to conventional water sampling methods use satellite based remote sensing techniques.

In the Baltic Sea coastal waters along the Lithuania there is one of the largest transitional water bodies (plume) due to dynamic water exchange between the Baltic Sea and Curonian Lagoon through the narrow, continuously dredging (mean depth approximately 14 m) Klaipėda strait, mainly driven by local hydrometeorological conditions. First time the water circulation and it's main features in the Klaipėda strait region was described by E. Červinskas (1959). Later the studies were exclusively focused on the sea level changes and water balance (Dubra, Červinskas, 1968; Dubra, 1970, Pustelnikovas, 1998). Along with the progress of modelling approaches, first time the currents and it's structure were described by Gailiušis et al. (2004; 2005). The extremely unstable plume area was investigated from the perspective of aquatic organisms and their response to the changing environment: zooplankton (Korshenko, 1991), phytoplankton (Olenina, 1997; 2004; Gasiūnaitė et al., 2005; Pilkaitytė et al., 2004) However, conventional sampling methods cannot produce enough data about spatial and temporal distribution of phytoplankton and waters quality parameters within the conditions of hypertrophic waters of the Curonian Lagoon in the Sea outflow. The satellite based remote sensing techniques appears an advanced state of the art tool, in addition to traditional field sampling techniques, for an accurate assessment of water quality parameters over large areas and extremely dynamic plumes, investigation of water bloom events. Satellite based remote sensing have never been applied for the assessment of ecological status of Lithuanian coastal waters. However, before the direct use of satellite products for the monitoring, Earth observation data should be validated with *in situ* measurements. Once the appropriate algorithms are established for the prediction of optically active water quality components, satellite based remote sensing technique may serve as a valuable tool for the investigation of ecological processes within the water basins, improve the typology of different water masses, and be an additional information source for the assessment of water quality.

Aim and objectives of the study. The aim of this study was to assess the distribution patterns of optically active components and phytoplankton in the estuarine plume in the Lithuanian Baltic Sea coastal waters applying traditional *in situ* methods and satellite remote sensing technique.

Tasks of this study:

- 1) to validate satellite derived and *in situ* measured concentration of optically active components (chlorophyll *a*, coloured dissolved organic matter, total suspended matter) and evaluate the applicability of remote sensing for the water quality assessment;
- 2) to delineate plume area using salinity and concentration of optically active components during the intensive vegetation period;
- 3) to assess the patterns of plume distribution with the application of remote sensing technique during the intensive vegetation period;
- 4) to compare the concentration of optically active components, phytoplankton biomass and structure in different water masses.

Novelty of the study This study for the first time in Lithuania provides comprehensive analysis of spatial distribution of all optically active components using both *in situ* and satellite technique along the salinity gradient in the SE Lithuanian Baltic Sea. The obtained result of validation of satellite-based water quality parameters provides key information about the most suitable processor for the chlorophyll *a*, coloured dissolved organic matter (CDOM) and total suspended matter (TSM) in order to monitor water quality in the coastal regions of the SE Baltic Sea with Envisat/MERIS data. Satellite derived CDOM was suitable parameter for the delineation of the plume area based on long-term satellite images was established. Finally, the ecological role of salinity gradient for the phytoplankton community was determined.

Scientific and applied significance of the results The results of this study increased understanding of the spatial distribution of optically

active components, phytoplankton communities and their abilities to represent the plume area in the Lithuanian Baltic Sea coastal waters. Moreover, it increased understanding of the satellite based remote sensing technique and its applicability for the investigation of the environmental processes in the other highly turbid regions of the Baltic Sea. This study is a valuable addition to existing results and confirms satellite remote sensing to be an advanced but cost effective tool, in addition to traditional field sampling techniques, for an accurate assessment of water quality parameters, detection of toxic cyanobacteria blooms and investigation of highly variable frontal zones over the large areas. The obtained annual changes of the summer plume area reveal it's variability in time and space. The use of both satellite imagery and environmental conditions allows predicting of the spatial distribution and spread of the lagoon waters. This information could be valuable information for the improvement of the monitoring strategy, for the fishery, recreation and scientific purpose. The occurrence of the plume area derived from satellite can explain the maximum depth limit of benthic vegetation, which form natural spawning grounds for fish and provide habitats for many benthic invertebrates in the coastal area (Bučas, 2009).

Defensive statements

1. Bio-optical processors of coastal and inland waters are suitable to derive the concentration of optically active components and to monitor water quality in the Lithuanian Baltic Sea coastal waters.
2. Lithuanian Baltic Sea coastal waters are characterized by higher salinity and lower concentration of optically active components, therefore these parameters could be used to delineate the estuarine plume.
3. Plume area in the Lithuanian Baltic Sea coastal waters covers the whole territorial sea, however mainly is directed towards the mainland coast to the north.
4. During the intensive vegetation period the outflow of the estuarine waters increases the concentration of optically active

Scientific approval

The results of this study were presented at fifteen international and five national conferences and seminars:

- scientific-practical conference “Sea and Coastal research–2008”, Palanga, Lithuania, April 2008;
- 3rd international student conference „Biodiversity and Functioning of Aquatic Ecosystems in the Baltic Sea Region“, Klaipėda, Lithuania, October 2008;
- scientific-practical conference “Sea and Coastal research–2009”, Nida, Lithuania, April 2009;
- 7th Baltic Sea Science Congress, Tallinn, Estonia, August 2009;
- seminar “Remote sensing and water optics specifically for Baltic Sea conditions”, Tallinn, Estonia, August 2009;
- 4th international student conference „Biodiversity and functioning of aquatic ecosystems in the Baltic Sea region“, Dubingiai, Lithuania, October 2009;
- Nordic Remote sensing Days, Helsinki, Finland, October 2009;
- Workshop “Introduced marine species: what should we study now and why?”, Bergen, Norway, October 2009;
- BONUS annual conference 2010, Vilnius, Lithuania, January 2010;
- scientific-practical conference “Sea and Coastal research–2010”, Palanga, Lithuania, April 2010;
- 6th annual conference for heads “Lužio taškas”, Palanga, Lithuania, September 2010;
- 5th international student conference „Biodiversity and functioning of aquatic ecosystems in the Baltic Sea region“, Palanga, Lithuania, October 2010;
- NordAquaRemS workshop on Remote Sensing of lakes, Oslo, Norway, February 2011;

- MarCoast Validation Workshop 3, Ispra, Italy, March 2011;
- scientific-practical conference “Sea and Coastal research–2011”, Palanga, Lithuania, April 2011;
- 8th Baltic Sea Science Congress, Sankt Petersburg, Russia, August 2011;
- Seminar “Bio-optics of the Baltic Sea and Remote Sensing”, Sankt Petersburg, Russia, August 2011;
- IEEE/OES Baltic INTERNATIONAL SYMPOSIUM, Klaipėda, Lithuania, May 2012;
- ECSA 51th International Symposium "Research and management of transitional waters", Klaipėda, Lithuania, September 2012;
- 6th international student conference “Aquatic environmental research”, Palanga, Lithuania, October 2012.

The material of this dissertation was presented in 3 original publications, published in peer-reviewed scientific journals.

Vaičiūtė, D., Bresciani, M., Bučas, M., 2012. Validation of MERIS bio-optical products with *in situ* data in the turbid Lithuanian Baltic Sea coastal waters. Journal of Applied Remote Sensing 6(1), 063568-1 - 063568-20.

Ianora A., Bentley, M., Caldwell, G., Casotti, R., Cembella, C., Engstrom-ost J., Halsbank-lenk, C., Sonnenschein E., Legrand, C., Llewellyn C., Paldaviciene, A., Pohnert G., Pilkaityte, R., Razinkovas, A., Romano, G., Tillmann, U., **Vaičiūtė, D.**, 2011. The Relevance of Marine Chemical Ecology to Plankton and Ecosystem. Marine Drugs, 9: 1625-1648.

Olenina, I., Wasmund, N., Hajdu, S., Jurgensone, I., Gromisz, S., Kownacka, J., Toming, K., **Vaičiūtė, D.**, Olenin, S. 2010. Assessing impacts of invasive phytoplankton: The Baltic Sea case. Marine Pollution Bulletin, 60: 1691–1700;

Thesis structure. The dissertation includes 8 chapters including Introduction, Literature review, Description of study area, Material and methods, Results, Discussion, Conclusions and References. Four

appendixes contain supplementary information. The material is presented in 126 pages, 28 figures and 11 tables. The dissertation refers to 229 literature sources. Dissertation is written in English and summary in Lithuanian and English languages.

Abbreviations used in the study

AOP's – Apparent Optical Properties;
Boreal – Boreal Lakes processor;
C2R – Case 2 Regional processor;
CDOM – Coloured Dissolved Organic Matter;
CZCS – the Coastal Zone Color Scanner, a multi-channel scanning radiometer aboard the Nimbus 7 satellite;
ESA – European Space Agency;
EU – European Union;
Eutrophic – Eutrophic Lakes processor;
FR – Full Resolution (for MERIS it is 300 m at nadir);
FUB – processor developed by the German Institute for Coastal Research, Brockmann Consult and Freie Universität Berlin;
GKSS – German Institute for Coastal Research;
GMT – Greenwich Mean Time;
HELCOM – HELsinki COMmission;
IOP's – Inherent Optical Properties;
MAE – the Mean Absolute Error;
MCI – Maximum Chlorophyll Index;
MERIS – MEidium Resolution Imaging Spectrometer;
MODIS – MODerate-Resolution Imaging Spectroradiometer aboard Terra and Aqua satellites;
MOS – Moderate Optoelectrical Scanner aboard the IRS P3 satellite;
MSFD – Marine Strategy Framework Directive (2008/56/EC);
NASA – National Aeronautic and Space Administration;
NIR – electromagnetic waves of Near InfraRed spectrum, wavelength range from 750 nm to 1 mm;
NN's – Neural Networks;
OAC – Optically Active Components, includes chlorophyll *a*, CDOM and TSM;
PSU – Practical Salinity Units;

RMSE – the Root Mean Square Error;
SeaWiFS - the Sea-viewing Wide Field-of-view Sensor aboard the SeaStar Spacecraft;
SHYFEM – Shallow water Hydrodynamic Finite Element Model;
SPM – Suspended Particulate Matter;
TSM – Total Suspended Matter;
UV – electromagnetic waves of UltraViolet spectrum, wavelength range from 10 nm to 400 nm;
UVB – UltraViolet medium (UltraViolet B), wavelength range from 280 nm to 315 nm;
VIS – VISible spectrum, the portion of the electromagnetic spectrum, wavelength range from 400 nm to 750 nm;
WFD – Water Framework Directive (2000/60/EC).

Acknowledgements

I would like to thank my supervisor Renata Pilkaitytė for her trust, tolerance and allowing me freely choose the study object and ideas. I am especially grateful to my scientific advisors: Darius Daunys for valuable comments, discussions, explanations, effort my ideas to become truth and essential input preparing this thesis; Zita Rasuolė Gasiūnaitė for the help, support, critical and valuable comments.

A sincere thank to the supervisor of my master thesis and first scientific teacher Jūratė Kasperovičienė, first my chief Ričardas Paškauskas and colleagues from Nature Research Centre for the scientific background, practical lessons, enthusiasm, that is leading me now, and encouragement of further scientific career. This work would be impossible without their support.

Special thank Sergej Olenin for the ideas, support and valuable discussions. Inga Dailidienė, Loreta Kelpšaitė, Igor Kozlov (Russian State Hydrometeorological University, Russian), Victor V. Klemas (University of Delaware, USA) and colleagues from cathedra of Geosciences, Klaipėda University for their support in the new scientific field of remote sensing.

Thanks Artūras Razinkovas for the valuable remarks and comments on my work. Petras Zemlys and all modeling group for funny time.

Saulius Gulbinskas for the possibility to attend field campaigns in the Baltic Sea.

My friend and colleagues Marija, Irma, Jolita, Ingrida, Anastasija, Ilona, Jūratė, Andrius, Aleksej, Aleksas, Viačeslav, Nerijus, Aurelija, Rasa and Julius, Greta, Tomas, Mindaugas, Arūnas, Aistė, Sigitas, Raimonda for their friendship, inspiring discussions, work together in the field and in the lab.

Special thank to my special team of field campaigns Erikas Visakavičius, Viktorija Savickytė, Evelina Grinienė, Aidas Figoras and Edgaras Lukšys for their assistance during the work and the best time onboard.

My special thanks to my colleagues and friend from the Department of Marine Research, especially Irina Olenina for the valuable knowledge's in taxonomy of phytoplankton and scientific discussions, Nijolė Remeikaitė-Nikienė advising regarding WFD. The time working together was full of practical knowledge in the field of marine monitoring that was fully used preparing this work.

Thanks to my first teachers of ocean colour and optical remote sensing: Kerstin Stelzer, Jasmin Geißler, Carsten Brockmann (Brockmann Consult, Germany).

Particular thanks to Susanne Kratzer, her team from Stockholm University (Sweden) and Annelies Hommersom (Water Insight, the Netherlands) for the gained wisdom in the field of bio-optics, for the opportunity to work together in the lab and infected with the laugh and optimism.

Special thanks to Mariano Bresciani, Claudia Giardino and Erica Matta (CNR-IREA, Milan, Italy), Federica Braga (ISMAR-CN, Venice, Italy) and Maria Patrizia Adamo (CNR-ISSIA, Bari, Italy) for the opportunity to work together, learn more about remote sensing and bio-optics and a good time in Italy and Lithuania.

Thank to Daniela Stroppiana (CNR-IREA, Italy) and Marco Bartoli (Parma University, Italy) for their sincerity, fruitful scientific discussions and comments on the manuscript, wonderful time together.

Thanks to Artūras Zaiko for the help organizing the fastest boat in Klaipėda port “Žaibas”, baywatchers from Melnragė II and Palanga

for the ride on the water motorcycle to take samples, special thank for the all flotilla of Klaipėda: “Darius”, “Putā”, “Odisėja”, “Brabander” and “Romastė”.

My deepest thanks and love goes to my family: to my Mom, Dad, Sister, Varnelė, Džeromas, Dyzelis and Mazutas and especially to my dear Martynas!

Finally, many thanks for the clouds and sunny days.

This study was partially supported by the EU FP7 project MEECE (Marine Ecosystem Evolution in a Changing Environment, 212085), by a Norwegian financial mechanism and the Republic of Lithuania project EEE (A system for the sustainable management of Lithuanian marine resources using novel surveillance, modeling tools and an ecosystem approach, LT0047).

Satellite data was provided by Brockmann Consult/ESA in the frame of MarCOAST 2 project and via Principal Investigator proposal for ESA “Monitoring of water quality parameters using multi spatial and temporal MERIS FR data in the Lithuanian Baltic Sea coast – LitBaltSeaSAT” (ID 7835, IP D. Vaičiūtė).

1. LITERATURE REVIEW

1.1. Riverine fronts and their role in shaping environment characteristics

A front is defined as a region characterized by the local maximum in the horizontal and/or vertical gradient of some water property (e.g. temperature, salinity, nitrate concentration, chlorophyll concentration) (Largier, 1993; Franks, 1992). Franks (1992) described four common types of coastal oceanic fronts: (i) wind-driven upwelling fronts generated by an alongshore wind stress at the water surface, creating a strong surface thermal gradient; (ii) tidal fronts formed in shallow seas that have strong tidal currents and sloping bathymetry; (iii) topographic fronts formed in the lee of stationary objects embedded in a flow; (iv) water mass or buoyancy fronts created at the abutment of two dissimilar water masses. The discharge of fresh water onto a continental shelf typically results in the formation of a buoyant (hypopycnal) plume (Gelfenbaum, Stumpf, 1993). The density contrast at a water mass front is caused by a salinity difference between the the two water masses (Figure 1): the lighter fresh riverine water masses will tend to flow over the heavier saline water masses (Bowman and Iverson, 1978).

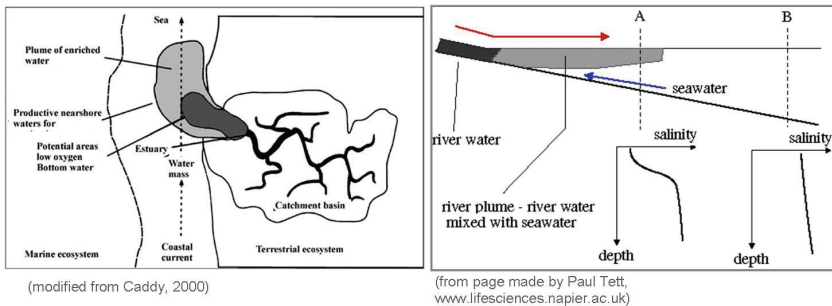


Figure 1. Schematic representation of frontal zone: spatial distribution (left) and vertical stratification (right).

The size and shape of a plume depends on the river discharge, wind and Coriolis force (Ou, 1984; Gelfenbaum, Stumpf, 1993).

Actually, Coriolis forcing plays an important role in plumes of moderate to large scale, e.g. Chesapeake Bay (Chao, 1988). While, for plumes of small scale, the Coriolis effect become secondary. It should be noted, however, that fronts are not always singular. At times, a series of embedded small-scale fronts and associated circulation cells can be observed within one frontal region (Largier, 1993). Haury et al. (1978) described the spatial dimensions of patches in respect to the aggregated distribution of biomass or number of individuals: i) mega-scale, when high biomass or species presence and absence extend over very large areas, i.e. greater than 3000 km; ii) macro-scale, where the patches are extended in the 1000 km up to 3000 km range; iii) meso-scale, the patches ranges from the 100 km up to 1000 km range; iv) coarse-scale, distinct aggregation at 1-100 km scales; v) fine-scale, patches of meters to hundreds of meters; vi) micro-scale, the small patches up to 1 m. Consequently, these smaller fronts exhibit much shorter time scales than their larger scale relatives. By the same token, these small fronts can be established very rapidly, whereas the larger geostrophic fronts require at least an inertial period before they are established.

The impact of large rivers as a primary interface between terrestrial and ocean environments is important on a regional/continental and on a global scale (Dagg et al., 2004). The formation of the frontal plume zones changes the hydrodynamic of the coastal waters enhancing vertical exchange (Largier, 1993). River plumes are a primary pathway for the dispersal of allochthonous materials both dissolved and particulate, organic and inorganic into the coastal ocean (Garvine, 1974). The precipitation of metals (e.g., iron and manganese) and the deposition of other pollutants accompany the delivery of terrestrially fine sediment. It may lead to toxic levels of metals being accumulated in the sediment (Largier, 1993). River systems deliver substantial amounts of inorganic nutrients, including nitrogen (N), phosphorus (P) and silica (Si) to coastal environments, mainly enhanced by anthropogenic sources (Gelfenbaum, Stumpf, 1993; Mayer et al., 1998). Rivers also contribute significant amounts of dissolved organic materials (DOM) and particulate materials, deposited near the mouth,

to the coastal ocean. A significant fraction of riverine DOM is biologically reactive on time scales (days–weeks) relevant to plume processes (Dagg et al., 2004). The physical processes responsible for nutrient transport into the euphotic zone, in particular the enhanced vertical motion at fronts, and the associated biological responses in these systems are well reviewed by Mann and Lazier (1991).

Buoyant plume regions are likely to be characterized by high phytoplankton biomass (Franks, 1992) and, in many cases, enhanced activity at higher trophic levels as well. The accumulation of plankton may be due to *in situ* production in the front or due to passive convergent transport toward the front. Numerous studies have shown phytoplankton biomass close relation to fronts in the ocean (Richardson, 1985; Franks and Anderson, 1992; Franks, 1992; Kononen et al., 1996; Moisander et al., 1997). Across hydrophysical boundaries of quasi-permanent salinity front non nutrient-limited growth conditions for pelagic ecosystems exists (Reynolds, 1989). Studies of plankton patchiness have shown that the regulation of the pelagic community by physical factors takes place at two levels: at the level of the functional groups of organisms and at the level of species composition (Kononen, 1992). As the result of the enrichment by nutrients transported by the rivers the enhanced primary production was recorded in the Mississippi River delta region (Lohrenz et al., 1997), Amazon plume (DeMaster, Pope, 1996), various estuarine systems, e.g. James River estuary (Filardo, Dunstan, 1985), Chesapeake Bay (Fisher et al., 1992), in the Kattegat/Skagerrak frontal zones (Richardson, 1985) and in the thermohaline front of the open Baltic Sea (Kahru et al., 1984). Consequently, the conditions for phytoplankton growth in buoyant discharge plumes of rivers are typically very good because of high available nutrient concentrations and high light associated with the buoyant plume (Dagg et al., 2004). However, the location of the maximum biomass along the salinity gradient differs between rivers and within rivers for different discharge conditions and seasons. This appears to be due to differences in salinities at which suspended matter concentrations decline to a level sufficient light to enhance phytoplankton growth

(Dagg et al., 2004). Thus, mixing, dilution, increased grazing and sinking causes the declining of the phytoplankton biomass (Liu, Dagg, 2003).

Riverine plume plays a significant role in the transporting zooplankton biomass seaward, where it has a strong stimulatory role in population growth due to enhanced biomass of phytoplankton, bacteria and lithogenic particles, and has a significant influence on the vertical composition (Amon, Benner, 1998). Rates of bacterial production in river plumes are typically higher than in river waters and adjacent marine waters. Distinct zooplankton communities also exist within and below the plume (Korshenko, 1991; Dagg, Ortner, 1995; Telesh, 2004). Alternatively, transformations associated with plumes may sometimes be destructive because of mortality resulting from salinity and temperature stresses, and because the forces that aggregate zooplankton may also aggregate larval fish and other predators. Feeding conditions in the highly productive plume regions appear favorable for ichthyoplankton (e.g. larval fish) because of the high concentrations of planktonic prey (Grimes, Finucane, 1991). Regions associated with river plume are often sites of high fisheries production (Chesney et al., 1998) suggesting stimulation of upper trophic levels. Finally, in economic terms, estuarine fronts are important to fisheries since estuarine fronts may be a feeding site for commercial fish.

Fronts may also be important for benthic communities (Largier, 1993). Enhanced turbidity and water column productivity reduces light penetration into the deeper water layers, i.e. reduces the photic zone depth, thus limiting the photosynthesis level necessary for the benthic vegetation. The enhanced phytoplankton production and accumulated biomass in the frontal waters can settle down, resulting in increased benthic productivity and enriched muddy sediments. Moreover, the blooms intensity produce high load of organic matter and cause oxygen depletion nearbottom unbalancing function of the system (Bianchi et al., 2000). Perhaps the most evident effect of fronts on society is the reduction of water quality due to accumulation of pollutants, heavy metals and toxins. The enhanced phytoplankton

production leads to the massive blooms caused by harmful algae (Largier, 1993). The toxic algae chemical activity can directly affect environmental and human health due to production and accumulation of nuisance or toxic metabolites (Ianora et al., 2011). The turbid waters are unpleasant not only for bathers and divers, but for local residents and tourists, and even can cause financial loss for resorts. River fronts in the Baltic Sea region.

1.2. River fronts in the Baltic Sea region

The non-tidal Baltic Sea is one of the largest (382 000 km²), semi-enclosed, brackish seas in the world with a relatively stable isohalines due to gradual changes of environmental factors and limited exchange of the water with the North Sea (Wallentinus, 1991; Storch, Omstedt, 2008). Salinity balance is maintained by outflow of rivers and precipitation in the surface layer, and a variable near bottom inflow of higher saline water (32 PSU) through the Danish Straits. The surface salinity decreases from 6-8 PSU in the Baltic Sea proper, to 5-6 PSU in the Bothnian Sea and 2-3 PSU in the Bothnian Bay. The river drainage basin covers an area of 1 739 000 km² (Figure 2) causing the salinity changes in regional scale. There are five main big rivers entering the Baltic Sea: Neva, Vistula, Nemunas, Daugava and Oder. These estuaries form fronts in the coastal waters that are important for both physical and ecological processes. Thus, the salinity gradient is one of the main features characteristic of any estuarine ecosystem (Telesh, Khlebovich, 2010). The large freshwater content is strongly associated with nutrient input from the densely populated and intensively cultivated catchment areas and atmosphere and therefore is one of the main elements causing the eutrophication processes in the sea (Rönnberg and Bonsdorff, 2004). An evident increase in eutrophication leading by toxic algae blooms, sediments pollution with heavy metals, enrichment by suspended matter and considerable drop in water transparency, changes in plankton and benthos communities due to the massive load of the rivers, has been observed in all regions (Buszewski et al., 2005; Pastuszak et al., 2003; Pöder et al., 2003).



Figure 2. The Baltic Sea drainage basin and the largest rivers (modified from Håkanson et al., 2003).

The annual freshwater discharge into the Gulf of Gdańsk is 34.5 km^3 , of which the Vistula (Wisła) River contributes approximately 30%, i.e. 7% of the total input of freshwater (Buszewski et al., 2005). The majority of the nutrients and toxic substances are carried by rivers mainly in the Gulf of Gdańsk and the Pomeranian Bay. About 5–10% of the time the Vistula river water discharged into the Baltic flows westwards, resulting in dispersion of pollutants onto the beaches of the Gulf of Gdańsk and Puck Bay (Glasby, Szefer, 1998). The salinity is strongly influenced by the outflow from the Vistula River and there is salinity (hydrological front) about 10 km from the river mouth. The lowest salinity near the mouth of Vistula is about 4.5 PSU in spring and summer. The outflow is transported mainly in E, NE, and N directions (Glasby, Szefer, 1998).

The Pomeranian Bay—together with the Szczecin Lagoon and a couple of lakes—form a huge complex estuarine system supplied by the Oder River (Siegel et al., 1999) that enters into the western Baltic Sea. According to Lampe (1993) the freshwater discharged into the Pomeranian Bight amounts to 18 km^3 per year (Oder river 15-17 km^3 ,

Peene river 0.8 km³). The river outflow is driven by sea level differences between the Oder lagoon and the southern Pomeranian Bight and wind forcing. Easterly winds induce the formation of a broad plume of riverine water (usually 10 km wide) along the western coasts of the Pomeranian Bay (Pastuszak et al., 2003; Siegel et al., 1999). During persistent westerly winds, the riverine waters are transported by the coastal current towards the east.

The eastern part of the Gulf of Finland receives the discharge from the river Neva, which constitutes 15–20% of the total Baltic fresh water inflow with a mean runoff of 2700 m³/s (Alenius et al., 1998). This leads not only to salinity stratification in the vertical but also to pronounced east–west salinity gradients (Jönsson et al., 2011). The main part of this estuary is dominated by water from the Baltic Proper and that the most pronounced mixing with Neva water takes place over a rather small area in the inner parts of the Gulf of Finland. The salinity increases from east to west and from north to south. The surface salinity varies from 5–7 PSU in the western Gulf of Finland to about 0–3 PSU in the east (Alenius et al., 1998).

The Daugava enters the Gulf of Riga and is the third largest river discharging into the Baltic Sea. Daugava contributes about 5 % of the total water inflow to the Baltic Sea (Klavins et al., 2002). Salinity in the Gulf of Riga varies from 0.5–2.0 to >5.5 PSU (Seisuma, Kulikova, 2007).

1.3. Investigation of Nemunas River plume in the Lithuanian Baltic Sea coastal waters

For the first time the hydrodynamical phenomenon created by the discharge of Nemunas River was described from the perspective of zooplankton distribution during April–July in 1982–1988 (Korshenko, 1991). Several hydrological surface units were described: i) waters of the Curonian Lagoon where salinity ranges from 2–3 PSU to 6.6–7.0 PSU; ii) transitional waters mainly directed westwards to the open Sea where salinity is up to 7.2–7.8 PSU; iii) brackish waters with salinity up to 8.4 PSU; iv) hydrofront that separates the lagoon waters from the transitional waters; v) surface patches of transitional waters,

that mainly originated from the Vistula Lagoon. According to Korshenko (1991) the most productive regions were located at the frontal zone near the entrance of the Curonian Lagoon where the lagoon waters are mixing with brackish coastal waters. Moreover, different zooplankton communities were described over different hydrological units.

During 1980-1996 the role of riverine front for the seasonal changes of the floristic composition of phytoplankton were studied by Olenina (1997).

Table 1. Assemblage of the dominant phytoplankton species in the plume area (modified from Olenina, 1997; 2004).

Month/Season	Olenina, 1997	Olenina, 2004
Method of assessment of dominant species	Dominant species according to the presence in the samples (20% and more)	Dominant species according to the relative abundance (10% and more from total)
V/Spring	<i>Skeletonema costatum</i> <i>Peridiniella catenata</i> <i>Diatoma tenuis</i> <i>Chaetoceros wighamii</i> <i>Stephanodiscus hantzschii</i>	<i>Skeletonema costatum</i> <i>Peridiniella catenata</i> <i>Diatoma tenuis</i> <i>Chaetoceros wighamii</i> <i>Stephanodiscus hantzschii</i> <i>Cryptomonadales</i> spp. <i>Heterocapsa rotundata</i>
VIII/Summer	<i>Gomphospaeria pusilla</i> * <i>Skeletonema costatum</i> <i>Flagellata</i> undet. <i>Planktonema lauterbornii</i> <i>Heterocapsa triquetra</i>	<i>Coelomonon pusillum</i> <i>Skeletonema costatum</i> <i>Aphanizomenon flos-aquae</i> <i>Chrysochromulina</i> spp. <i>Heterocapsa triquetra</i> <i>Cylindrotheca closterium</i> <i>Cryptomonadales</i> spp.
X-XII/Autumn	<i>Stephanodiscus hantzschii</i> <i>Cryptomonadales</i> spp. <i>Aulacoseira islandica</i> <i>Aphanizomenon flos-aquae</i> <i>Skeletonema costatum</i>	<i>Stephanodiscus hantzschii</i> <i>Cryptomonadales</i> spp. <i>Aulacoseira islandica</i> <i>Aphanizomenon flos-aquae</i> <i>Skeletonema costatum</i> <i>Prorocentrum minimum</i> <i>Coscinodiscus granii</i>
-/Winter	Not given	<i>Skeletonema costatum</i> <i>Aulacoseira islandica</i> <i>Melosira varians</i> <i>Thalassiosira levanderii</i> <i>Cryptomonadales</i> spp. <i>Pseudopedinella tricostata</i>

* *Gomphospaeria pusilla* and *Coelomonon pusillum* are the synonyms of the same species (Guiry and Guiry, 2012).

According to the results of cluster analysis it was found, that the plume was significantly different in species composition from the rest three areas identified in the SE Baltic Sea. The phytoplankton of this area is characteristic with brackish water species which are abundant in the northern part of the Curonian lagoon (Table 1). Later the zonation of SE Baltic coastal waters has been improved on the basis of the phytoplankton investigation data in 1984-2003 (Olenina, 2004). Two different areas were identified according to the phytoplankton structure: the open coast and the plume area of the Curonian Lagoon. For each zone, characteristic seasonal complex of dominant species were identified (Table 1).

The typology of the coastal water masses (Figure 3) was presented in the national project (Implementation of the EU Water Framework Directive, 2004; Langas et al., 2009; Management plan of Nemunas River basin region, 2010) in order to assess the water quality based on selected environmental criteria. Transitional waters in respect to depth, mixing characteristics and mean substratum composition include i) plume of the Curonian Lagoon in the Baltic Sea; ii) northern part of the Curonian Lagoon; iii) central part of the Curonian Lagoon (Daunys et al., 2007; Management plan of Nemunas River basin region, 2010). Whereas coastal waters, i.e. 1 nautical mile from coast line, in respect to dominant sediment type include i) open Baltic Sea sandy coast, i.e. coast along Curonian Spit; ii) open Baltic Sea stony coast, i.e. northern mainland coast. Territorial Sea waters are located within the area between the coast line and 12 nautical miles (Management plan of Nemunas River basin region, 2010). The waters outside the Territorial Sea belong to the Lithuanian exclusive economical zone and in this work are named as offshore. The extent of the Curonian lagoon plume in the Baltic Sea was assessed by hydrodynamic finite element model SHYFEM (Daunys et al., 2007; Management plan of Nemunas River basin region, 2010).

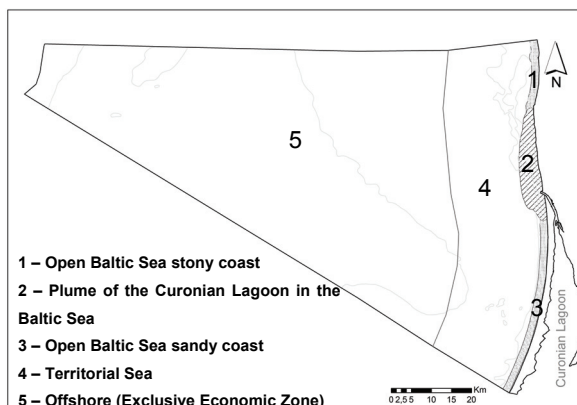


Figure 3. Different water regions of the Lithuanian Baltic Sea (adapted from Daunys et al., 2007; Langas et al., 2009; Management plan of Nemunas River basin region, 2010). The grey lines – isobaths (every 10 m).

1.4. Water optics and Remote Sensing

1.4.1. Optical Remote Sensing

The optical remote sensing operating in the visible-near-infrared (VIS/NIR) range, i.e. 400–900 nm, with passive satellite radiometers (Capone and Subramaniam, 2007). VIS/NIR radiation, i.e. the sun light, is scattered and absorbed on its way through the atmosphere (Figure 4). As the radiant flux reaches the sea surface, some of it is reflected, and some of it is refracted as it enters the water body. Once in the water, the radiant flux is either absorbed or scattered by the optical components in the water body, which changes its spectral signature. The radiance that is scattered back into the atmosphere, the so-called water-leaving radiance, now contains information about the optical water constituents. It is changed, again, on its way through the atmosphere. The VIS/NIR signal measured remotely by a sensor placed on an aircraft or a satellite therefore carries information on both the optical in-water constituents and the atmosphere. The NIR channels of the radiometer are used for atmospheric correction,

whereas the visible channels are used to derive information about water quality.

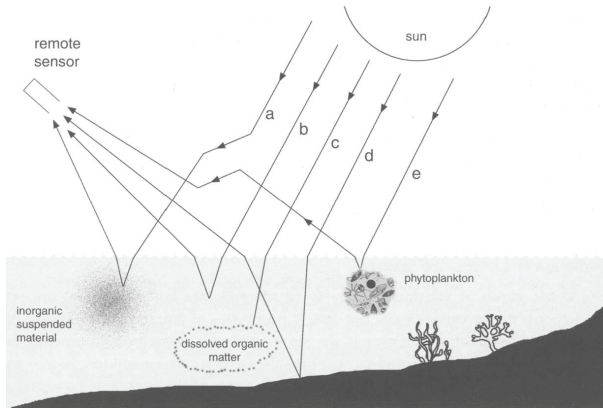


Figure 4. Factors affecting upwelling light leaving the sea surface: (a) upward scattering by inorganic suspended material; (b) upward scattering from water molecules; (c) absorption by CDOM; (d) reflection off the bottom; (e) upward scattering from the phytoplankton component. Modified from IOCCG Report (2000).

The first instrument (a multi-channel scanning radiometer) designed specifically for the estimation of water quality (particularly chlorophyll *a*) was Coastal Zone Colour Scanner (CZCS), on board the Nimbus 7 satellite, provided images in 1978–1986 with 825 m spatial resolution. Then next instrument followed by SeaStar SeaWiFS (1000 m resolution, 1997–2011). In the 2000s, the usability of satellite imagery for water quality mapping has improved considerably with the availability of several satellite instruments created for water applications in particular: Moderate-Resolution Imaging Spectroradiometer (MODIS) on board of Terra (2000–present) and Aqua (2002–present) satellites of the National Aeronautics and Space Administration (NASA) and Medium Resolution Imaging Spectrometer (MERIS) ocean color sensor (2002–2012) on board the ENVISAT satellite of the European Space Agency (ESA) provide frequent acquisitions with sufficient spatial coverage (Reinart, Kutser, 2006). In particular, the products of the MERIS ocean color sensor are

suitable to monitor coastal waters (Kratzer, Vinterhav, 2010; Doerffer et al., 1999) with a sufficient 300 m spatial resolution at nadir and currently the best spectral and radiometric resolution, i.e. MERIS has 15 spectral bands with 10 nm bandwidth each (Doerffer et al., 1999).

Morel and Prieur (1977) suggested the division of marine waters into two optical categories, according to the dominating optical water properties. They defined Case 1 waters as those with high phytoplankton concentration comparing with other constituents, which means that the light field is determined merely by the optical properties of phytoplankton (particularly pigment absorption) co-varying with yellow substances, and the optical properties of water itself (Figure 5). Oceanic waters are usually Case 1 waters. Coastal waters, lakes and continental shelf areas usually belong to Case 2 waters, where other substances (CDOM and inorganic particles) in addition to phytoplankton can make a significant contribution to optical properties and they can vary independently of phytoplankton (Morel and Prieur, 1977). The Baltic Sea is considered as optically complex Case 2 water basin. The optical water properties are strongly influenced by phytoplankton pigments, yellow substances and suspended matter (Morel and Prieur, 1977; Mobley, 1994; Kratzer et al., 2008).



Figure 5. Bio-optical classification of waters according to Morel and Prieur (1977). Adapted from IOCCG report 3 (2000).

Firstly, the algorithms for the estimating of the concentration of chlorophyll *a* have been developed over the last decades. Chlorophyll *a* retrieval algorithms for multi-spectral sensors, which have one to a few bands in the visible part of the spectrum, are based on single band algorithms or band ratio-type algorithms (Kutser, 2009). Single band chlorophyll-retrieval algorithms utilize red and near-infrared bands. For example, Kutser et al (2006) have shown that MODIS band 1 (620–670 nm) can be used not only for detailed mapping of the extent of cyanobacterial blooms but also for mapping cyanobacterial biomass. Reinart and Kutser (2006) have shown that MODIS band 2 (841–876 nm) is suitable for separating dense subsurface cyanobacterial blooms from surface scum. The most commonly used chlorophyll-retrieval band ratio algorithms especially for the mapping of phytoplankton blooms are based on the blue to green ratio (Sathyendranath et al., 2001). However, the standard products must be treated with caution in coastal and inland waters. For example, Darecki et al. (2005) have shown for the Baltic Sea that SeaWiFS and MODIS chlorophyll-retrieval algorithms are not suitable even in non-bloom conditions, where they significantly overestimate chlorophyll concentrations. The main cause of the error is using blue bands in chlorophyll-retrieval algorithms due to the interference with CDOM that highly dominates in coastal waters. The general tendency in successfulness of the band-ratio-type algorithms in coastal and inland waters seems to be that green to red (and NIR) bands are more suitable in the case of higher phytoplankton biomasses and/or more turbid waters than the algorithms using blue to green bands (Kutser, 2009).

It becomes necessary to develop processing algorithms suitable for optically complex coastal and inland waters (Doerffer et al., 1999). Different neural networks-based (NNs) processors of MERIS data, like case 2 regional (C2R), Eutrophic, Boreal, FUB and standard MERIS Level 2 has been developed to identify the most suitable one for optically Case 2 or coastal and inland waters. Recent works have shown that algorithms based on NNs are better suited than band ratio algorithms for Case 2 waters and they allow the estimation of

chlorophyll *a* concentration in presence of CDOM (Schiller and Doerffer, 1999). These processors have been already tested in different Baltic Sea regions: in northwestern part (Kratzer et al., 2008; Kratzer, Vinterhav, 2010), Skagerrak (Sørensen et al., 2002; 2007), open Sea areas (Ohde et al., 2007; Siegel et al., 2003) and Baltic Sea largest lagoons (Giardino et al., 2010a; Kruk et al., 2010) showing the advantage of satellite based remote sensing for environmental science, and as a helpful tool for the water authority and policy makers (Bresciani et al., 2011).

Recently developed Maximum chlorophyll index (MCI) algorithm become applied for the ecological studies (Rundquist et al., 1996; Gower et al., 2006). MCI algorithm in MERIS data is determined by the height of the peak near 709 nm in the radiance spectrum. The spectral features in this region include chl *a* absorption around 675 nm, chl *a* fluorescence around 683 nm, and in algae-laden waters the prominent reflectance peak around 690–700 nm caused by algal-cell scattering and a minimum in the combined absorption curves of algae and water (Rundquist et al., 1996). The MCI was applied for the detecting of floating *Sargassum* in the Gulf of Mexico (Gower et al., 2006) and later for the ‘superblooms’ of Antarctic diatoms (Gower, King 2007).

However, there are the limitations of satellite based optical remote sensing technique. The low sun elevation in the high-latitude regions of the Baltic basin limits the availability of satellite data from approximately early March to late October (Kratzer et al., 2011). Further limitations are caused by intermittent cloud cover. The extent of cloud cover in the Baltic Sea area is about 40–50% in summer and about 60–70% in winter (Karlsson, 1996). Due to high CDOM in the Baltic Sea, the absorption is very high, especially in the blue part of the spectrum. Thus, Baltic Sea water is relatively dark compared to other seas leading to extremely low water signals. The large amount of the signal coming back to the sensor is solar radiation originated from atmospheric processes, such as scattering by aerosols, while only 10% comes from the water (Brockmann, 2006). The atmospheric contribution of the detected signal is unwanted and needs to be

removed in order correctly retrieve of water quality products (Schroeder et al., 2007a; Giardino et al., 2010a). Moreover, areas close to the coast are usually influenced by high reflectance from land. Satellite data from water areas close to the coastline have to be corrected for the adjacency or environmental effects (Kratzer, Vinterhav, 2010). Finally, the environmental information from the satellites could be given only from the surface of the water basin or from the several meters, i.e. if the signal penetrates deeper (IOCCG report 3, 2000).

1.4.2. Optical properties of water basins

In 1961, Preisendorfer introduced a system which separated optical properties into two categories – inherent and apparent (Kirk, 2011). Apparent optical properties (AOP's) – radiance and irradiance – are those affected by a change in the radiance distribution, while inherent optical properties (IOP's) are independent of changes in the radiance distribution and depend only on the substances within aquatic medium also known as Optically Active Components (OAC).

Water typically includes three main groups of absorbing OAC: phytoplankton, coloured dissolved organic material (CDOM) and non-algal particles such as detritus and mineral particles. In addition, pure water absorbs light too. The total spectral absorption coefficient ($a_{tot}(\lambda)$) can be described as:

$$a_{tot}(\lambda) = a_w(\lambda) + a_{CDOM}(\lambda) + a_{ph}(\lambda) + a_{nap}(\lambda)$$

where $a_w(\lambda)$ is the absorption coefficient of pure water, $a_{CDOM}(\lambda)$ is the absorption coefficient of CDOM, $a_{ph}(\lambda)$ is the absorption coefficient of phytoplankton, $a_{nap}(\lambda)$ is the absorption of non-algal particles and λ is wavelength.

The total scattering coefficient ($b_{tot}(\lambda)$) can be divided into the following main components contributing to scattering:

$$b_{tot}(\lambda) = b_w(\lambda) + b_{TSM}(\lambda) + b_{ph}(\lambda)$$

where $b_w(\lambda)$ is the scattering coefficient of pure water, $b_{TSM}(\lambda)$ is the specific scattering coefficient of TSM, $b_{ph}(\lambda)$ is the scattering coefficient of phytoplankton.

Finally, the total attenuation coefficient ($c_{tot}(\lambda)$) is the sum of the absorption and scattering coefficients:

$$c_{tot}(\lambda) = a_{tot}(\lambda) + b_{tot}(\lambda)$$

The presented optical parameters serve as a source for bio-optical models, which can be formulated for total absorption, reflectance, diffuse attenuation coefficient etc.

1.4.3. Optically active components

Chlorophyll *a*, coloured dissolved organic matter and total suspended matter, are known as optically active components (OAC) that influences the optical properties of water basins and can be derived by satellite remote sensing techniques (Dekker et al., 2001; Kratzer and Tett, 2009). The estimation of optical in-water components are based on absorption and scattering properties. Water itself, controls the optical properties, i.e. the absorption and attenuation of the water at visible and near-infrared light depend on temperature and salinity (Pegau et al., 1997; Kirk, 2011).

Chlorophyll *a* (chl *a*) is the main photosynthetically active pigment of phytoplankton prevailing in all algal groups and therefore commonly used as a proxy for the microalgae biomass in the water (Wasmund and Uhlig, 2003). The concentration of pigments may be stimulated by various environmental factors, generally by water temperature and nutrients (Kononen, 1992; Wasmund et al., 2001; Gasiūnaitė et al., 2005; Wasmund et al., 2011). In a number of countries chl *a* is used as first metric in water quality assessment according to Water Framework Directive (2000/60/EC).

Coloured dissolved organic matter (CDOM) also known as humic substances, yellow substances, gelbstoff or gilvin, is a mixture of compounds that are products of plant and animal decomposition (Coble et al., 2004). Water originating from rainfall drains through

soil, extracting humic substances, which are carried into rivers and then into the estuaries and sea. Most of the soluble humic material in river water is precipitated when it comes into the contact with sea water. Most of the CDOM in coastal waters originates from land run off (Kratzer et al., 2008). However, it may be released by macroalgae as well (Hulatt et al., 2009). In natural waters CDOM plays an important role: due to strong absorption of CDOM in the UV portion of the spectrum, it protects phytoplankton, macroalgae and other biota from damaging UV medium wave (UVB) radiation (Blough and Green, 1995) and plays an important role in carbon cycle as in addition to primary production (Moran and Zepp, 1997). On the other hand, CDOM can reduce dissolved oxygen concentration causing release of nutrients (Bushaw et al., 1996). The increased level of CDOM can reduce the amount and quality of photosynthetically active radiation to phytoplankton and other primary producers (Bidigare et al., 1993).

There are typical absorption spectra by CDOM, with absorption being very low or absent at the red end of the visible spectrum and rising steadily with decreasing wavelength towards the blue and can be measured optically in the coastal areas (Kratzer et al., 2008; Kratzer et al., 2011). The absorption spectra as well as the concentration of CDOM vary between marine and freshwater (Kirk, 2011). Changes in the concentration and properties of CDOM in coastal regions can be used to trace physical circulation and water mass history. This information can be useful in tracking freshwater plumes to assess the impact of river-born components, such as nutrients and pollutants that may impact fisheries and water quality (Coble et al., 2004).

Total suspended matter (TSM) also referred to as suspended particulate matter (SPM) generally originated from terrestrial and river runoff or wind-driven re-suspension of sediments in the coastal areas (Kratzer and Tett, 2009; Kratzer et al., 2011). High turbidity in the waters reduces radiation and limits aquatic primary production, therefore it is a key element of water quality in coastal areas (Premazzi et al., 1999). From the optical point of view, primary effect

of TSM on water colour usually originates from scattering (Kirk, 2011). TSM plays an important role in regulation of the two major transport pathways: the dissolved pelagic route and the particulate sedimentation and benthic route (Håkanson et al., 2005). Moreover, TSM transports all kinds of pollutants, such as organics (Clark, 1986), nutrients (Håkanson, 1999), heavy metals and radionuclide (Wieland et al., 1991). At lower trophic levels, the carbon content of SPM is crucial as a source of energy for bacteria, phytoplankton and zooplankton (Wetzel, 1983).

1.5. Optical Remote Sensing in the Baltic Sea region and in the Lithuanian waters

The application of satellite data in the Baltic Sea started in the 1970s with Landsat MSS before the first ocean colour sensors CZCS and intensified in the last decade continuing with sensors such as MOS, SeaWiFS, MODIS and MERIS (Kahru et al., 1994). The ocean colour satellite data in the Baltic Sea were mainly applied for coastal discharge (Horstmann, 1983; Siegel et al., 1996; 1999), in order to derive information about water quality indicators, e.g. chlorophyll *a*, TSM, CDOM (e.g. Giardino et al., 2010a; Kratzer et al., 2008; Vaičiūtė et al., 2012) and phytoplankton blooms (Öström, 1976; Ulbricht, Schmidt, 1977; Kahru et al., 1994; Kahru, 1997; Kononen, Leppänen, 1997, Kutser, 2004; Seppälä et al., 2005). Algorithms for derivation of biogeochemical products are being adapted to the conditions of the Baltic Sea as well (Darecki et al., 2005; Schiller and Doerffer, 1999; Doerffer et al., 1999; Ohde et al., 2007; Kratzer et al., 2003).

Nowadays, few environmental institutes make retrieved biogeophysical satellite products for the whole Baltic Sea available online to a wide range of end-users, such as environmental agencies, tourism, or fisheries (Kratzer et al., 2011). The Swedish Meteorological and Hydrological Institute (SMHI) and the Finnish Environmental Institute (SYKE) have developed online information systems for water quality monitoring of the Baltic Sea, which are operational since 2002 and 2003, respectively. The Water Quality

Service System (WAQSS) was developed by Brockman Consult, Germany within the ESA project MarCoast for Global Monitoring of Environment and Security GMES.

For the first time in Lithuania calibration and validation activities associated with satellite MERIS image processing were performed in the Curonian Lagoon by Giardino et al. (2010a). Field data were used to validate the performances of two atmospheric correction algorithms, to build a band-ratio algorithm for chlorophyll *a* and to validate MERIS-derived maps. In the results they found that the neural network-based Case 2 Regional processor was found suitable for mapping CDOM and the band-ratio algorithm applied to image data corrected with the 6S code was appropriate for chlorophyll *a*. In general maps were in agreement with *in situ* measurements. Later With respect to the work done by Giardino et al., 2010, the algorithm was developed for the estimation of chlorophyll *a* concentrations in the Curonian Lagoon during the specific case of hyper-trophic waters (Bresciani et al., 2012). Concentrations of chlorophyll *a* obtained from MERIS data corresponded to the hypertrophic water conditions during summer and showed great inter-annual variability.

2. DESCRIPTION OF THE STUDY AREA

2.1. Geolocation

The coastal waters of Lithuania belong to the southern Baltic Proper. The Lithuanian Baltic Sea region together with the part of Kaliningrad and the part of Latvia (to Pape) comprises the South Eastern (SE) Baltic Sea region. The area of Lithuanian Baltic Sea waters occupies about 6426.6 km² between Latvia in the north and Russia Federation in the south. The mean depth is ca 50 m while the maximum depth is 125 m (Gelumauskaitė et al., 1999). The maximum depth of Klaipėda Strait is approximately 14 m and changes because of dredging (Galkus, 2007). The coast of Lithuania represents a generic type of more or less strait coasts mainly formed by the activity of waves that contain a relatively large amount of fine and mobile sediments (Žilinskas, 2005; Žaromskis, 1996). Lithuanian Baltic Sea is connected with the largest European non-tidal Curonian Lagoon (1584 km²) by narrow Klaipėda Strait, where the water exchange between the Lagoon and the Sea occurs.

2.2. Local hydrometeorological conditions and hydrodynamics

Lithuanian Baltic Sea coast is exposed from any westerly direction, with a wind fetch exceeding >200 km (Olenin et al., 2003). Permanent influence of winds, waves and water currents produces a hydrodynamically very active environment resulting in no oxygen deficiency. The typical water mass transport in the Lithuanian Baltic Sea is towards the coast from the south to north caused by Coriolis force representative in the northern hemisphere. The dynamic of water masses mainly depends on the wind regime, riverine runoff and precipitation.

Generally, dominant wind of one direction cannot be clearly distinguished (Dailidienė et al., 2006). Strong western wind predominates, which forms the water level rising in the Baltic Sea coast, while the probability of southeastern wind has decreased. However, the winds of southern directions remain (Figure 6). Long-term seasonal change of water level in Klaipėda Strait reflects general

water rise in the Baltic Sea at the end of summer and the beginning of autumn when the seawater raises mainly due to the total inflow of river waters.

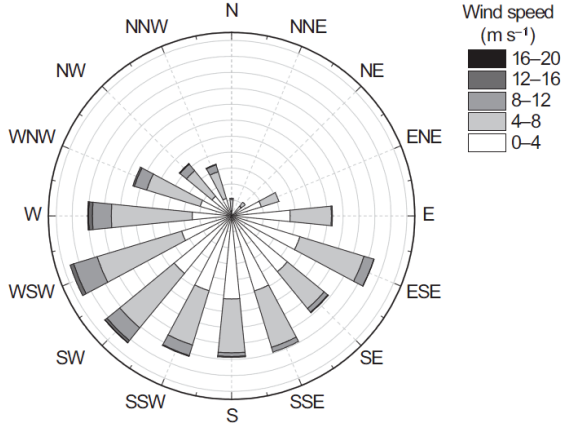


Figure 6. Wind rose at Klaipėda for 1993-2008 period (from Kelpšaitė et al., 2011).

However, the freshwater lagoon waters can reach the coastal water due to the nearly 15 cm higher water level of the lagoon with respect to the Baltic Sea waters (Dailidienė et al., 2006; 2011; Dailidienė, Davulienė, 2007; 2008). According to Gailiušis et al. (2001) in 18% of all cases brackish water penetrates the Curonian Lagoon. The Nemunas River runoff (22.1 km³/year), contributing approximately 96% to the total riverine runoff and 77% to the water balance of the Curonian Lagoon, carries most of the nutrient loads from the neighboring countryside (Ferrarin et al., 2008). Fresh water runoff from the Curonian Lagoon to the Baltic Sea through the Klaipėda Strait approximately is 27.7 km³/year (Jakimavičius, Kovalenkoviėnė, 2010). The seasonal Nemunas river runoff distribution is the following: 38% of annual runoff in spring, 16% in summer, 20% in autumn and 26% in winter season (Jakimavičius, Kovalenkoviėnė, 2010; Gailiušis et al., 2011). In this region several types of water circulation between two water bodies exists: i) the outflow of the Lagoon waters; ii) the inflow of the Sea waters; iii) two-layer system

of water exchange; iv) water exchange by two different directions of the Strait (Dubra, Červinskas, 1968; later improved by Galkus, 2007). Long-term mean precipitation in Nemunas River basin is about 1194 km³. The slight long-term changes in precipitation among the seasons were recorded: the quantity of precipitation increases in winter season and decreased in spring season (Jakimavičius, Kovalenkoviėnė, 2010).

2.3. Hydrophysics and hydrochemistry

The water temperature regime in the study area exhibits the typical boreal pattern, with the highest temperatures in July–August (15 ± 3.3 °C) and the lowest ones in January–February (1.3 ± 0.8 °C) (calculations of temperature are based on unpublished monitoring data, Department of Marine Research).

The average concentration of phosphates in summer is 0.22 ± 0.16 μmol/l and the winter maximum is 2.45 μmol/l, total phosphorus summer concentration ranges from 0.20 to 4.81 μmol/l and the winter maximum is 3.55 μmol/l. The average concentration of nitrates in summer is 1.13 ± 0.72 μmol/l, while in wintertime the maximum exceeds 51 μmol/l. Total nitrogen concentration ranges from 4.64 to 164.88 μmol/l during summer, with lower concentrations in winter (up to 116 μmol/l) (calculations of nutrients are based on unpublished monitoring data, Department of Marine Research). In general, the highest measured concentrations of nutrients are in the vicinity of the outlet of Curonian Lagoon (Olenina and Kavolytė, 1996).

Generally the surface salinity is in the range of 7–8 PSU, whereas near the mouth of the Curonian Lagoon salinity may decrease to almost freshwater and salinity gradient may extend for tens of kilometers out into the sea (Olenina and Olenin, 2002; Olenin and Daunys, 2004).

The plume area is strongly affected by hypereutrophic lagoon waters (Pilkaitytė, Razinkovas, 2007). The shallow (mean depth of 3.8 m) and weakly stratified Curonian Lagoon remains very turbid because of the resuspension (favor sediments mainly sand and silt)

induced by water mixing driven by the action of the local wind and intense primary production (Galkus, 2003; Žaromskis, 1996). The Secchi disk depth varies from 0.3 to 2.2 m (Gasiūnaitė et al., 2008). Annually, the Curonian Lagoon receives 170000 t of particulate organic material from 100500 km² catchment area, 98% of which belongs to the Nemunas River (Žaromskis, 1996; Galkus, Jokšas, 1997). The greatest concentrations of particulate matter occur during spring ~ 30 and summer ~25 mg/l, the lowest – in winter (Jokšas et al., 2005). Marine water mass is characterized by 3-6 fold lower concentration of suspended particulate matter than in the Curonian Lagoon or the Nemunas River; it varies in the range of 5–7 mg/l and contains 50–60% of organic matter during the spring-autumn period (Jokšas et al., 2005). The outflow of highly productive lagoon waters reduces light penetration into the deeper water layers of the Baltic Sea (Olenina and Olenin, 2002).

3. MATERIAL AND METHODS

In this study summer period or intensive vegetation period covers June–September according HELCOM (1996). The summary of used samples and MERIS images is given in Appendix 1, p. 125.

3.1. Validation of satellite data

The validation of satellite data was based on *in situ* data collected during eight field surveys carried out from May to September 2010 in the SE Baltic Sea coastal waters (Figure 7). Water samples were taken just below the sea surface with a sampling bucket. Over 8 surveys a total of 77 water samples were collected and transported by ice-bags to laboratory, where they were analyzed following the methods described in Chapter 3.3.

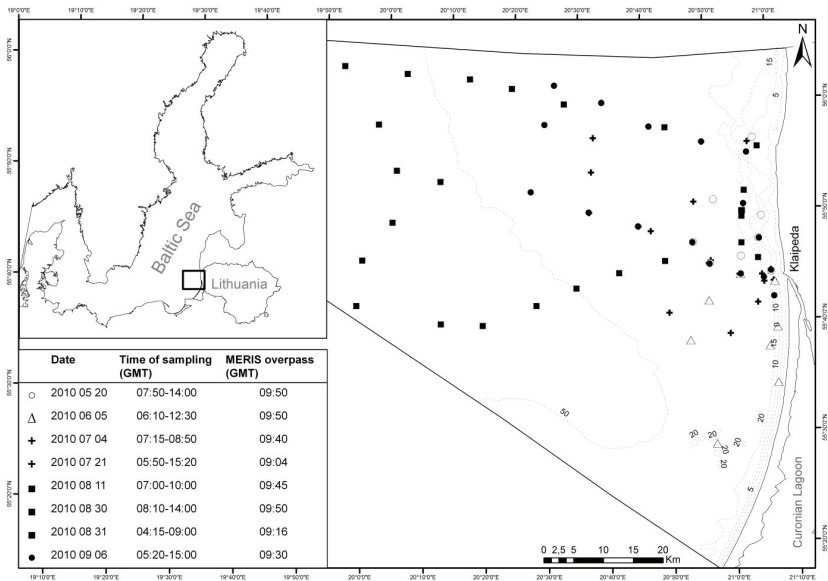


Figure 7. Study area and sampling locations during 8 surveys in 2010 over the Lithuanian part of the Baltic Sea. Different sampling month are indicated by different symbols.

Simultaneously with the dates of the field campaigns (see Figure 7) MERIS full resolution (FR, 300 m) cloud free images were acquired. MERIS operates in the visible and near-infrared spectral range (from 400 to 900 nm) with a wavelength configuration sensitivities to the most important optically-active water constituents. MERIS acquired 15 spectral bands, the band 11 (760 nm) is driven to resolve spectral features of the oxygen absorption and the band 14 (890 nm) and 15 (900 nm) is using for water vapor absorption.

After 2nd reprocessing MERIS Level 1b images firstly were corrected to account for the difference between actual and nominal wavelengths of the solar irradiance in each channel (Fomferra and Brockmann, 2006) with the Smile tool (1.2.101 version) of the BEAM VISAT (4.8.1) software provided by Brockmann Consult/ESA, in order to perform an irradiance correction for all bands. Later, the images were processed using four different plug-in optical processors of the BEAM VISAT (4.8.1) software in order to retrieve the water quality parameters chl *a*, CDOM and TSM. Three of the available processors were developed by the German Institute for Coastal Research GKSS (Doerffer and Schiller, 2008a; Doerffer and Schiller, 2008b): Case 2 Regional processor (C2R, 1.4.1 version), Eutrophic Lakes processor (Eutrophic, 1.4.1 version) and Boreal Lakes processor (Boreal, 1.4.1 version). In these processors, atmospheric correction is performed using 12 bands without extrapolation and the reflectance values are converted into water quality information with different neural networks (NN) (Koponen et al., 2008; Doerffer and Schiller, 2008a). These NNs were calibrated with simulations performed with bio-optical models and using specific inherent optical properties (IOPs) of different water types (Table 2): coastal waters (C2R), waters with high phytoplankton and chl *a* concentrations (Eutrophic) and boreal lakes typical of the boreal forest regions where the absorption by gelbstoff (CDOM) is high (Boreal). In particular, the C2R water processor presents a bio-optical model adapted to the variation in a wide range of the IOPs. In contrast, the Eutrophic and Boreal processors share the same architecture, but the bio-optical

models were optimised for extreme concentrations of chl *a* and CDOM respectively (more in Schroeder et al., 2007b).

Table 2. The ranges of concentrations used to parameterise the different processors (based on Koponen et al. (2008), Schroeder et al. (2007a)) and in the standard MERIS Level 2 products.

	C2R	Eutrophic	Boreal	FUB	MERIS Level 2
Chl <i>a</i> , mg/m ³	0.003-50	1-120	0.5-50	0.05-50	0.02-43
TSM, g/m ³	0.03-50	0.25-30	0.1-20	0.05-50	0.01-51
CDOM, 1/m	0.002-2	0.1-3	0.25-10	0.005-1	0.005-5

The fourth processor was developed by the German Institute for Coastal Research (GKSS) and Brockmann Consult and Freie Universität Berlin (FUB, 1.2.4 version). FUB is designed for European coastal waters and uses MERIS Level 1b Top-Of-Atmosphere radiances to retrieve the concentration of the optical water constituents (Schroeder et al., 2007a). For all processors the default conversion factors of water quality parameters were used (Doerffer and Schiller, 2008a).

Finally, standard MERIS Level 2 products for the validation analysis were also obtained. The NN uses all visible bands (except the band at 681 nm). The outputs of the processing were the scattering coefficient (*b*), absorption by pigments (*a_{pig}*) and absorption by CDOM and detritus (*a_{CDOM}*). Concentrations of chl *a*, TSM and CDOM were calculated from the scattering and absorption coefficients according to empirical relationships (Doerffer, 2006; ESA, 2006). In this study the “*algal_2*” pigment index for the chl *a* were used, since it is appropriate for Case 2 coastal waters and waters rich in sediment particles and yellow substances (Doerffer and Schiller, 2000), “*total_susp*” for the TSM concentrations and “*yellow_subs*” for the CDOM concentrations.

All the above described processors are provided with quality flags (more about the flags in the MERIS product hand book (ESA, 2006)) which give an indication on the confidence of the quality of the retrieved parameter besides helping in the interpretation of the data. Therefore, the flagged pixels were inspected and discarded or used very carefully (ESA, 2006).

The standard MERIS Level 2 products, after application of the Case 2 waters atmospheric correction, contain the water leaving reflectance information and accompanying flags (Brockmann, 2006). The following flags have been removed from the analysis: cloud (CLOUD), Ice at high aerosol load pixel (ICE_HAZE), High uncorrected glint (HIGH_GLINT), Uncertain normalized surface reflectance (PCD_1_13), Uncertain normalized surface reflectance (PCD_16), Uncertain algal pigment index 2 or bottom of atmosphere vegetation index (PCD_17) and Uncertain aerosol type and optical thickness or cloud optical thickness (PCD_19). In case of FUB the flag (ATM_OUT) that identifies unrecognized reflectance data after atmospheric correction has been used for filtering. In C2R and Lake Processors pixels flagged as L2 are invalid if one of the seven flags are raised: Top Of Atmosphere Radiance out of valid range (RAD_ERR), land pixel (LAND), cloud or ice (CLOUD_ICE), Top Of Standard Atmosphere out of range (TOSA_OOR), water leaving radiance Out Of Training Range (OOTR), the air/water emulsion occurring at the top of ocean surface waves under high winds (WHITECAPS) and water leaving radiance reflectance Out Of Scope (WLR_OOR). The highlighted pixels were removed from the validation procedure.

Pixels within a cloud shadow may not be flagged due to limitation of atmosphere correction of a particular processor (Brockmann, 2006) and can probably result in less accurate estimation of water quality parameters. In respect to this the total albedo reflectance for each station was computed for each MERIS acquisition, since it shows the effect of clouds. This analysis revealed that in the image acquired on August 30, 2010, three stations were affected by the clouds shadow since the total values of albedo were ten times lower than for other stations. Consequently, these stations were discarded from further analysis.

Sun glint often occur in MERIS images when the sensor azimuth is high and solar zenith is low, and depends on local wind fields and slicks (Hochberg et al., 2003; Doerffer, 2008; Kutser et al., 2009). These conditions were found in our dataset for the acquisition on July

4, 2010. However, the analysis of the spectral signature of this image suggested that it was affected by cirrus clouds rather than sun glint (Pepe et al., 2005). Consequently, seven stations were removed from this date.

The MERIS validation dataset was built by extracting a window of size 3x3 pixels centered on the location of the *in situ* measurement in order to reduce the influence of geo-location errors (Patt, 2002; Bailey and Werdell, 2006). For each 3x3 window, the proportion of flagged (invalid data identified by the processor-specific flags) pixels was computed and if it was more than 50%, the site was discarded. For the remaining windows (with less than 50% of flagged pixels) the homogeneity of the valid pixels was tested according Bailey and Werdell (2006).

Differences of water quality parameters between satellite and *in situ* data were quantified using different statistical error metrics: the coefficient of determination (R^2), the mean absolute error (MAE) using Eq. 1 and the root mean square error (RMSE) using Eq. 2:

$$MAE = \frac{\sum_{i=1}^n |y_{sat} - x_{in_situ}|}{N} \tag{1}$$

$$RMSE = \sqrt{\frac{\sum_{i=1}^n (y_{sat} - x_{in_situ})^2}{N}} \tag{2}$$

where

x_{in_situ} is the field measurement, y_{sat} is the satellite estimation, N is the total number of observations.

MAE and RMSE measures residual errors, estimating a global difference between the observed (*in situ*) and predicted (satellite) values. RMSE gives higher weight to relatively large errors than to the low ones, whereas MAE weights equally all the differences.

Nonlinear regression analysis (generalized additive modeling) was used to find the set of environmental factors that may explain the differences between satellite-derived and *in situ* measured in-water constituent concentration. The tested independent variables: salinity, Secchi depth, distance from the coast, distance from the outlet of the lagoon and sampling time. Before the regression analysis the multicollinearity was tested among the independent variables (Zuur et al., 2007). The Secchi depth highly correlated (Pearson correlation coefficient $r > 0.7$) with the salinity and the distance from the outlet of the lagoon, and therefore were removed from the regression. Dependent variables were transformed (e.g. by square root or logarithm) in order to fit the normal distribution. The regression analysis was performed with the “mgcv” package for R, version 2.13.2. The residuals of the regression models were checked for adherence to the assumption of variance equality and normality by using scatterplots (residuals vs. the independent variables) and histograms (Zuur et al., 2007). Spatial autocorrelation of the residuals was checked by correlogram and semivariogram using the available functions in R, version 2.13.2 (spline.correlog() from the package “ncf” or variog4() from the package “GeoR”). The summary of used samples and MERIS images is given in Appendix 1, p. 125.

3.2. Analysis of the plume area

The analysis of the summer plume area was based on *in situ* data and satellite images. *In situ* data were collected along the east-west (EW) and south-north (SN) transects during five field surveys carried out in July, August and September in 2010 and in August in 2011 in the SE Baltic Sea coastal waters (Figure 8). Totally 43 surface samples were collected and analyzed following the methods described in Chapter 3.3.

Analysis of plume spatial distribution was based on MERIS FR for the period 2005–2011 after the processing, as it is described in the section 3.1. Totally 147 images for the summer period were analysed (Table 3).

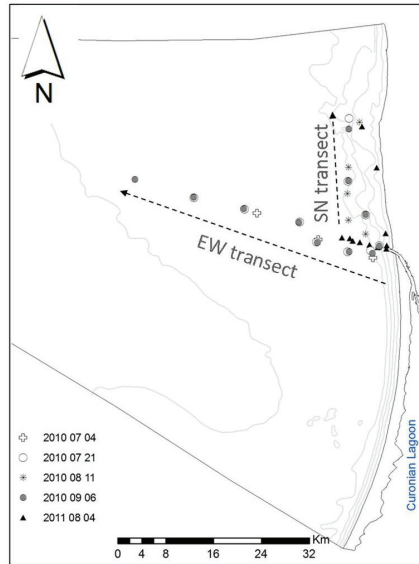


Figure 8. Study area and sampling locations during 5 surveys in summer 2010 and 2011. Each sampling month is indicated by different symbol.

The analysis of plume spatial distribution was performed using ArcGIS 9.3.1 software. The size of the plume was calculated using Patch Analyst (version 5.0.1.60) extension for ArcMap (Rempel et al., 2012). The direction of the distribution (N – north, NW – north-west, W – west, SW – south-west and S – south – expressed as the percentage from the total area) was analysed. The spreading direction was set taking into account the direction of maximal distribution.

Table 3. The number of analysed satellite images.

Month	Year						
	2005	2006	2007	2008	2009	2010	2011
June	6	7	4	6	2	6	6
July	7	5	4	6	6	9	4
August	4	4	3	2	5	8	9
September	2	7	5	3	5	6	6
TOTAL	19	23	16	17	18	29	25

3.3. Analysis of samples

Phytoplankton species composition, abundance and biomass. In the SE Baltic the surface phytoplankton samples were taken at 43 sites (Figure 8). All samples were preserved with acetic Lugol's solution. Treatment of the phytoplankton samples was done using the inverted microscope technique (Utermöhl, 1958). Samples were analysed using LEICA DMI 3000 inverted microscope at the magnification x200 and x400. Species were identified according Царенко, 1990; Komárek, Foot, 1983; Komárek, Anagnostidis, 1999; Kramer, Lange-Bertalot, 1886; 1988; 1991a; 1991b; Starmach, 1989, Hindák, 2001. The systematic of the microalgae represented in this work follows van den C. Hoek et al. (1995) and L. E. Graham, L. W. Wilcox (2000). The used systematic ranges and common names are given in Table 4. The Others contains the Chrysophyceae, Euglenophyceae classes and division Zoomastigophora that comprises very low part (<1%) of the total biomass.

Table 4. Systematic and common names of microalgae used in this work.

Division	Class	Abbreviation	Order	Common name
Cyanobacteria	Cyanophyceae	Cyano	Chroococcales Oscillatoriales Nostocales	cyanobacteria
Cryptophyta	Cryptophyceae	Crypto		cryptophytes
Dinophyta	Dinophyceae	Dino		dinoflagellates
Prymnesiophyta	Prymnesiophyceae	Prymnesio		prymnesiophytes
Ochrophyta	Chrysophyceae Bacillariophyceae	Chryso Bacillario		diatoms
Euglenophyta	Euglenophyceae	Eugleno		euglenophytes
Chlorophyta	Prasinophyceae	Prasino		prasinophytes
	Charophyceae Chlorophyceae	Charo Chloro		green algae
Zoomastigophora	Ebriidae Choanoflagellidea Incerta Sedis			

The phytoplankton abundance (thousand cells/l) was calculated using Eq. 3 (HELCOM, 1988).

$$Abundance = \frac{A \times 100}{N \times a_1 \times V} \quad (3)$$

where A – cross-section area of the top cylinder of the combined sedimentation chamber the usual inner diameter is 25.0 mm, giving $A = 491 \text{ mm}^2$ (the inner diameter of the bottom-plate being irrelevant); N – number of counted transects; a_1 – area of single field or transect; V – volume of sedimented aliquot;

The phytoplankton biomass (mg/l) was calculated by stereometrical formulae according methodology described in Olenina et al. (2006) using Eq. 4.

$$\text{Biomass} = \text{Abundance} \times \text{VCU} \times 10^{-9} \quad (4)$$

where VCU – volume of counting unit.

‘cf.’ is an abbreviation from a Latin word (confer) and means ‘refer to’ or ‘compare with’, it means that it could possibly be some certain species (cf. *Aphanizomenon flos-aquae*) or closely related, or similar. This abbreviation has no taxonomic status.

Optically active components. Water for chlorophyll *a* analysis was taken from the same samples as for biological and other analyses. Water samples for chlorophyll *a* measurement were filtered through 47 mm in diameter glass fiber GF/F filters. The volume of filtered water was 0.25-2l, depending on the chlorophyll *a* contents. Usually the analysis was carried out directly after filtration, otherwise filters were stored frozen at -80 °C no longer than 2 month. Later the filters were flooded with the 90% acetone and were kept for 24 hours in darkness in a fridge. The extract was centrifuged (~5000 rev/min, 20 min). The optical density (OD), i.e. absorbance spectra in the range 350–750 nm were collected using GENESYS 6 UV/VIS spectrophotometer in 1 cm path cuvette. Photosynthetic pigments were measured spectrophotometrically and estimated according to the trichromatic method as it is described in Eq. 5 (Jeffrey, Humphrey, 1975):

$$\text{Chla} = \frac{(11.85 \times OD_{663} - 1.54 \times OD_{647} - 0.08 \times OD_{630}) \times v}{l \times V} \quad (5)$$

where *Chl a* – chlorophyll *a* concentration, mg/m³; *OD* - optical density, i.e. absorbance at wavelength indicated by subscript, after correction by the blank and subtraction of the blank corrected absorbance at 750 nm; *v* - volume of acetone, ml; *l* - cell (cuvette) length, cm, *V* - volume of filtered water, l.

CDOM was measured spectrophotometrically after filtration through 47 mm diameter 0.22 µm membrane filters. Filtrate was kept in amber glass bottles and measured immediately after filtration. The absorption spectra in the range 350–750 nm were collected using GENESYS 6 UV/VIS spectrophotometer in 5 cm path cuvette. The CDOM absorption coefficient at 440 nm (*g*₄₄₀) was derived according to Kirk (2011) as follows:

$$g_{440} = \ln(10) \times (OD_{440} - OD_{750}) / l \quad (6)$$

where *OD* – optical density, i.e. absorbance at 440 nm and 750 nm, *l* – the path length of the cuvette in meters (in this case 0.05 m);

TSM was assessed gravimetrically using the method proposed by Strickland and Parson (1972) and following recommendations described in Doerffer (2002), Kratzer et al. (2003), Kratzer and Tett (2009). Water samples were filtered through pre-weighed 47 mm in diameter glass fiber GF/F filters. The volume of filtered water was 0.5-2 l, depending on the TSM contents. For the TSM measurement filters were dried at 110 °C overnight in an oven. A balance weighing Kern ABJ to 4 decimal places was used.

3.4. Measurement of environmental parameters

Water temperature and salinity at the surface during 2010 was measured using conductometer Cond 330i WTW, later in 2011 using multimeter Ysi Professional Plus. Water transparency was measured using standard 30 cm white Secchi disk.

Vertical distribution of water temperature and salinity was measured with the multiparametric CTD 90M probe. Vertical concentration of chlorophyll *a* of different microalgae groups was measured using fluorometer FluoroProbe II.

During all campaigns wind speed and direction, wave conditions, sampling time, site coordinates and other important observations were registered simultaneously to the water sampling.

3.5. Long-term data and satellite images

The long-term 1992–2007 salinity data from August were used. The data originated from the national monitoring program performed by Department of Marine Research, Environmental Protection Agency.

Satellite data was provided by Brockmann Consult/ESA in the frame of MarCOAST 2 project and via Principal Investigator proposal for ESA “Monitoring of water quality parameters using multi spatial and temporal MERIS FR data in the Lithuanian Baltic Sea coast – LitBaltSeaSAT” (ID 7835, IP D. Vaičiūtė).

3.6. Statistical analysis

Data were tested for normality and homogeneity of variances before analysis employing Kolmogorov-Smirnov and F’ tests respectively. In cases where these conditions were not met, transformations were applied (Sokal and Rohlf, 1995). The Spearman rank correlation (ρ) was used for determination of relationship between categorical variables, whereas linear regression was used for prediction of continuous variables. A t-test was applied to test for differences between the means of two independent groups. Means and standard deviations were used in the study to represent the estimated parameters and their variability.

Different phytoplankton communities in the plume and not plume area were derived by multidimensional scaling (MDS) analysis, the difference between the communities was tested by ANOSIM analysis using PRIMER 6 software.

4. RESULTS

4.1. Validation of satellite remote sensing technique

4.1.1. Validation of chlorophyll *a* concentration

The maximum *in situ* chlorophyll *a* concentration 156.18 mg/m³ was recorded in coastal waters in July during cyanobacteria bloom originated from the lagoon (Table 5). This concentration was comparable with maximum concentration predicted by FUB (116.18 mg/m³). Other processors gave extremely low maximum values of chl *a*. Minimum of chl *a* concentration measured *in situ* and by FUB were also in accordance. Minimum concentrations were overestimated about 4 times by lake processors (Eutrophic and Boreal) and marginally by C2R, whereas more than twice underestimated by MERIS Level 2.

Table 5. Descriptive statistics of water quality parameters (chlorophyll *a*, CDOM and TSM) estimated *in situ* and derived from MERIS satellite data by different processors: FUB, C2R, Eutrophic, Boreal and standard MERIS Level 2.

Parameter	Statistics	<i>In situ</i>	FUB	C2R	Eutrophic	Boreal	Level 2
Chl <i>a</i> , mg/m ³	minimum	0.69	0.59	0.98	2.87	2.10	0.26
	maximum	156.18	116.18	13.43	9.35	26.80	23.60
	mean	12.03	15.41	9.54	7.30	16.96	6.68
	standard deviation	20.75	25.66	2.66	1.47	5.56	6.75
	median	4.57	2.56	10.41	7.66	17.68	4.51
CDOM, 1/m	minimum	0.01	0.06	0.03	0.10	0.25	0.03
	maximum	2.01	1.79	0.90	0.99	1.11	0.55
	mean	0.42	0.34	0.19	0.32	0.37	0.15
	standard deviation	0.40	0.37	0.21	0.18	0.17	0.14
	median	0.33	0.17	0.09	0.27	0.29	0.09
TSM, g/m ³	minimum	1.05	0.24	0.22	0.44	0.21	0.36
	maximum	32.00	27.05	7.44	9.53	5.28	7.91
	mean	6.01	2.41	2.32	2.95	1.73	2.13
	standard deviation	4.61	4.04	1.89	2.49	1.33	1.80
	median	4.40	0.96	1.54	1.80	1.07	1.56

Mean and median of chl *a* concentration derived by FUB and Boreal were closest to the measurements *in situ*, although there was relatively high variance in the data (standard deviation was twice the mean for *in situ* and FUB). Mean and median of chl *a* concentration derived by C2R, Eutrophic and MERIS Level 2 were markedly underestimated.

The best fit of relationship ($R^2=0.87$, MAE=2.49 mg/m³) between chl *a* measured *in situ* and derived by algorithm was found for standard Level 2 (Figure 9). On the other hand, more than 60% of data was discarded from the analysis due to flagged pixels, especially with high (>25 mg/m³) concentrations of chl *a*. Relatively good fit of relationship was determined for FUB algorithm ($R^2=0.69$, MAE=7.76 mg/m³), where only 10% of data was removed due to flagged pixels. *In situ* concentrations from 15 to 50 mg/m³ were slightly overestimated.

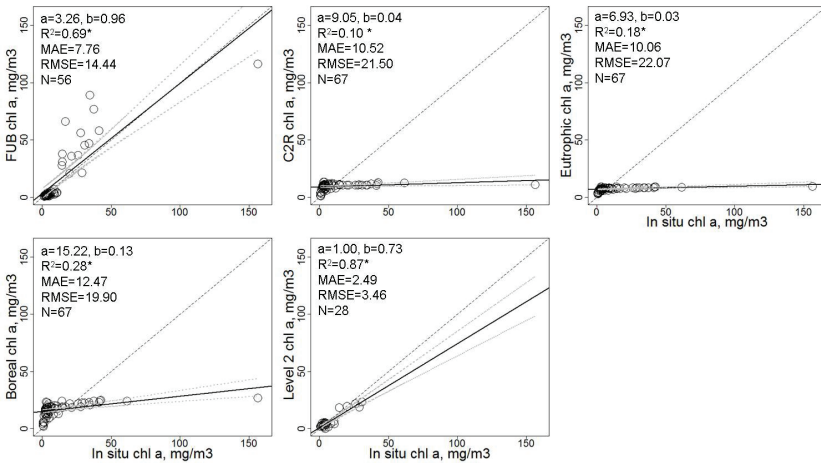


Figure 9. Relationships between *in situ* measured and satellite derived chl *a* by different algorithms. Black dashed line shows ideal fit 1:1, black solid line – linear trend line, grey dashed line – 95% confidence level. Statistically significant relationships are indicated in asterisks.

C2R and lake processors (Eutrophic and Boreal) explained relatively small amount ($R^2=10-30\%$) of variation in the data and

produced relatively high MAE (10–12 mg/m³). Moreover, the satellite derived estimates could not predict more than 10 mg/m³ of chl *a* concentration showing the acceptable agreement only for lower values of chl *a* (Figure 9).

Absolute differences between *in situ* chl *a* measurements and satellite estimates were mainly explained by the Secchi depth (Table 6).

Table 6. Relative importance (F value) of explanatory variables for the validation results of water quality parameters (chl *a*, CDOM and TSM) among the processors (FUB, C2R, Eutrophic, Boreal and standard Level 2), and explained deviance by the explanatory variables. Statistically significant effects indicated in bold.

F-values		FUB	C2R	Eutrophic	Boreal	Level 2	
Chl <i>a</i>	Transformation	sqrt	sqrt	sqrt	sqrt	log	
	N	56	67	67	67	28	
	<u>Explanatory variables:</u>						
	<i>Secchi depth</i>	7.51	22.39	22.30	19.35	0.62	
	<i>Sampling_time</i>	0	0	0	0	1.87	
	<i>Dist_from_coast</i>	0	0	0	0	0	
Deviance explained,%		37	59	59	55	26	
CDOM	Transformation	sqrt	sqrt	sqrt	sqrt	sqrt	
	N	56	67	67	67	28	
	<u>Explanatory variables:</u>						
	<i>Secchi depth</i>	0.86	12.28	14.34	17.50	31.28	
	<i>Sampling_time</i>	0	1.87	0.04	0.28	1.34	
	<i>Dist_from_coast</i>	0	0	0	0	0	
Deviance explained,%		15	47	46	51	86	
TSM	Transformation	log	log	sqrt	log	log	
	N	56	67	67	67	28	
	<u>Explanatory variables:</u>						
	<i>Secchi depth</i>	3.14	13.99	20.18	17.30	2.85	
	<i>Sampling_time</i>	0	0	0.64	0	0	
	<i>Dist_from_coast</i>	0	0	0	0	0	
Deviance explained,%		7	49	59	53	13	

The FUB processor overestimated *in situ* measured chl *a* concentrations at a Secchi depth below 3 m, while at a Secchi depth greater than 3 m the estimates of the FUB processor were in relatively good agreement with *in situ* measurements (Figure 10). The effect of Secchi depth for the absolute differences between the FUB derived and *in situ* measured chl *a* concentrations explained 37% of deviance.

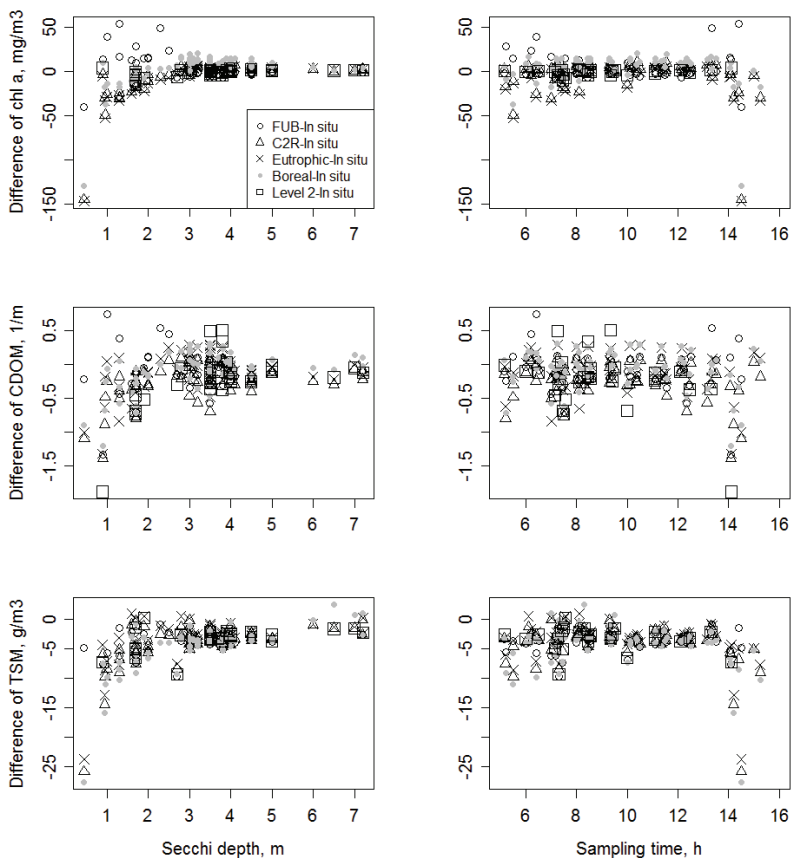


Figure 10. Scatterplots of differences, between the water quality parameters (chl *a*, CDOM and TSM) derived by the algorithms (FUB, C2R, Eutrophic, Boreal and standard Level 2) and measured *in situ*, Secchi depth and sampling time in GMT.

More than half of explained deviances (55–59%) by the effect of Secchi depth were found for the C2R, Eutrophic and Boreal (Table 6). The processors strongly underestimated chl *a* concentrations at a Secchi depth below 2.5 m. At a Secchi depth above 3 m the C2R, Eutrophic and Boreal slightly overestimated *in situ* measurements (Figure 10). Relatively weak effect of Secchi depth for the difference between *in situ* chl *a* measurements and satellite estimates (26% explained deviance) was found for the standard Level 2 (Table 6).

The effect of the sampling time was found only for the standard Level 2 processor, although it was not statistically significant (Table 6). However, the difference between *in situ* and satellite derived estimates by all processors were relatively high 3 hours before and 4 hours after the satellite overpass (Figure 10), that occurred over the investigation area approximately at 9:00–9:50.

4.1.2. Validation of dissolved coloured organic matter (CDOM) absorption

The maximum coloured organic matter CDOM absorption *in situ* closely agreed only with prediction by FUB, whereas the other algorithms underestimated by approximately two times. The minimum CDOM absorption *in situ* was relatively similar to derived minimum estimates by C2R and Level 2, and marginally by FUB, whereas minimum CDOM absorption by Eutrophic and Boreal was strongly overestimated. Mean and median of CDOM absorption derived by Boreal were the closest to the measurements *in situ*, and predictions by FUB and Eutrophic as well (Table 5). Mean and median of CDOM absorption derived by C2R, and MERIS Level 2 were markedly underestimated.

The best fit of relationship ($R^2=0.69$, MAE=0.20 1/m) between CDOM measured *in situ* and derived by algorithm was found for Boreal (Figure 11), although processor underestimated maximum and overestimated minimum absorption.

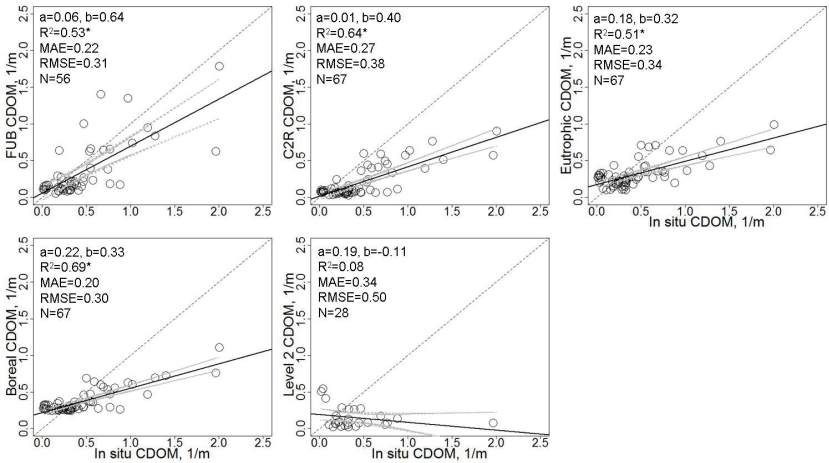


Figure 11. Relationships between *in situ* measured and satellite derived CDOM by the different processors. Black dashed line shows ideal fit 1:1, black solid line – linear trend line, grey dashed line – 95% confidence level. Statistically significant relationships are indicated in asterisks.

Similar trends were observed with FUB, C2R and Eutrophic processors, which explained more than 50% of variation and produced relatively low MAE 0.22–0.27 1/m. CDOM absorption derived by C2R and Eutrophic could not predict absorption more than 1 1/m showing the acceptable agreement only for lower absorption, whereas estimates by FUB showed agreement high absorption, although with high variance. CDOM absorption values derived by standard Level 2 did not correspond to *in situ* measurements.

Absolute differences between *in situ* CDOM measurements and satellite estimates were mainly explained by the Secchi depth, followed by the sampling time, except for the FUB (Table 6). The values of explained deviance varied from 15% for the FUB to 86% for the standard Level 2 processor. The differences of all processors with *in situ* CDOM measurements highly varied at a Secchi depth lower than 4.5 m (Figure 10), whereas the CDOM estimates of processors were comparable with *in situ* CDOM measurements at a Secchi depth

greater than 4.5 m. The C2R and the standard Level 2 strongly underestimated CDOM absorptions at a Secchi depth below 2 m.

The effect of sampling time showed the similar pattern as in the case of chl *a* (Figure 10), where the differences between *in situ* CDOM measurements and satellite estimates were high at 2 hours before and after the satellite overpass. However, the differences between *in situ* CDOM measurements and the standard Level 2 estimates were relatively high even during the time of satellite overpass.

4.1.3. Validation of total suspended matter TSM concentration

The *in situ* TSM varied from 1.05 to 32 g/m³ with the highest values measured the 21st of July and 11th of August 2010 in the plume area of the lagoon (Table 5). The minimum TSM concentration derived by all processors was underestimated compared to *in situ* measurements. The maximum TSM concentration predicted by FUB was the only close to *in situ*, whereas the other algorithms strongly (from 3 to 6 times) underestimated. Mean and median of TSM concentrations derived by all processors were underestimated (from 2 to 3 times) compared to *in situ* measurements, where Eutrophic being the closest to the *in situ* values.

The best fit of relationship ($R^2=0.87$, MAE=3.93 g/m³) between TSM measured *in situ* and derived by algorithm was found for FUB (Figure 12), although this algorithm underestimated *in situ* measurements. Match of TSM estimated by C2R, Eutrophic and standard Level 2 algorithms and *in situ* measurements was relatively good (explained more than 50% of variation and produced relatively low MAE=3.29–4.05 g/m³). However, the derived TSM concentrations by these processors could not predict more than 10 g/m³ showing the acceptable agreement only for lower concentrations. Boreal algorithm had the worst fit ($R^2=0.37$ and MAE=4.76 g/m³) and strongly underestimated TSM above 5 g/m³.

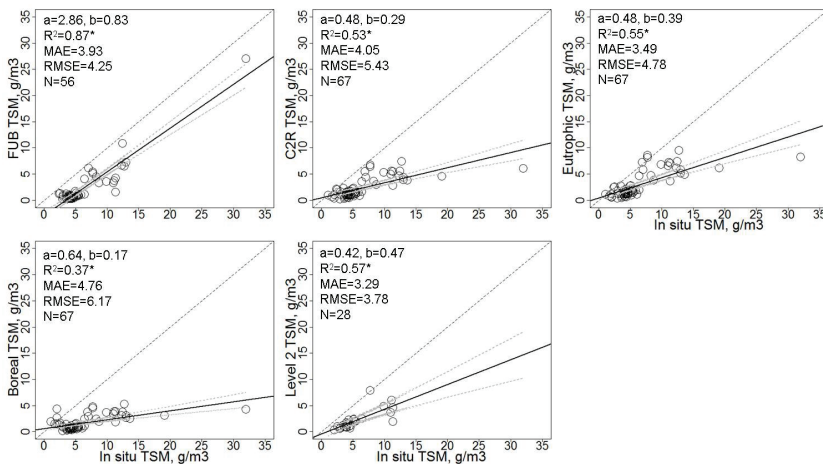


Figure 12. Relationships between *in situ* measured and satellite derived TSM by the different processors. Black dashed line shows ideal fit 1:1, black solid line – linear trend line, grey dashed line – 95% confidence level. Statistically significant relationships are indicated in asterisks.

Absolute differences between *in situ* TSM measurements and satellite estimates were mainly explained by the Secchi depth (Table 6). The values of explained deviance varied from 7% for the FUB to 59% for the Eutrophic processor. Secchi depth had a relatively small effect for the differences between *in situ* TSM measurements and derived by the FUB and the standard Level 2 processor. Overall, all tested processors underestimated the concentration of TSM: the greater difference were observed at a Secchi depth lower than 3 m, while at a Secchi depth above 3 m the differences were relatively smaller.

The effect of sampling time on the differences between *in situ* TSM measurements and satellite estimates was found only for the Eutrophic processor, although it was not a statistically significant (Table 6). However, the differences by all processors were relatively high 3 hour before and 4 hour after the satellite overpass (Figure 10).

As an example of chl a, CDOM and TSM distribution over the study area retrieved by MERIS imagery acquired during one

validation survey in 21st of July in 2010 is given in Figure 13. The highest values of all optical components were recorded close to the outlet of the lagoon.

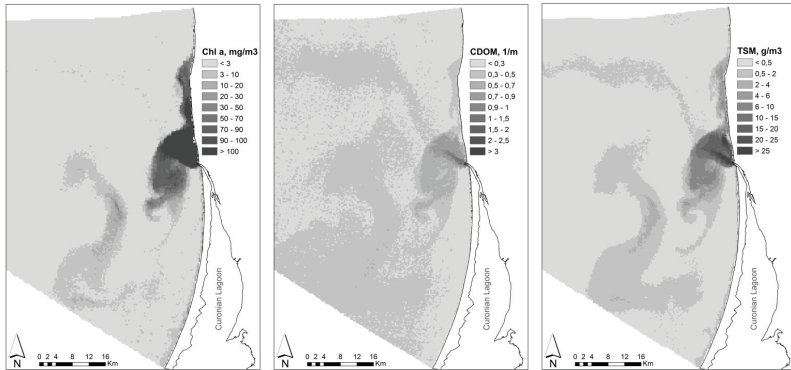


Figure 13. Chlorophyll *a* (left), CDOM (middle) and TSM (right) maps after application of different processors for MERIS images: FUB for chlorophyll *a* and TSM and Boreal for CDOM during 21st of July 2010. Maps show the outflow of eutrophic fresh water from the Curonian lagoon into the SE Baltic Sea coastal waters.

Plume area could be divided into two major branches most probably due to hydrometeorological conditions: the first branch of plume directed towards south-west and meandering more than 20 km from the outlet of the Curonian lagoon; the second branch spread 30 km northwards from the outlet. The lens of water mass with concentrations of all optical components higher than surrounding water could be seen in the southern part 10–20 km off the coast. This lens most likely originated from the plume and meandered southwards due to hydrometeorological conditions. Plume area in all three satellite based maps indicated large enrichment of Baltic Sea coastal waters according to concentrations of all optically active components emphasizing the dynamic changes of waters trophic status and reduction of water quality level.

4.2. Delineation of the plume

4.2.1. Identification of the plume by salinity threshold

The changes of the long-term surface salinity were investigated during the summer period of 1992–2010 in five different areas of the Lithuanian Baltic Sea waters (see Figure 3, Management plan of Nemunas River basin region, 2010). Three areas are based on typological unites of WFD (open Baltic Sea stony coast, open Baltic Sea sandy coast, plume of the Curonian Lagoon in the Baltic Sea). Fourth area covers Territorial Sea (i.e. 12 nautical miles from the coast). The fifth area is located in the offshore (i.e. Exclusive Economic Zone). The mean salinity of waters of open Baltic Sea stony coast was 6.60 ± 0.42 PSU, $N=7$, in the waters of open Baltic Sea sandy coast was 6.86 ± 0.26 PSU, $N=34$, in the plume of the Curonian Lagoon – 5.96 ± 1.17 PSU, $N=61$, in the Territorial Sea – 6.70 ± 0.50 PSU, $N=174$ and in the offshore – 6.99 ± 0.18 PSU, $N=101$ (Figure 14).

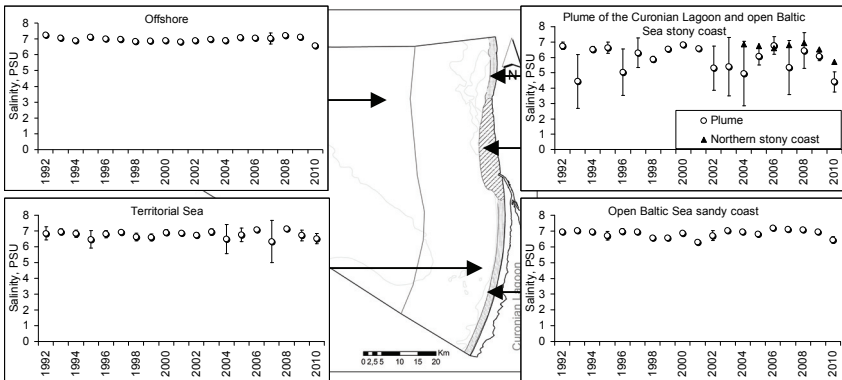


Figure 14. Long-term surface salinity (PSU) changes in five regions of the Lithuanian Baltic Sea waters in summer of 1992–2010.

The salinity threshold of the plume was derived from the selected monitoring stations. The stations in the waters of open Baltic Sea stony coast and sandy coast, plume of the Curonian Lagoon in the Baltic Sea were excluded due to the effects from land: other small rivers and drainage or precipitation (Leppäranta and Myrberg, 2009).

According to Wasmund et al. (2001) the influence of fresh water was indicated by the salinity value below the typical range of salinity in the open sea (6.8 PSU). Consequently, the monitoring stations with salinity values below this threshold were selected and the threshold for the delineation of the plume area was calculated as mean salinity minus standard deviation. Therefore, the plume area is considered where the salinity is lower than 6.20 PSU, whereas the waters with salinity equal or above this threshold correspond to offshore waters.

4.2.2. Delineation of the plume by the optically active components

The spatial observation of OAC and salinity along two transects in the summer period indicate the presence of strong relationship between the parameters (Figure 15). Strong negative correlation was found between salinity and chl *a* ($\rho=-0.87$, $N=43$, $p<0.05$), TSM ($\rho=-0.92$, $N=43$, $p<0.05$) and CDOM absorption ($\rho=-0.94$, $N=43$, $p<0.05$).

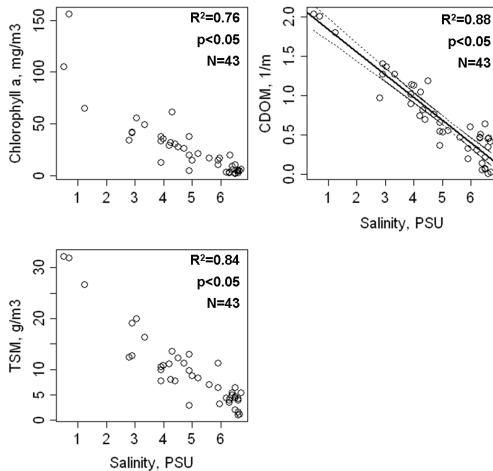


Figure 15. Relationships between *in situ* measured concentration of optically active components and salinity during the summer period of 2010 and 2011. Black solid line – regression line; dotted lines – 95% confidence intervals.

The later empirical relationship (i.e. the upper value of the 95% of confidence level) was the strongest and therefore was used to delineate the plume area. Using the salinity threshold value 6.20 PSU in the regression model (Eq. 7) the obtained CDOM value 0.408 1/m characterizes the thresholds between plume waters (>0.408) and not plume waters (≤ 0.408).

$$CDOM = -0.29 \times Salinity + 2.135 \quad (7)$$

4.2.3. Spatio-temporal variability of the plume

The number of satellite images was limited by the amount of cloudy days during the summer time of the year and the quality of the images. The number of images used for the analysis of the plume differed within study period from 16 in 2007 to 29 in 2010. In total 147 satellite images were processed by Boreal and using the CDOM threshold obtained in this study (see chapter 4.2.2) the plume was delineated. The spatial distribution and temporal variability of the plume was analyzed and results are described below.

In 2005 the size of the plume ranged from 14 up to 630 km². The largest plume was directed north-westwards from the Klaipeda Strait, and the majority of the plume cases (N=9) represented the same direction (Figure 16). Only three cases of the plume were recorded directed towards south-west, however the mean size of the plume was relatively large - 194±74 km². The smallest mean areas (31±23 km²) of the plumes were directed westwards. The plume extended to the north crossing over the national border of Lithuania, however with the frequency of occurrence up to 20% (Figure 17). The frequency of spread of the plume <15 km to the same direction was 50–70%. The maximum distance of the plume was determined at 45 km to the north-west direction from the lagoon with 10% frequency of occurrence. The frequency of spread of the plume <25 km to the same direction was 40%. The maximum westward spread of the plume was 20 km with the minimum 10% of frequency of occurrence. With the same frequency of occurrence the plume spread <30 km to the south and south-west. In general, the plume occurred 70–100% in all

directions approximately in the distance of 4–6 km from the lagoon, except to the south, where it was spread 1 km only.

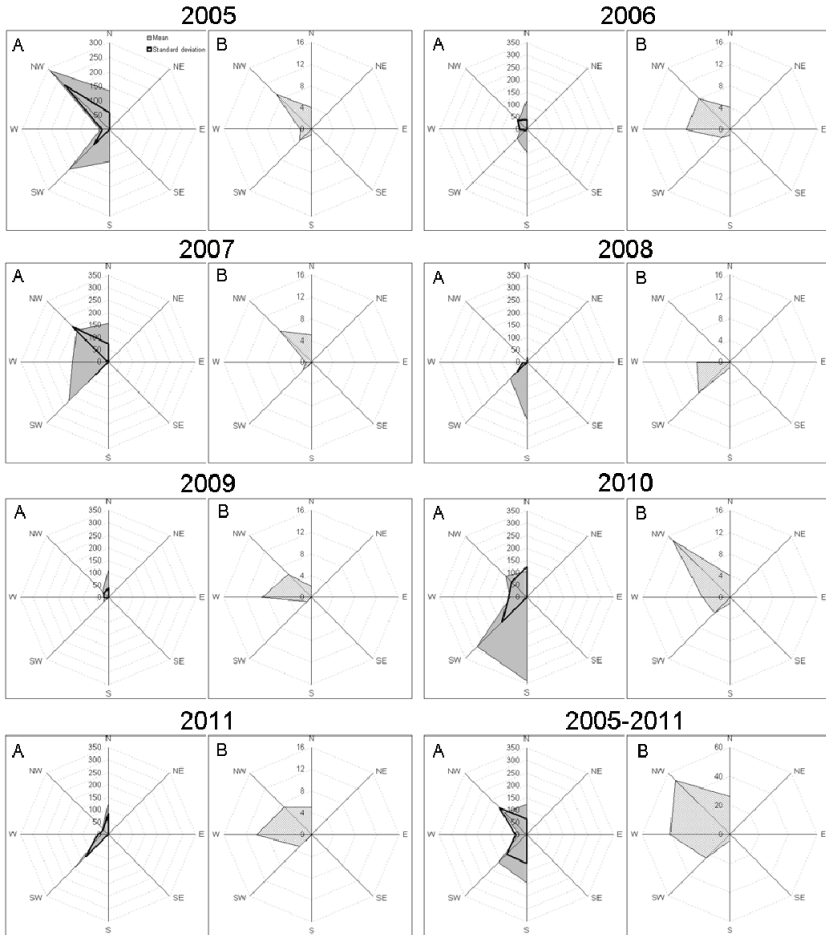


Figure 16. Mean and standard deviation of the plume size (km^2) (A) and its frequency at the given directions (B) during the intensive vegetation period of 2005–2011.

In 2006 the mean size of the plume was four times smaller than in 2005 and ranged from 0.7 up to 148 km^2 . The largest plume was

directed both northwards and southwards, however with different frequency of cases, i.e. four cases represented the northern direction, while only one – the southern direction (Figure 16). The smallest plumes were mainly directed to west and north-west. The plume area was spreading northwards and southwards in similar distances as in 2005, although with lower frequency of occurrence (Figure 17). However, in contrast to 2005, the plume did not occur much in the territorial sea and it spread only up to 10 km westward. The high frequency of occurrence (70–100%) of the plume was found in similar 4–6 km distance from the lagoon as it was in 2005.

In 2007 the size of plume ranged from 27 up to 570 km². The largest plume was directed north-westwards and with similar frequency as in 2005 (N=8) (Figure 16). Although only two cases represent south-west direction, the mean size of the plume was relatively large - 222±72 km². The spatial distribution of the plume was similar to that in 2005 (Figure 17). The plume spread mainly to the north and north-west approximately 45 km and to the west and south-west approximately 20 km. The high frequency of occurrence (70–100%) of the plume was found in similar 4–6 km distance from the lagoon as it was in 2005.

In 2008 the size of plume ranged from 1 up to 232 km². In contrary for the other years the largest plume was directed southwards, however only one case was observed (Figure 16). The majority of cases (N=8) with the mean size 91±53 km² represented the south-west direction. The smallest plumes were directed westwards with mean size of 12±16 km². The south-west spread of the plume was 40–50 km in distance from the lagoon with frequency of occurrence <20%, whereas the spread of the plume 10 km to the same direction occurred <40% (Figure 17). The spread of the plume was mainly to the south and south-west. The later was 40–50 km in distance from the lagoon with frequency of occurrence <20%, whereas the spread of the plume 10 km to the same direction occurred <40%. The high frequency of occurrence (70–100%) of the plume was <3 km from the lagoon.

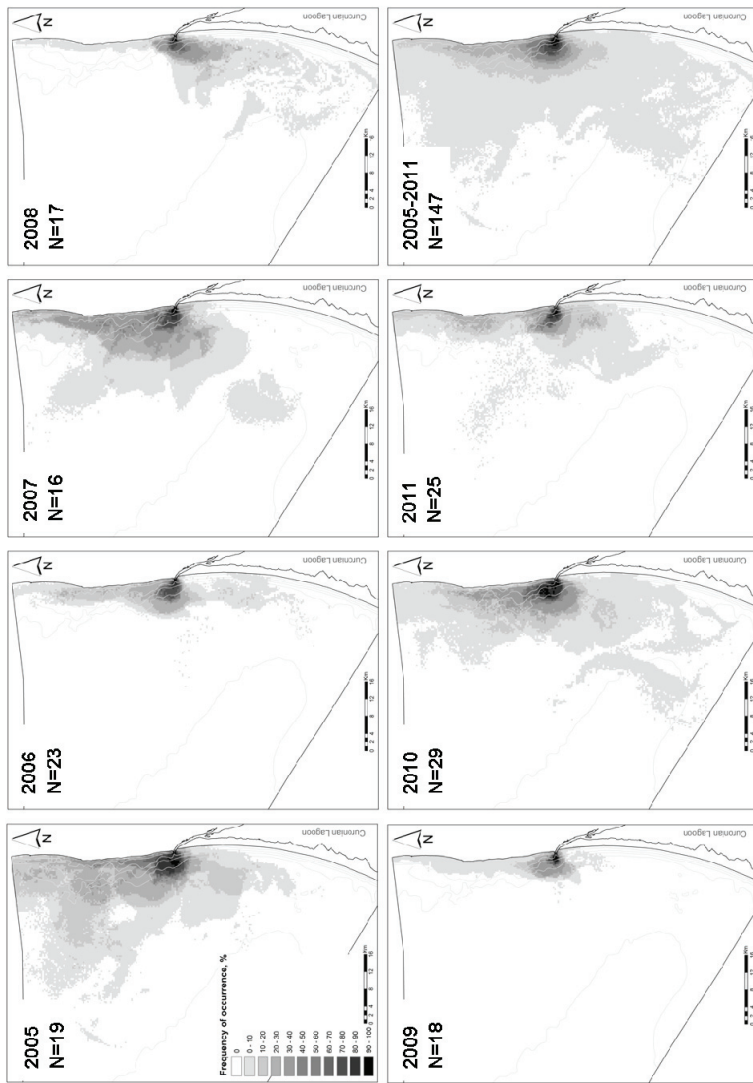


Figure 17. Spatial distribution and frequency (%) of the plume during the summer period of 2005-2011. N indicates the number of used satellite images.

In 2009 the size of plume ranged from 0.8 up to 138 km². The largest plume was directed northwards (Figure 16). The majority of the plume cases (N=9) with the smallest mean size (13±16 km²) represented the west direction. The distribution of the plume in 2009 was similar to the 2006, except that the spread of the plume was shorter southwards and frequency of occurrence was lower in 2009 than in 2006 (Figure 17).

In 2010 the size of plume ranged from 0.7 up to 378 km². The largest plume was directed south-westwards (Figure 16). Although only one case represents south direction, the size of the plume was relatively large (338 km²). The majority of the plume cases (N=15) were directed the north-westwards, however with the relatively small mean size (67±72 km²). In 2010 the plume occupied the whole area of the territorial sea and even exceeded the border: <40 km northwards, <40 km southwards and <20 km westwards (Figure 17).

In 2011 the size of plume ranged from 0.3 up to 300 km². Although only three cases represented south-western direction (Figure 16), the mean size of the plumes was relatively large (189±125 km²). The majority of the plume cases were spread to western (N=10) and north-western directions with relatively small mean size of the plumes (30±40 km² and 31±25 km² respectively). The northward spread of the plume exceeded the Lithuania-Latvia border, whereas to the south the plume extended <20 km only (Figure 17).

In summary, during the whole period (2005–2011) the size of plume ranged from 0.3 up to 630 km². The most frequent direction of the spread was north-westwards (N=53, 36%) with the mean size of 124±153 km² (Figure 16). Although 28% of the plume cases represent western direction, relatively small in size plumes predominated (30±41 km²). Surprisingly, 16% of the plume cases represented south-western and only 3% – southern directions, however largest plumes predominated with the mean size 156±112 km² and 193±115 km² respectively. The averaged map of the plume for the whole period showed, that the Territorial Sea of the Lithuanian Baltic Sea was affected by the outflow of the lagoon waters with frequency of

occurrence <10% (Figure 17). The highest frequency of occurrence of the plume (70-100%, N=143) was observed 10 km northwards, 6 km westwards and 4 km southwards.

4.3. The role of the plume for spatial variability of the optical water properties and phytoplankton

4.3.1. Optical water properties

The concentration of all optically active components measured *in situ* clearly differed between the delineated plume area and brackish coastal waters (Figure 18). Chl *a* concentration in the plume area ranged from 4.70 to 156.18 mg/m³, where the mean concentration was 38.35±31.47 mg/m³. Outside the plume area the chl *a* concentration was lower and ranged from 2.23 to 20.16 mg/m³, and the mean concentration was 5.70±4.51 mg/m³. There was statistically significant difference (t=5.30, df=27.78, p<0.05) between the chl *a* concentration estimated in the plume area and outside.

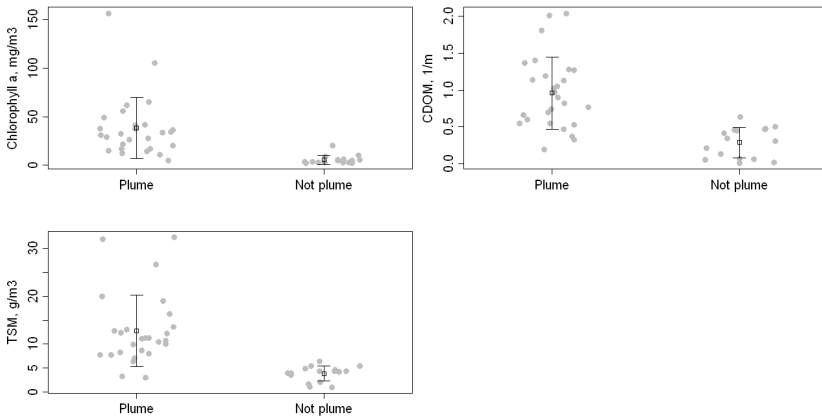


Figure 18. Concentration of optically active components in the plume and not-plume areas during the summer period of 2010 and 2011.

In situ CDOM absorption in the plume area ranged from 0.19 to 2.04 1/m, the mean absorption was 0.96±0.49 1/m (Figure 18). Outside the plume area the absorption was lower and ranged from

0.01 to 0.64 1/m, and the mean absorption was 0.29 ± 0.21 1/m. There was statistically significant difference ($t=6.25$, $df=38.12$, $p<0.001$) between the CDOM absorption estimated in the plume area and outside.

In situ TSM concentration in the plume area ranged from 2.94 to 32.33 g/m^3 , where the mean concentration was $12.79 \pm 7.48 \text{ g/m}^3$ (Figure 18). Outside the plume area the concentration was lower and ranged from 1.00 to 6.40 g/m^3 , with the mean of $3.84 \pm 1.59 \text{ g/m}^3$. There was statistically significant difference ($t=5.99$, $df=29.82$, $p<0.05$) between the TSM concentration estimated in the plume area and outside.

4.3.2. Phytoplankton biomass and community structure

Totally 228 taxa were identified at genera and species levels, which belong to 13 classes and groups: 10 classes of microalgae and 3 groups of the division Zoomastigophora: class Choanoflagellidea, class Ebriidea and group Incertae Sedis. The latter contained microorganisms with unknown or undefined relationships. The division Zoomastigophora contained mainly heterotrophic microorganisms.

The majority 68 (30%) of taxa belonged to Cyanophyceae and 58 (25%) Chlorophyceae, whereas 45 (20%) taxa were identified as Bacillariophyceae and 20 (9%) as Dinophyceae. The other classes comprised the small part of the total amount of the taxa: 11 (5%) were identified as Charophyceae, 8 (4%) – Prasinophyceae, 7 (3%) – Cryptophyceae, 4 (2%) – Incerta Sedis, 2 (1%) – Prymnesiophyceae and Chrysophyceae, and 1 (0.4%) – Euglenophyceae, Choanoflagellidea and Ebriidea.

In total 215 (94%) taxa were found in the samples from the plume area, whereas 133 (58%) taxa were found in the samples outside the plume. However, the taxa composition was the same in both areas, in the Plume and outside, and belonged to all classes and groups mentioned above.

Total phytoplankton biomass obtained in the plume area ranges from 3.88 to 43.58 mg/l, mean biomass was 17.13 ± 10.26 mg/l, and was significantly different and more than eight times higher than that outside the plume waters (Table 7, Figure 19). Outside the plume the biomass ranges from 0.27 to 7.98 mg/l, mean biomass was 2.32 ± 1.82 mg/l. More than 50% of total phytoplankton biomass was comprised by cyanobacteria in both the plume area and outside. However, the phytoplankton community was more divers outside the plume area. In the plume the second dominating groupe was diatoms and comprised approximately 30% of total phytoplankton biomass, following by green algae (15% of total phytoplankton biomass) that belong for two classes: Chlorophyceae and Charophyceae.

Table 7. Results of statistical comparison (Welch t-test) of two mean biomasses (mean±standard deviation, mg/l) of total phytoplankton and its different taxonomical groups in the plume (Plume) and outside the plume (Not plume) areas. Statistically significant differences are indicated with asterisks.

	Plume	Not plume	t value	Degree of freedom
Phytoplankton	17.13±10.26	2.32±1.82	7.31	28.68*
Cyanophyceae	9.34±5.87	1.32±1.63	6.68	32.23*
Dinophyceae	0.21±0.29	0.54±0.56	-2.21	19.94*
Bacillariophyceae	5.02±4.65	0.14±0.15	5.44	26.09*
Prasinophyceae	0.11±0.12	0.09±0.06	0.73	39.23
Prymnesiophyceae	0.05±0.05	0.08±0.07	-1.07	24.38
Charophyceae	0.51±0.84	0.003±0.01	3.13	26.01*
Chlorophyceae	1.74±1.80	0.07±0.08	4.81	26.16*
Cryptophyceae	0.11±0.12	0.06±0.06	1.86	38.91
Others	0.04±0.06	0.03±0.03	0.95	39.12

Outside the plume area the second dominating group was dinoflagellates, creating approximately 25% of total biomass (Table 7, Figure 19). Cryptophytes, prymnesiophytes, diatoms, pasinophytes and green algae each comprised approximately 5–10% of total biomass. However, the mean biomass of small cryptophytes was higher in the plume waters compared to the waters outside the plume, although the difference was not statistically significant.

On the other hand, the mean biomass of Dinophyceae was lower in the plume waters than outside the plume area, although, the high variation of the biomass was in both areas (Figure 19, Table 7). The mean biomass of microalgae that belongs to Prymnesiophyceae class and together prasinophytes, euglenophytes and small phototrophic and mixotrophic flagellates did not show statistically significant difference between both areas.

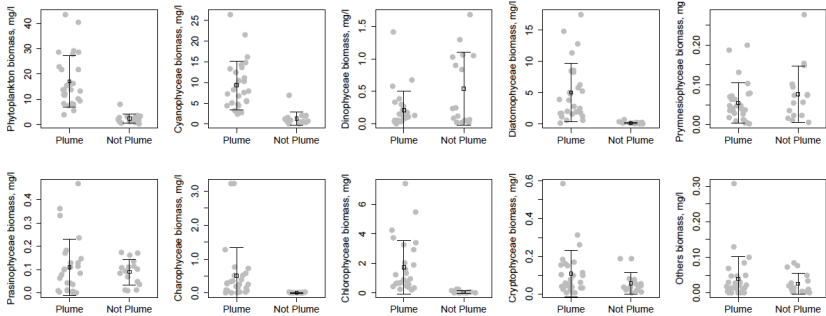


Figure 19. Mean and dispersion of total phytoplankton biomass and different phytoplankton taxonomical groups biomass in the Plume and outside the Plume (Not plume) areas during the summer period. Open square indicates mean and error bars - standard deviation of the data.

The changes of phytoplankton and its main groups were investigated along the salinity gradient in the plume area. The constant decreased along the salinity gradient was found. The highest biomass (31.7 ± 10.7 mg/l) was observed where salinity was < 2 PSU, i.e. close to the lagoon entrance, whereas the lowest phytoplankton biomass (2.3 ± 1.8 mg/l) was found outside the plume area (Figure 20). About 50% of total phytoplankton biomass was comprised by cyanobacteria. Diatoms comprised from 20 to 40% of total phytoplankton biomass at salinity < 5 PSU, whereas the biomass sharply decreased with more saline waters. The similar pattern was found for the green algae, although the biomass contribution to the total phytoplankton biomass was twice lower than that of diatoms. In contrary, dinoflagellates being minority at salinity < 5 PSU, comprised more than 5% of total phytoplankton biomass within the salinity 5–6 PSU and approximately

30% at salinity ≥ 6.2 PSU. Moreover, it is obvious that in waters with salinity >5 PSU phytoplankton communities started to be much heterogeneous (comprised of more microalgae classes) than those, where salinity was <5 PSU (Figure 20). The investigation confirms that the frontal, i.e. transitional zone can of phytoplankton changes can vary in the certain range of salinity.

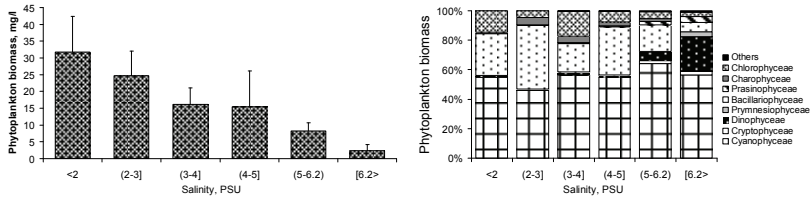


Figure 20. Distribution of total phytoplankton biomass (left) and relative contribution (%) of different phytoplankton classes in the total biomass (right) in the plume area and outside during the summer period in 2010–2011.

The different orders of cyanobacteria: Chroococcales, Oscillatoriales and Nostocales, showed the evident changes of the biomass in the plume area and outside (Figure 21). The highest mean biomass was for Nostocales order ranging from 6.51 ± 5.16 mg/l in the plume to 0.65 ± 0.70 mg/l outside the plume, where salinity was ≥ 6.2 PSU. The changes along the salinity gradient in the plume area show that the highest mean biomass was for Nostocales order ranging from 12.20 ± 10.82 mg/l at salinity <2 PSU. The maximal biomass estimated in the stations with highly reduced salinity gradually decreased to 4.25 ± 1.83 mg/l while salinity increased up to 4 PSU. At the salinity <5 PSU showed evident increase by factor two. The biomass of Nostocales decreased and riched the minimum value at the statios outside the plume.

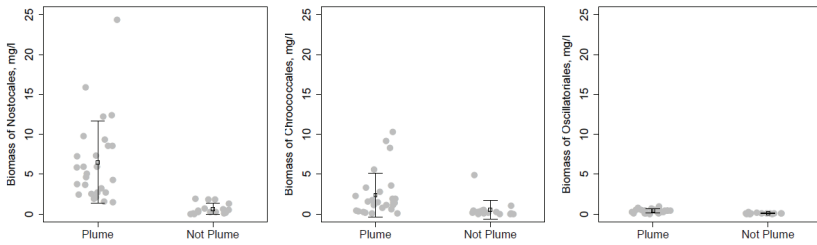


Figure 21. Mean biomass and its dispersion of different orders of cyanobacteria in the plume and outside the plume (Not plume) areas during the summer period. Open square indicates mean and error bars - standard deviation of the data.

The mean biomass of order Chroococcales ranged from 2.40 ± 2.77 mg/l in the plume to 0.56 ± 1.18 mg/l outside the plume. The changes along the salinity gradient in the plume area show that at the salinity up to 3 PSU the biomass decreased approximately by factor 3. From the salinity 4–5 PSU the biomass of Chroococcales decreased gradually and reached the minimum at the stations outside the plume area, however, comprising 25% of mean total biomass, i.e. the same part as Nostocales.

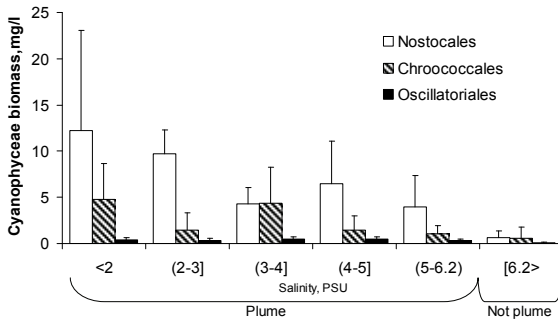


Figure 22. Biomass of different orders of class Cyanophyceae along the salinity gradient during the summer period in 2010–2011.

The mean biomass of Oscillatoriales was relatively low and comprised small part of the mean total biomass (1.25–4.46%). The mean biomass in the plume area was 0.43 ± 0.24 mg/l, while outside

the plume the mean biomass was 0.10 ± 0.06 mg/l. The changes along the salinity gradient in the plume area show that the salinity < 3 PSU the biomass was marginally lower ranging from 0.40 ± 0.22 mg/l at the salinity lower than 2 PSU to 0.31 ± 0.22 mg/l at the salinity > 3 PSU. The gradual decrease of the biomass (up to 0.10 ± 0.06 mg/l) was observed at the stations outside the plume. However, the contribution to the mean total biomass increased while salinity increased: at salinity < 2 PSU the relative biomass of Oscillatoriales was 1.25% from the mean total biomass, while at salinity > 6.2 PSU the relative biomass was 4.46%.

Statistically significant difference (ANOSIM, Global R=0.76, $p=0.001$, N=43) was found between the phytoplankton communities in the plume area with reduced salinity and outside the plume area, where salinity was typical for the Baltic Proper. Two distinct groups of stations with different phytoplankton communities can be evidently seen in the multi-dimensional scaling plot (Figure 23).

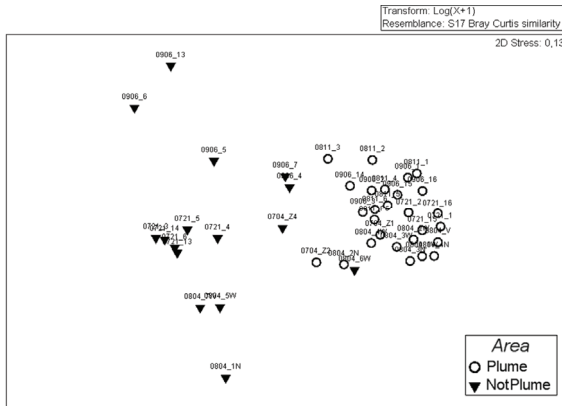


Figure 23. Multi-dimensional scaling plot of phytoplankton communities based on their biomass (log transformed) in the plume waters (Plume) and outside the plume waters (NotPlume).

However, there is no clear boundary between them as phytoplankton structure and biomass gradually changes with salinity. Thus, several samples from the plume waters (0704_Z2, 0804_2N and

0811_3) were rather close to the samples from the other group, whereas several samples (0704_Z4, 0906_4, 0906_7 and 0804_6W) from the outside plume area were close to the stations from the plume waters. The salinity within both groups of stations ranged from 6.3 to 6.5 PSU, and therefore all these samples could be characterized as transitional between the two investigated surroundings.

The set of phytoplankton species, which describes the phytoplankton community within the plume and outside the plume areas were defined (Table 8).

Table 8. Results of statistical comparison (Welch t-test) of two mean biomasses (mean±standard deviation, mg/l) of important phytoplankton species in the plume (Plume) and outside the plume (Not plume) areas. Statistically significant differences are indicated with asterisks.

Class	Species	Plume	Not plume	t value	Degree of freedom
Cyano	<i>Aphanizomenon flos-aquae</i>	5.88±5.15	0.58±0.67	5.28	27.48*
Diatomo	<i>Actinocyclus spp.</i>	2.86±3.74	0.06±0.13	3.89	26.10*
Diatomo	<i>Aulacoseira islandica</i>	1.28±3.36	0.0004±0.001	1.97	26.00
Chloro	<i>Pediastrum boryanum</i>	0.71±1.12	0.002±0.004	3.31	26.00*
Cyano	<i>Microcystis wesenbergii</i>	0.64±1.71	0.08±0.33	1.63	29.17
Charo	<i>Mougeotia sp.</i>	0.42±0.82	0.001±0.01	2.62	26.00*
Dino	<i>Scrippsiella spp.</i>	0.01±0.04	0.35±0.50	-2.71	15.10*
Cyano	<i>Planktothrix agardhii</i>	0.24±0.16	0.002±0.004	7.63	26.06*
Cyano	<i>cf. Woronichinia compacta</i>	0.33±0.49	0.02±0.03	3.27	26.42*
Cyano	<i>Microcystis aeruginosa</i>	0.28±0.59	0.20±0.77	0.39	25.35
Cyano	<i>Anabaena spp.</i>	0.22±0.24	0.02±0.03	4.27	27.59*
Cyano	<i>Microcystis viridis</i>	0.40±1.05	0.01±0.05	1.92	26.20
Cyano	<i>Coelosphaerium kuetzingianum</i>	0.26±0.44	0	3.04	26.00*
Chloro	<i>Pediastrum duplex</i>	0.25±0.46	0.004±0.01	2.75	26.03*
Cyano	<i>Anabaena spiroides</i>	0.16±0.32	0.01±0.01	2.38	26.15*
Chloro	<i>Desmodesmus communis</i>	0.15±0.14	0.01±0.02	4.87	27.74*
Chloro	<i>Dictyosphaerium spp.</i>	0.14±0.18	0.01±0.02	3.46	27.07*
Diatomo	<i>Thalassiosira spp.</i>	0.13±0.34	0	1.94	26.00
Diatomo	<i>Stephanodiscus rotula</i>	0.10±0.17	0.005±0.02	2.84	27.11*
Prasino	<i>Pyramimonas spp.</i>	0.09±0.11	0.07±0.05	0.65	37.69
Cyano	<i>Cyanonephron sp.</i>	0.01±0.01	0.09±0.14	-2.38	15.07*
Dino	<i>Gymnodinium spp.</i>	0.06±0.26	0.01±0.04	1.03	27.61

In total 22 taxa of phytoplankton from the five phytoplankton classes were selected as important for the both communities. The majority (20 taxa) of their biomasses was higher in the Plume area than outside, except the two taxa: dinoflagellate *Scrippsiella* spp. and cyanobacteria *Cyanonephron* spp. Two main taxa, cyanobacteria *Aphanizomenon flos-aquae* and diatom *Actinocyclus* spp., contributed to evident difference between the two areas. *A. flos-aquae* was the dominant species during the whole investigation period and its mean biomass was 10 times higher in the plume area than outside indicating the bloom conditions (Table 8). The diatom showed the similar pattern having higher mean biomass in the Plume area than outside.

The phytoplankton community in the plume area was described mainly by six phytoplankton species (Table 9). Cyanobacteria *A. flos-aquae* was the main component of the phytoplankton community of the plume leading by two other cyanobacteria: *Planktothrix agardhii* and cf. *Woronichinia compacta*, two diatoms *Actinocyclus* spp. and *Aulacoseira islandica* and one species of green algae *Pediastrum boryanum*. All species biomass strongly correlated with salinity ($r=-0.47 - -0.81$, $p<0.05$, $N=43$).

Table 9. Phytoplankton species composition in the plume area and outside the plume area (cumulative contribution >70% of contributing taxa to community is given) and spearman rank correlation with salinity (significant correlations are indicated in asterisks).

Plume		Not plume	
Species	Correl.	Species	Correl.
<i>Aphanizomenon flos-aquae</i>	-0.81*	<i>Aphanizomenon flos-aquae</i>	-0.81*
<i>Actinocyclus</i> spp.	-0.75*	<i>Scrippsiella</i> spp.	0.19
<i>Planktothrix agardhii</i>	-0.68*	<i>Pyramimonas</i> spp.	0.24
<i>Pediastrum boryanum</i>	-0.79*	<i>Chrysochromulina</i> spp.	0.13
<i>Aulacoseira islandica</i>	-0.47*	<i>Limnothrix planctonica</i>	-0.07
cf. <i>Woronichinia compacta</i>	-0.65*	<i>Cyanonephron</i> spp.	0.23

The phytoplankton community outside the plume area was described by six phytoplankton species (Table 9). Cyanobacteria *A. flos-aquae* was the main component of this phytoplankton community, although with much lower biomass than in the plume area. The other contributing taxa to community were dinoflagellates *Scrippsiella* spp., prasinophytes *Pyramimonas* spp., prymnesiophytes *Chrysochromulina*

spp., and two other cyanobacteria *Limnothrix planctonica* and colonial chroococoids *Cyanonephron* spp. All species except *A. flos-aquae* showed weak statistically not significant correlation with salinity ($r=-0.07-0.24$, $p>0.05$, $N=43$).

5. DISCUSSION

5.1. Validation: different algorithms and effect of environmental conditions

In general, results from the FUB processor showed a good agreement with *in situ* measurements for all optically active components, especially chl *a* and TSM (Figure 9 and Figure 12). Our results highlighted that the FUB processor with the sufficient confidence level was useful in the offshore area and in the plume area, where relatively high concentration of pigments and other in-water constituents occurred. The same processor was tested in Skagerrak (Sørensen et al., 2007) and in the Himmerfjärden Bay, northwestern part of the Baltic Sea (Kratzer et al., 2008). Similarly to our results, investigations in Skagerrak demonstrated the ability of the FUB processor to predict well both chl *a* and TSM concentrations. Kratzer et al. (2008) found that the FUB processor performed very well in the open Baltic Sea. The promising results from the validation of estimates derived by the FUB processor over different parts of the Baltic Sea suggest that it could be used as a common tool for monitoring the spatial distribution of water quality parameters in the Baltic Sea.

The C2R, Eutrophic and Boreal processors strongly underestimated chl *a* concentration, showing obvious threshold within 10–27 mg/m³. The C2R processor was tested in the NW part of the Baltic Sea and contradictory results were obtained (Kratzer, Vinterhav, 2010). In the open Sea chl *a* was overestimated by the processor (Mean Normalised Bias MNB=118.7%, Root Mean Square RMS=141.6%), whereas in the coastal waters chl *a* was underestimated (RMS=-68.2%, MNB=63.3%). According to the results obtained in the northern Curonian lagoon (Giardino et al., 2010a), the strong underestimation of chl *a*, particularly during cyanobacteria bloom, could be due to uncorrected C2R derived remote sensing reflectance (R_{rs}) at red/near-infrared wavelengths. It is known, that the C2R processor is unable to capture the typical peak of remote sensing reflectance (R_{rs}) around 700 nm, due to a combination of high backscattering, exponentially

increasing absorption by water molecules and low absorption by CDOM and phytoplankton (Kutser, 2009). The results obtained by Giardino et al. (2010a) confirmed the remarks regarding the plume area, where higher chl *a* concentration is often measured. However, in our study we directly validated water quality parameters and the validation of remote sensing reflectance (R_{rs}) will be addressed in the future. The best agreement between *in situ* and satellite-derived CDOM absorption was found for the Boreal processor (Figure 11), in which the neural network was trained with data from the boreal forest region with high absorption of gelbstoff (Doerffer and Schiller, 2008a, Koponen et al., 2008). Moreover, CDOM absorption derived by the Eutrophic processor were also in moderate agreement with *in situ* measurements suggesting that the algorithms developed for fresh waters can be used also for the brackish waters of the Baltic Sea. The estimates of CDOM absorption derived by the FUB and C2R processors were comparable to *in situ* measurements as well, demonstrating the ability of these processors to accurately predict CDOM. According to Giardino et al. (2010a) the C2R processor gave CDOM in the same ranges as *in situ* measurements in the highly eutrophic Curonian Lagoon waters. CDOM concentration derived by the C2R, Eutrophic and Boreal processors were in moderate agreement with *in situ* measurements showing some underestimation (see Figure 12). In summary, the C2R, Boreal and Eutrophic processors provided ranges of CDOM comparable to *in situ* measurements and could be used for the CDOM mapping over the lacustrine and brackish coastal waters.

The validation results of the standard MERIS Level 2 products showed, that the fit between satellite derived and *in situ* measured chl *a* was in an exceptionally good agreement (see Table 5), although maximum chl *a* predictions were below 25 mg/m³. This was the effect of the high proportion (>60%) of flagged pixels that were discarded from the analysis. In order to compare the relevance of predicted water quality parameters with other processors, we tested the goodness of fit with a reduced number of observations (N=26) for all processors (Table 10).

Table 10. Explained variance (R^2), regression coefficients (slope and intercept), mean absolute error (MAE) and root mean squared error (RMSE) of the processing schemes (FUB, C2R, Eutrophic, Boreal and standard Level 2) for water quality parameters (chl *a*, CDOM and TSM) from reduced number of samples (N=26).

		Chl <i>a</i> , mg/m ³	CDOM, 1/m	TSM, g/m ³
FUB	R^2	0.84	0.55	0.62
	Slope and intercept	$1.29 \times \text{Chl}_{in\ situ} - 2.89$	$0.34 \times \text{CDOM}_{in\ situ} + 0.07$	$0.38 \times \text{TSM}_{in\ situ} - 0.71$
	MAE	3.59	0.23	4.20
	RMSE	5.32	0.34	4.61
C2R	R^2	0.17	0.54	0.68
	Slope and intercept	$0.10 \times \text{Chl}_{in\ situ} + 8.51$	$0.34 \times \text{CDOM}_{in\ situ} + 0.03$	$0.53 \times \text{TSM}_{in\ situ} - 0.86$
	MAE	6.31	0.26	3.50
	RMSE	7.94	0.37	3.87
Eutrophic	R^2	0.30	0.58	0.69
	Slope and intercept	$0.07 \times \text{Chl}_{in\ situ} + 6.69$	$0.21 \times \text{CDOM}_{in\ situ} + 0.17$	$0.70 \times \text{TSM}_{in\ situ} - 1.23$
	MAE	5.61	0.22	2.99
	RMSE	8.01	0.35	3.33
Boreal	R^2	0.46	0.68	0.65
	Slope and intercept	$0.36 \times \text{Chl}_{in\ situ} + 13.68$	$0.26 \times \text{CDOM}_{in\ situ} + 0.23$	$0.37 \times \text{TSM}_{in\ situ} - 0.57$
	MAE	9.82	0.18	4.17
	RMSE	10.52	0.30	4.58
Level 2	R^2	0.86	0.09	0.54
	Slope and intercept	$0.74 \times \text{Chl}_{in\ situ} + 0.94$	$-0.12 \times \text{CDOM}_{in\ situ} + 0.21$	$0.47 \times \text{TSM}_{in\ situ} - 0.38$
	MAE	2.59	0.36	3.42
	RMSE	3.58	0.52	3.90

The accuracy of chl *a* estimates derived by the FUB processor were comparable to those derived by the standard Level 2 ($R^2=0.84$, MAE=3.59 mg/m³), although with the higher prediction error. It should be mentioned, that in this study CDOM absorption was estimated in terms of yellow substance, whereas CDOM absorption by the standard Level 2 product is the sum of yellow substance and detritus in terms of the bleached particle (BP) absorption (Ohde et al., 2007). This difference might explain the observed disagreement. Ohde et al. (2007) and Siegel et al. (2003) showed that absorption by BP can contribute to the total absorption by both CDOM and BP by about

15% in the clear open Baltic Sea and up to 25% in the coastal waters. Thus, it should be taken into an account and tested in the near future in order to make the final conclusion regarding the prediction of CDOM absorption by the standard MERIS Level 2 product.

All processors predicted TSM exceptionally well in the similar confidence level range (Table 10). After the reduction of the number of observations used for the analysis, the best fit between the TSM measurements *in situ* and derived by algorithm was found for the Eutrophic processor ($R^2=0.69$, $MAE=2.99 \text{ g/m}^3$), whereas with the full data set the best agreement was found with the FUB processor. The fit between standard Level 2 estimates and *in situ* was an intermediate ($R^2=0.54$, $MAE=3.42 \text{ g/m}^3$) and the predictions by the processor were below 12 g/m^3 concentrations.

The large amount of data in the standard Level 2 products is usually dropped due to quality flags and therefore the extreme concentrations, which are important for the assessment of water quality, meant to be overlooked. According to Stelzer et al. (2008) the ESA Case 2 Regional C2R processor is one option for overcoming this problem, as well as Boreal and Eutrophic. For example, only 13% of the pixels were flagged in this study by these processors, whereas FUB flagged only 27% of all measurements. Nevertheless, standard Level 2 products were broadly investigated over the whole Baltic Sea basin soon after the launch of Envisat satellite: in the NW part of the Baltic Sea (Kratzer et al., 2008), Skagerrak (Sørensen et al., 2007), in the SW part and in the open Baltic Sea (Ohde et al., 2007), and in the Vistula lagoon (Kruk et al., 2010). These studies demonstrated the highly variable results of comparison between the *in situ* and satellite derived values. The studies performed in the open Sea waters of northern Baltic Sea showed that the standard Level 2 processor overestimated chl *a* by about 59%, and TSM (in terms of suspended particulate matter) by about 28%, and underestimated CDOM by about 81% (Kratzer et al., 2008). Sørensen et al. (2007) described the validation results from the northern part of Skagerrak with additional measurements in Kattegat. *In situ* measured chl *a* explained 86% of the variance in standard MERIS Level 2 ($RMS=1.17 \text{ mg/m}^3$), whereas

the *in situ* measured TSM explained 71% of the variance (RMS=0.30 g/m³). The results were presumable, since conversion factors used in empirical relationships of processor were determined in Skagerrak and later included in the second reprocessing of the MERIS data (Sørensen et al., 2007). The results highlighted the advantage of regional conversion factors to be implemented into the models of processors. In the western part of the Baltic including open Sea and discharge areas of the Oder River in the Pomeranian Bay, the standard Level 2 products underestimated *in situ* measurements (Ohde et al., 2007). According to Kruk et al. (2010) the correlation between in-water constituents measured *in situ* and derived by standard Level 2 products was weak in the Vistula Lagoon. In summary, one can state that the standard MERIS Level 2 products are applicable to monitor chl *a* and TSM concentrations over the Baltic Sea.

The differences between *in situ* measurements and satellite derived water quality parameters could be related to i) water types, especially coastal waters influenced by eutrophic lacustrine waters, that differ in their specific inherent optical properties (IOPs); ii) IOPs used for the parameterization of the MERIS Neural Network algorithms that differ from those measured in the region of interest; iii) aerosol types within the coastal region challenging the atmospheric correction process (Zibordi et al., 2011) and iv) adjacency effect of the coast (Kratzer, Vinterhav, 2010). As it was noted before, the SE Baltic Sea coastal waters are extremely influenced by fresh, productive, highly eutrophic Curonian lagoon waters. The later waters constantly mix with brackish coastal water masses causing very rapid changes in the concentration of chl *a*, CDOM and TSM, herewith certainly causing an increase of absorption by pigments and CDOM, and scattering by suspended material, i.e. rapid changes in the IOPs. However, re-parameterization of the MERIS Neural Network algorithms was outside of the scope of this study owing to the scarcity IOPs and radiometric measurements in the study area. Instead, we focused on the analysis of environmental and sampling conditions that may cause differences between satellite-derived and *in situ* measured concentrations of in-water constituents.

From the nonlinear regression analysis we found that Secchi depth was the mainly important factor, whereas the effects of distance from the coast and sampling time were not statistically significant. The Secchi depth strongly correlated ($r > 0.7$) with salinity, chl *a*, CDOM and TSM concentrations, and distance from the outlet of the lagoon being a proxy of rapidly changing IOPs within the investigated region. In general, the absolute differences between satellite-derived and *in situ* measured values increased with the decrease of the Secchi depth (Figure 10). Low differences (close to zero) were between 4 and 7 m of the Secchi depth, where water salinity ranged 6–7 PSU, which is typical for the Lithuanian Baltic Sea coastal waters (Storch, Omstedt, 2008; Gasiūnaitė et al., 2005; Žaromskis, 1996).

The data presented here showed, that the C2R, Boreal and Eutrophic processors strongly underestimated *in situ* chl *a* concentrations over the sampling locations with reduced Secchi depth, whereas the FUB algorithm overestimated chl *a* concentrations. As mentioned before, C2R was unable to capture the typical peak of remote sensing reflectance (R_{rs}) around 700 nm, especially during intensive production of phytoplankton (Giardino et al., 2010a, Kutser, 2009). This is highly probable in the coastal areas impacted by productive waters of the Curonian lagoon, where drastic changes of IOPs occur. Similarly, the greatest differences of CDOM and TSM concentrations given by all processors were found within the locations with reduced Secchi depth, suggesting the need of *in situ* measurements of IOPs in very mixed waters.

Kratzer et al. (2008) emphasized the difficulty to get a temporal match between the satellite overpass and *in situ* data due to the frequent cloud cover over the Baltic Sea. Moreover, *in situ* data are usually taken in a wider time frame than the satellite overpass due to design of sampling locations and usually extra measurements of other water parameters (e.g. nutrients, primary production, plankton community structure). For this reason we tested the effect of sampling time on the differences between *in situ* measurements and the satellite derived estimates. In the regression analysis the sampling time was not a statistically significant factor, whereas the Secchi depth

explained most of the variance in the estimated differences. However, there was an evident match of *in situ* measurements and satellite-based estimates within 1–2 hours before the overpass of satellite to approximately 2–3 hours after it (Figure 10). These results may give useful information for future validation analysis, since the appropriate time for sampling differed among the water quality parameters.

5.2. Indicators of dynamically active hydrofront

Estuarine salinity gradient is a primary conservative factor indicating the influence of riverine freshwater into the marine environment. This hydrochemical parameter has been used for the delineation of different environments in order to interpret species ecology as well as to monitor water trophic status in the Baltic Sea (Moisander et al., 1997; Wasmund et al., 2001; Gasiūnaitė et al., 2005; Daunys et al., 2007; Jurgensone et al., 2011). However, there is no one common method how to delineate water bodies according to salinity. For example, the salinity gradient in the Gulf of Finland was divided into two subareas by Kononen et al. (1996): frontal waters in the gulf with relatively low salinity (5.8-6.2 PSU) and waters outside the frontal region with relatively high salinity (6.5-6.8 PSU) in the northern Baltic proper. On the other hand, the Gulf of Finland was divided into five subareas according to salinity and temperature by Moisander et al. (1997). Another example, where Wasmund et al., (2001) suggested different salinity thresholds to delineate river plume areas in the waters of Pomeranian Bay (7.3 PSU), Gulf of Gdansk (7.0 PSU), Lithuania (6.8 PSU) and Gulf of Riga (5.0 PSU). The same threshold (6.8 PSU) was used in the coastal waters of Lithuania by Gasiūnaitė et al. (2005), who summarized the long-term 1984-2001 monitoring data from the coastal stations influenced by the outflow of eutrophic waters from the Curonian Lagoon. However, during the implementation of Water Framework Directive (2000/60/EC) delineation of the plume area in the coastal waters of Lithuania was based on 5 PSU salinity threshold according to COAST (2002) and modelled salinity with finite element SHYFEM (Daunys et al., 2007).

In this study the estimated mean salinity of waters not affected by the plume (6.70 ± 0.50 PSU) were close to the threshold (6.8 PSU) suggested by Wasmund et al. (2001) for the Lithuanian coastal waters. However, in this study the used threshold of plume and offshore waters was 6.2 PSU, obtained by subtracting the standard deviation from the mean, in order to eliminate variability associated with offshore waters.

CDOM in coastal environments generally has a terrestrial origin and is transported to the ocean via rivers (Kratzer et al., 2008; Kirk, 2011). Thus, CDOM is decreasing with increase of salinity (Blough and Del Vecchio, 2002). In this study strong negative linear relationship ($r = -0.94$, $p < 0.05$, $N = 43$) between salinity as a primal indicator of riverine runoff and CDOM was found. Similar relationship ($r = -0.89$, $N = 476$) between two parameters was observed in the southern Baltic Sea (Kowalczyk et al., 2010). It was considered that the discharge and mixing of riverine waters is a primary driver of variability in CDOM absorption in the surface waters of the southern Baltic Sea. In the Gulf of Bothnia CDOM in terms of a_{440} absorption was analysed as a function of salinity and high negative correlation ($r = -0.96$) was found also (Harvey et al., 2011). In respect to these strong correlations and CDOM being a common component of remotely sensed ocean colour (Siegel et al., 2002) it is evident that CDOM derived by satellite images can be used to map freshwater intrusions into the coastal areas, reflecting changes in river discharge rates in more sufficient temporal and spatial scales.

The concentration of chlorophyll *a* is often used as a proxy of phytoplankton biomass and water quality indicator (Wasmund and Uhlig, 2003; Directive, 2000; 2008). This parameter is primary limited by environmental factors such as nutrients, light intensity and temperature. Water salinity can play an important role too, especially in estuarine or lagoon systems, which are commonly exposed to rapid and irregular changes of salinity. There are examples, where in the Baltic Sea the salinity has been shown to be one of the key factors influencing phytoplankton composition (Moisander et al., 1997, Kononen et al., 1996, Gasiūnaitė et al., 2005) and photosynthetic

behavior of several phytoplankton species (Schubert et al., 1993). The salinity change can result in osmotic stress on cells, uptake or loss of ions and effects on the cellular ionic ratio in phytoplankton (Guillard, 1962). To maintain osmotic balance due to frequent alterations in salinity level result in an increased respiratory activity in phytoplankton. Hence, the community response to physical events, like changes in salinity, is complex and dependent on time (Franks, 1992). On the other hand, high concentrations of chlorophyll *a* can occur in high salinity, indicating favorable growth conditions for the phytoplankton in the non light limiting and nutrient rich waters (Devlin et al., 2012). The lags between nutrient inputs and phytoplankton production have been recorded in different estuarine ecosystems (Kemp, Boynton, 1984; Flint et al., 1986; Malone et al., 1988). Described conditions could be named as a secondary plume characterised by high phytoplankton production as measured by elevated chlorophyll *a* (Devlin et al., 2012) already as a sequence of initial discharge. Therefore, chlorophyll *a* could not be considered as an appropriate optical parameter for the delineation of the plume area, unless the time lags between nutrient inputs and phytoplankton production can be assessed and initial outflow can be distinguished from secondary plume. However, the strong negative relationship between the concentration of chlorophyll *a* and salinity was found in this study, showing that chlorophyll *a* might be used with certain care. Its use could be restricted during coastal and offshore phytoplankton blooms, when it is difficult to distinguish limits of brackish and freshwater originated blooms. Moreover, underestimated concentration of chlorophyll *a* by the satellites may result during rough hydrometeorological conditions due to mixture of surface waters or due to vertical migration, e.g. of cyanobacteria (Kutser et al., 2008).

TSM mainly originates from terrestrial and river runoff, although high concentration of TSM in the coastal waters may show re-suspension of water sediments by wind-wave stirring (Erm et al., 2011). Consequently, TSM was suggested as indicator of coastal waters (Kratzer and Tett, 2009). The Lithuanian coastal waters having

the highest wave exposure in the Baltic Sea (Kelpšaitė et al., 2011) are influenced by both factors that may enrich waters by TSM: intrusion of fresh, eutrophic and turbid lagoon waters, and wind-driven re-suspension of bottom sediments. Therefore, concentration of TSM could not be directly used as an indicator of the plume area. In this study the correlation between concentration of TSM and salinity was strongly indicating a possible application of TSM as indicator of water quality, however similar care should be taken as for concentration of chlorophyll *a*, because TSM, as a sum of organic and inorganic material, highly depends on phytoplankton production especially in the bloom conditions (Kratzer, Vinterhav, 2010). It was show that the outflow of the lagoon is relatively large source of organic matter, i.e. riverine and lagoon phytoplankton in the Sea. Most of suspended sedimentary material outflow from the Curonian Lagoon deposits in the close proximity or is transported along the coast by dominant water stream of northern direction (Galkus, Jokšas, 1997).

5.3. Phytoplankton communities in the plume and coastal waters

The salinity plays as both external ecological factor and physiological characteristic of aquatic organisms; it divides living conditions appropriate for freshwater and marine (Telesh, Khlebovich, 2010). It is well known that the salinity gradient is one of the main factors limiting number of species in the Baltic Sea. For a long time it was accepted that estuaries and other ‘transitional’ marine-freshwater areas host species-poor communities, demonstrating the ‘species minimum’ described by Remane (1934). However, the phytoplankton species diversity displays a maximum within the marine-freshwater salinity gradient (Muylaert et al., 2009). In this study, in phytoplankton of the plume cyanobacteria (Cyanophyceae), diatoms (Bacillariophyceae) and green algae (Chlorophyceae) predominated, while the assessed phytoplankton community of brackish coastal waters was more heterogeneous in the level of cyanobacteria and microalgae classes: together with cyanobacteria (Cyanophyceae), dinoflagellates (Dinophyceae), cryptophytes (Cryptophyceae), prymnesiophytes (Prymnesiophyceae) with diatoms (Bacillariophyceae) predominated.

Several studies documented the changes of phytoplankton communities along the salinity gradient in various regions of the Baltic Sea: in open Baltic Sea (Kahru et al., 1984), in the eastern and western parts of the Gulf of Finland (Kononen et al., 1996; Moisander et al., 1997; Gasiūnaitė et al., 2005), in the SE Baltic Sea and Curonian Lagoon (Olenina, 1996; 1997; Gasiūnaitė et al., 2005), in the Mariager Fjord, Skive Fjord and Gulf of Riga (Gasiūnaitė et al., 2005). Moreover, experimental studies showed, that addition of NaCl largely influenced the taxonomic composition of the phytoplankton communities (Pilkaitytė et al., 2004), i.e. the evident increase in filamentous cyanobacteria was observed, while coccoid cyanobacteria decreased. By this study response of cyanobacteria to hyperosmotic NaCl stress and iron depletion by activating molecular acclimation mechanisms was highlighted.

In this study the complex of microalgae was determined in the plume area consisting of six dominant phytoplankton species: cyanobacteria *A. flos-aquae*, *Planktothrix agardhii*, cf. *Woronichinia compacta*, two diatoms *Actinocyclus* spp. and *Aulacoseira islandica*, green algae species *Pediastrum boryanum* (Table 9). On the other hand, the species complex differed from the phytoplankton composition found in the plume area during the summer from the long-term (1980-1996) national monitoring data (Olenina, 1997), where five dominant species were found: cyanobacteria *Gomphosphaeria pusilla*, diatoms *Skeletonema costatum*, Flagellata undet., green algae *Planktonema lauterbornii* and dinoflagellate *Heterocapsa triquetra*. These species were considered as indicators of the plume area. Moreover, *A. flos-aquae* was not dominant and common among the other species in the plume area, whereas *A. flos-aquae* dominated in the whole Curonian Lagoon area during the same investigation period. In this study on the contrarily, the *A. flos-aquae* bloom was clearly restricted to the frontal area, although the species was present in the coastal waters outside the plume. The same pattern was observed in other Baltic Sea regions, where *A. flos-aquae* dominated in summer samples from the adjacent areas with lower salinities (Kahru et al., 1984; Kononen et al., 1996; Moisander et al.,

1997; Gasiūnaitė et al., 2005). Later, a different long-term (1984-2003) data set was investigated, and seven dominant species were found: *A. flos-aquae*, *Coelomonon pusillum*, *Chrysochromulina* spp., *Heterocapsa triquetra*, *Skeletonema costatum*, *Cylindrotheca closterium* and Cryptomonadales spp. (Olenina, 2004).

Nevertheless, the differences in the dominant species composition of the plume area between two datasets, firstly could be explained by phytoplankton temporal variation, length and frequency of data series (Wasmund et al., 2011). In respect to the differences between the datasets, short data series with relatively frequent surveys (e.g. this study) could describe more the development of phytoplankton only in some certain situations compared to long-term data. However, even long data series with relatively low frequency (e.g. 1-3 surveys during summer, which is typical for the Lithuanian monitoring program), can be too rough to determine the patterns and composition of dominating phytoplankton species in such dynamic waters as plume areas.

On the other hand, all species indicators of the plume waters were determined in this study, but in very small biomass. The difference of dominant phytoplankton species biomass between two datasets could be related to the sampling methods. In this study only surface samples were analysed in order to assess phytoplankton changes at the surface in relation to the OAC derived from the satellite images. In the second and third dataset (Olenina, 1997, 2004) the species composition and biomass were determined from integrated water samples: samples taken from surface, 2.5 m, 5 m, 7.5 m and 10 m depth were mixed. Taking into account that the waters of lagoon may spread differently along the depth (Figure 24), the integrated samples of phytoplankton, taken from separate sites within the plume area, can give different results.

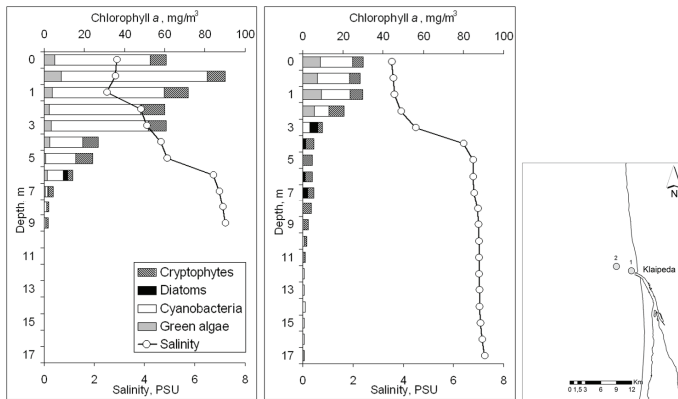


Figure 24. Vertical distribution of salinity and different phytoplankton groups in terms of chlorophyll a (mg/m^3) measured by fluorometer FluoroProbeII in two stations of the Lithuanian Baltic Sea, 29th of July, 2012 (the results obtained by author).

Finally, different methods for the determination of the dominant species were used and therefore could influence the result. In the study presented by Olenina (1997) the dominant species was assessed according to the presence in the samples (20% of samples and more). While Olenina (2004) use the methodology described by Давыдова (1985), where relative abundance greater than 10% indicates the dominance of the species. In this study the biomasses of species were used, and multidimensional scaling with ANOSIM were applied.

In this study the phytoplankton composition in the coastal waters outside the plume was typical of the season and the area (Olenina, 1996, 1997; Gasiūnaite et al., 2005). The species composition consisted of cyanobacteria *A. flos-aquae*, dinoflagellates *Scrippsiella* spp., prasinophytes *Pyramimonas* spp., prymnesiophytes *Chrysochromulina* spp., and two other cyanobacteria *Limnothrix planctonica* and colonial chroococcoids *Cyanonephron* spp. Cyanobacteria *A. flos-aquae* was the main component of the phytoplankton community, although with much lower biomass than in the plume area. Biomass of *Chrysochromulina* spp. and *Pyramimonas* spp. correlated with salinity indicating as typical brackish water

species. The same tendency regarding these microalgae was observed in the open Gulf of Finland (Kononen et al., 1996). Again, the complex of dominant species outside the plume determined in this study differed from the species composition of long-term monitoring data (Olenina, 1997), except cyanobacteria *A. flos-aquae*. The other complex of dominant species consisted of *Gomphosphaeria pusilla*, *Flagellata* undet, Cryptomonadales B and Centrales spp. Later investigation (Olenina, 2004) using different long-term (1984-2003) determined six dominant species: *Chrysochromulina* spp., *A. flos-aquae*, *Nodularia spumigena*, Cryptomonadales spp., *Heterocapsa triquetra*, *Skeletonema costatum*, that differs from the goupe mentioned before presumably due to reasons described before.

The permanent fluctuations of fresh and rich in nutrients waters may control the success of invasions by non-indigenous species (Telesh, 2006; Olenin, 2005), especially those with a broad tolerance for the salinity. As an example, the invasion and establishment of the euryhaline and eutythermal, potentially toxic dinoflagellate *Prorocentrum minimum* (Pavillard) Schiller 1933 was recorded in the Baltic Sea (Hajdu et al., 2000; Olenina et al., 2010). Since its first bloom in the Skagerrak, *P. minimum* has spread successively into the low-saline waters of the Baltic Sea. Moreover, experimentally was shown that *P. minimum* can thrive in a broad range of salinity: cells adapted to salinities outside the optimum range (from 15 to 17 PSU) grow well even below 5 PSU, suggesting a potential to penetrate farther into the low saline part of the Baltic Sea (Hajdu et al., 2000). In the Lithuanian waters the peak of *P. minimum* bloom was observed in 2003 (Figure 25). The species was found in the near shore plankton already in April and starting from July till the end of October the species bloom expanded to all study areas, including the northern part of the Curonian Lagoon. The most abundant *P. minimum* was in the near shore areas.

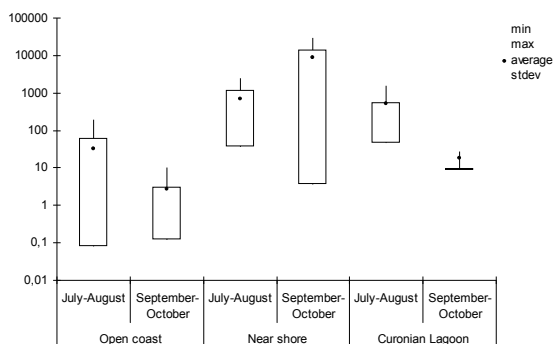


Figure 25. *Prorocentrum minimum* bloom intensity (logarithmic scale, 10 thousand cells/l) during two periods (summer and autumn) and different areas of the Lithuanian Baltic Sea waters in 2003 (Olenina et al., unpub.).

Besides the water salinity, plankton communities in different Baltic Sea estuaries can be influenced by other common environmental and anthropogenic factors (Telesh, 2004). The plumes are usually enriched with high concentration of nutrients, which is important source of nutrients for phytoplankton production (Loder and Platt, 1985; Kononen et al., 1996). However, the timescales of frontal development and phytoplankton growth may mismatch (Franks, 1992), making it a stiff task to assess direct effects of increased concentration of nutrients on, phytoplankton production rates *in situ* of highly dynamical frontal zone. During this investigation sharp decrease in phytoplankton biomass as an outcome of salinity gradient was observed: from 31.7 ± 10.7 mg/l up to 2.3 ± 1.8 mg/l (Figure 20). However, due to coarse sampling, the obtained result could not explain the effect of nutrients load.

5.4. Remote sensing application in the assessment of the plume area

In the frame of WFD it is necessary to produce a simple physical typology of waters that is both ecologically relevant and practical to implement (Daunys et al., 2007). Few studies attempted to assess the

distribution of the plume area in the coastal waters. Different approaches were used in each of them. Olenina (1997; 2004) classified water areas according to phytoplankton composition in 1980-1996 and later in 1984-2003. The Baltic Sea phytoplankton communities were affected by the plume waters within approximately 35 km to the north, 30 km to the north-west, 14-15 km to the west and south-west from the outlet of Lagoon to the Sea (Figure 26). The size of this area was ca 531 km² (Table 11).

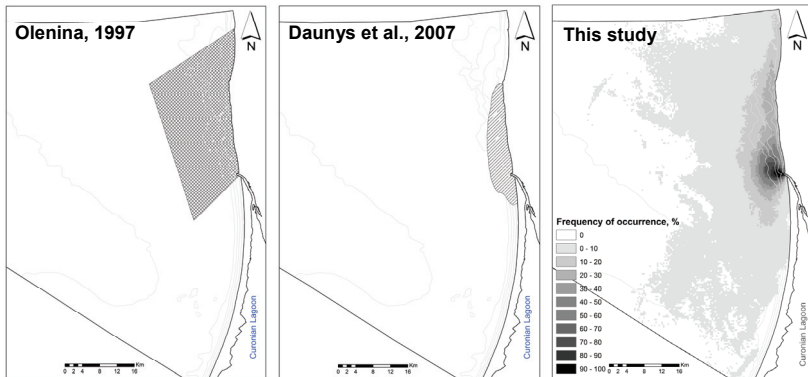


Figure 26. Spatial distribution of the plume area using different approaches in the Lithuanian Baltic Sea waters.

In other study the plume area was assessed applying spatial and temporal distribution of salinity during 2004-2006, which was modeled using finite element SHYFEM model (Daunys et al., 2007). Two thresholds of salinity (0.5 and 5-6 PSU) were suggested for the use in water typology according to CIS Working Group COAST Guidance (COAST, 2002). However, 5 PSU salinity threshold was selected because of better correspondence with the existing phytoplankton data (Olenina, 2004) and therefore having higher ecological relevance. The delineated plume area was 112 km² (Table 11) mainly directed northward along the coast (Figure 26).

In this study, the satellite remote sensing technique was used for the delineation of the plume area. The CDOM threshold of the plume waters (>0.408 1/m) was selected according to the mean salinity and

its variability in the territorial sea region (see chapter 4.2.2.). Figure 26 shows the spatial distribution of the plume, which is based on CDOM values derived from MERIS images (during 2005-2011) after application of Boreal processor. The spread of the plume was mainly directed to the north, although with less frequency it occurred in the whole area of territorial sea and even up to 40 km from the shore line, covering 728 ± 397 km² (Table 11).

Table 11. Size of the plume area and its frequency of occurrence according to the three different approaches.

Reference	Frequency of occurrence, %	Area, km ²
Olenina, 1997	Whole plume area	531
Daunys et al., 2007	Whole plume area	112
	Whole plume area	728±397
This study	10-100	367±230
	20-100	202±137
	30-100	101±74
	40-100	60±47
	50-100	34±21
	60-100	23±13
	70-100	16±11
	80-100	9±9
	90-100	5±5

The delineated plume areas in three studies do not overlap in time frame, therefore the results of comparison should be interpreted with care. Nevertheless, it is evident that in all the studies the occurrence of the plume probability was relatively high in the northern coastal part (Figure 26). It could be explained by predominant SE and SW winds and currents in the study area (Dailidienė et al., 2012). On the other hand, the southern part of the coast appears to be less influenced by the lagoon waters according to the modelled salinity and satellite images. Moreover, the phytoplankton data corresponded well with the delineated plume area by salinity.

The presented comparison of three different approaches shows, that more frequent in time and space scale measurements or

observations, like in this study satellite imagery, could improve the understanding about the distribution of dynamical plume area and the magnitude of it's influence for the coastal waters. The combination of different techniques: satellite images (different types of optical and synthetic aperture radars – SAR), data about the weather conditions and modeling technique would improve the typology of the plume.

5.5. Remote sensing application for water quality assessment

Long-term changes of optically active water quality indicators

In the frame of national monitoring of Lithuania, sampling in the coastal waters is generally carried out on a seasonal basis, i.e. four times per year (Appendix 2, p. 125). Due to hydrodynamically active environment (exposed coast and large inflow of the waters from the Curonian Lagoon) the trophic state parameters (concentration of nutrients, chlorophyll *a*, Secchi disk depth, phytoplankton structure and biomass) considerably vary in spatial and time (from hours to months) scale especially during the vegetative period (Salmaso, 1996). Therefore, few samples per summer season may not reflect the general trophic state of the coastal waters. The limitation of sampling in the Lithuanian waters can be solved by analysing optically active compounds from satellite images, since data from different ocean colour sensors is provided every 72 h for MERIS and every 24 h for MODIS (i.e. approximately each day).

The limitations of *in situ* sampling were tested on three monitoring stations during the intensive vegetation period of 2005-2011 (Figure 27). Two stations are located in the transitional waters (plume zone), delineated in the WFD (Daunys et al., 2007): the 4th station (just in front of the entrance of Curonian Lagoon) and the 3rd station (ca 11 km to the north from the entrance). The third station (46th) is located at the end of the exclusive economic zone of Lithuania (ca 125 km from the entrance, see Appendix 2, p. 125). The concentration of chlorophyll *a* (chl *a*), derived by FUB processor from satellite images (MERIS), was compared with *in situ* measurements in three stations. According to both measurements, mean concentration of chl *a* decreased with the distance from the entrance of the Lagoon.

However, the maximum estimates derived from the satellite were significantly higher up to five times than measured *in situ*. This shows how important the satellite method can be, because *in situ* data did not record many phytoplankton blooms, yet it missed the hyperblooms, which were caught by satellites.

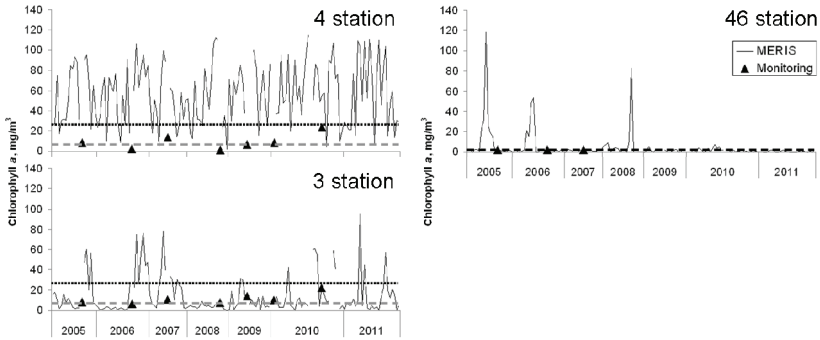


Figure 27. Long-term (2005-2011) changes of chlorophyll *a* concentration according to *in situ* data (Monitoring) and derived from satellite images after application of FUB processor (MERIS) at three monitoring stations (their location see Appendix 2, p. 125). In the 4th and 3rd stations the concentration of chlorophyll *a* below the black dotted line (25.8 mg/m³) and grey dotted line (4.9 mg/m³) is considered “good” water quality when salinity is <4 PSU and >4 PSU respectively; in the 46th station the concentration of chlorophyll *a* below the black dotted line (1.5-1.9 mg/m³) indicates “good” water quality in the open sea waters (HELCOM, 2007; MSFD 3rd intermediary report, 2012).

In Figure 27 the thresholds of “good” water quality are indicated according to MSFD (HELCOM, 2007, MSFD 3rd intermediary report, 2012). Long-term concentration of chlorophyll *a* derived from the satellite data in the 4th and 3rd stations usually indicated “bad” state of waters even if salinity is unknown, while *in situ* monitoring data showed mainly “good” environment state. In the end of the exclusive economical zone of Lithuania (46th station) only three peaks in 2005, 2006 and 2008 of extreme phytoplankton biomass were recorded from the satellite images, whereas no “bad” state of waters was recorded by the monitoring data.

The use of satellite images can support monitoring data not only temporally but also spatially. For example, the images from MERIS usually cover the whole exclusive economic zone of Lithuania in the Baltic Sea (Figure 28), especially the most dynamic areas in terms of trophic state. One of them is offshore waters, which during vegetation period are often impacted by cyanobacteria bloom originated in the central part of the Baltic Sea.

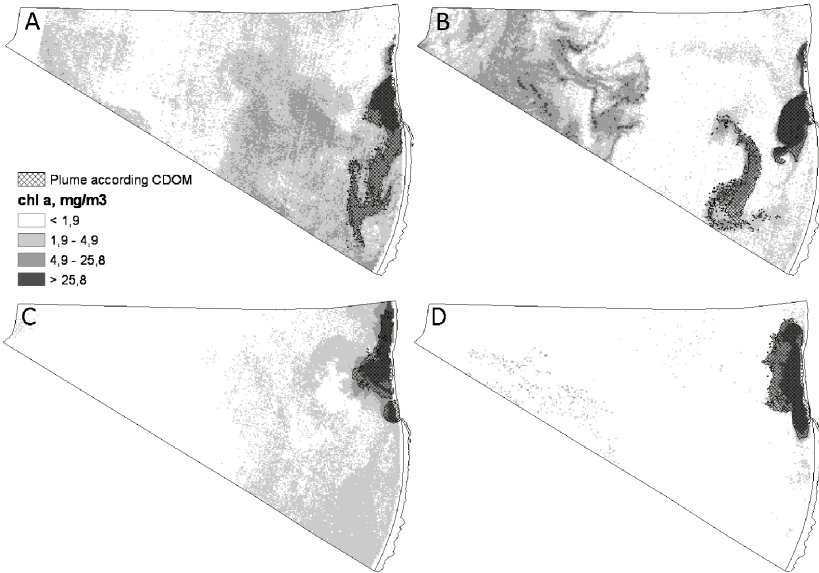


Figure 28. Examples of spatial and temporal (29th June (A), 21st July (B), 11th August (C) and 7th September (D) of 2010) variation of chl *a* and the plume area in the Lithuanian Baltic Sea. Chlorophyll *a* maps based on MERIS/Envisat data after application of FUB and the maps of the plume area based on CDOM of MERIS/Envisat data after application of Boreal.

The second area is the coastal waters influenced by the waters of lagoon. The improvement of water quality assessment with remote sensing in these areas was tested in four satellite images, where the water state was evaluated using the thresholds of chlorophyll *a*

determined in WFD and MSFD (HELCOM, 2007, MSFD 3rd intermediary report, 2012).

In the transitional waters (<4 PSU) the concentration of chlorophyll *a* >25.8 mg/m³ indicates “bad” environment state. The coastal waters with this environmental state were recorded in the satellite data and precisely fit the delineated plume area by the method used in this study (Figure 28). The waters with concentration of chlorophyll *a* between 4.9 and 25.8 mg/m³ can be classified either “good” or “bad” waters according to salinity: <4 PSU or >4 PSU respectively, suggested by WFD and MSFD. This salinity threshold was selected due to statistically significant correlation between the phytoplankton biomass and nutrients (Olenina, 2004; Daunys et al., 2007). Thus, the boundary between “good” and “bad” waters according to WFD and MSFD can not be directly compared with the plume area delineated in this study. Moreover, it has been shown (Kemp, Boynton 1984; Flint et al. 1986; Malone et al., 1988) that in the coastal waters the phytoplankton biomass may achieve the level similar to the one found in the plume waters, most likely, because of the input of additional nutrients by the riverine waters or precipitation. Nevertheless, in this work the delineated plume area corresponded to the waters with the concentration of chlorophyll *a* between 4.9 and 25.8 mg/m³, indicating that method used in this work could be successfully applied for the classification of water quality.

CDOM is generally considered as good indicator of direct effect of terrestrial influence (Kratzer et al., 2008), although it has not been included in the monitoring program yet, it would be highly recommended its measurements in the future as an indicator of the plume area. Moreover, CDOM correlates with salinity, therefore the CDOM maps derived from satellite images can be transformed into salinity maps, which may be useful for ecological interpretation of marine species distribution and dynamics in the coastal waters.

Assessment of cyanobacteria blooms

As it was indicated in this study, cyanobacteria are the main components of summer phytoplankton and summer blooms are regular

annual phenomena (Olenina and Olenin, 2004). As it was mentioned before, the most abundant species *Aphanizomenon flos-aquae* is constantly presented in the phytoplankton throughout the year, but rapidly increases in abundance (by 100-1000 fold) when the water temperature reaches 20°C. The bloom usually lasts until the end of October/beginning of November. During the two recent decades, an intensive bloom caused by *Aphanizomenon flos-aquae* was observed, while during summer season of period 1986-1989 and later 1994-1996 seasons, it reached hyperbloom conditions (Olenina and Olenin, 2004). During this investigation, in the estuarine plume of the Lithuanian coastal zone the biomass of *A. flos-aquae* was 24 mg/l and according to Reimers (1990) scale reached the level of intensive bloom (Appendix 3, p. 126). The damage of recreational zones during the outflow of the Curonian Lagoon was evident (personal observations).

The synoptical view to the water bloom based on visible satellite imagery is essential in order to evaluate, follow and predict the situation (Kahru, 1997). Variouse algorithms, with the application of modelling approaches are being developed in order to retriev cyanobacterial bloom (Metsamaa et al., 2006; Kutser et al., 2006; Gower et al., 2008). On of the MERIS algorithms Maximum Chlorophyll Index (MCI) is a useful, new tool for detection and estimation cyanobacteria biomass, phytoplankton biomass and chlorophyll *a* concentration (Alikas et al., 2010). During the summer all these parameters, due to strong relationship with MCI, can by predicted from the satellite data. In this study the MCI was tested on some of the data and gave promising results. For example, during the summer 2005 in the central part of the Baltic Sea the biggest cyanobacteria bloom can be seen in RGB image (Appendix 4, p. 126) recorded by the MERIS/Envisat, and the bloom was clearly indicated by MCI.

Thuse, remote sensing of cyanobacteria blooms has some limitations. According to Webster, Hutchinson (1994) a wind speed of >2–3 m/s may cause floating phytoplankton cells to descend from the surface into the water column, which will bias the estimates derived

from the satellite image. Besides that, there are several problems related to the prediction of cyanobacteria from the satellite signal (Kutser et al., 2006): i) the remote sensing algorithms are often image specific and not applicable to images obtained in different conditions, ii) the *in situ* chlorophyll values used for developing the remote sensing algorithms and validating satellite maps do not represent the situation satellites are detecting unless special methods have been used to collect the cyanobacteria from subsurface layer or surface scum, iii) still, spatial resolution of nearly all satellites is too coarse compared to the spatial heterogeneity of cyanobacterial blooms. Kutser (2004) showed that chlorophyll concentration may vary by two orders of magnitude within one MERIS 300×300 m pixel. Moreover, MERIS detects absorption of phycocyanin only in waters dominated by cyanobacteria (Simis et al., 2005). Thus, MERIS can be used in cyanobacteria mapping if concentration phycocyanin corresponds to concentration of chlorophyll *a* around 10–30 mg/m³ (depending on species). This concentration is significantly higher than the level of chlorophyll *a*, which is generally considered as bloom condition in the Baltic Sea (4 mg/m³).

Nevertheless, the satellite images provide valuable information about spatial distribution of algal blooms and water quality. For example, according to Hansson and Öberg (2010) the cyanobacterial bloom occurred during the first three weeks of July and mostly affected the SE parts of the Baltic Proper in summer 2010 (Appendix 3, 126). This phenomenon was not documented in the monitoring observations of Lithuania, whereas it was recorded in the satellite image. Once again, it is obvious that, remote sensing technique could be a tool for collecting consistent spatial and temporal data for the assessment of water quality parameters in lakes (e.g., Bukata et al., 1991; Koponen et al., 2004; Giardino et al., 2010b; Bresciani et al., 2011), in large Baltic Sea lagoons (Bresciani et al., 2012) and in the coastal waters of the Baltic Sea (Neumann et al., 2002; Kratzer et al., 2008).

Assessment of water transparency

The plume waters with higher concentration of OAC changes the light conditions by limiting penetration of light to the deeper water layers (Kirk, 2011). The Secchi depth is one of the oldest methods for estimation of water transparency used in oceanography (Tyler, 1968). However, there is other available methods, where diffuse attenuation coefficient (K_d) is measured by applying satellite images (Kratzer et al., 2003). In the Lithuanian Baltic Sea K_d was not applied yet, however, waters maximal remote sensing signal depth Z_{90_max} derived from MERIS/Envisat using Eutrophic processor was successfully validated with *in situ* measured Secchi depth (Vaičiūtė, 2012).

Based on the results of this study the following recommendations are suggested:

In this study the absorption of coloured dissolved organic matter (CDOM) was the best indicator of the plume, and it would be highly recommended its measurements in the monitoring program in order to assess the quality of coastal waters.

CDOM maps derived from satellite images can be transformed into salinity maps, which could be useful for the validation of hydrological transport models, ecological interpretation of species distribution patterns and their dynamics in the coastal waters.

In this study the showed importance of the satellite methods for the estimation of phytoplankton blooms and water transparency suggests to continue routine measurements of chlorophyll *a* and Secchi depth in the monitoring program in order to improve the optical models.

6. CONCLUSIONS

1. The FUB and standard Level 2 processors were the most relevant to derive chlorophyll *a* concentration in the Lithuanian Baltic Sea coastal waters, the Boreal processor – coloured dissolved organic matter absorption, the FUB processor – the concentration of total suspended matter.

2. Mean salinity of the estuarine waters was significantly lower than salinity of Lithuanian Baltic Sea coastal waters and highly correlated with the absorption of coloured dissolved organic matter (CDOM). According to this relationship, a threshold CDOM value (0.408 1/m), indicating the plume waters, was determined.

3. During the intensive vegetation period of 2005-2011, the fresh estuarine waters two-thirds of all investigated cases (64%) were directed towards the mainland coast to the north, north-west and west from the Klaipėda Strait, thus covered two fold smaller area of the Sea than the estuarine water masses directed south-east, southwards (20% of all investigated cases).

4. The estuarine waters are characterized by 7 fold higher concentration of chlorophyll *a*, by 3 fold higher values of both absorption of coloured dissolved organic matter and concentration of total suspended matter in comparison to the brackish coastal waters. It confirms that the outflow of the Curonian Lagoon waters is the main source of optically active components in the coastal waters of Lithuanian Baltic Sea.

5. The estuarine waters are characterized by 7 fold higher phytoplankton biomass. Phytoplankton was dominated by algae and cyanobacteria belonging to three classes: Cyanophyceae comprised more than 50% of total phytoplankton biomass, Bacillariophyceae – 30% and Chlorophyceae – 15%. Phytoplankton of brackish coastal waters was characterized by more heterogeneous structure at the level of classes: Cyanophyceae - 50%, Dinophyceae– 25%, Cryptophyceae, Prymnesiophyceae, Bacillariophyceae, Prasinophyceae and Chlorophyceae comprised 5–10% of total biomass each.

7. REFERENCE

- Alenius, P., Myrberg, K. and Nekrasov, A., 1998. The physical oceanography of the Gulf of Finland: a review. *Boreal Environment Research* 3, 97–125.
- Alikas, K., Kangro, K., Reinart, A., 2010. Detecting cyanobacterial blooms in large North European lakes using the Maximum Chlorophyll Index. *Oceanologia* 52(2), 237–257.
- Amon, R.M.W., Benner, R., 1998. Seasonal patterns of bacterial abundance and production in the Mississippi River plume and their importance for the fate of enhanced primary production. *Microbial Ecology* 35, 289–300.
- Bailey, W. S. and Werdell, J. P., 2006. A multi-sensor approach for the on-orbit validation of ocean color satellite data products, *Remote Sensing of Environment* 102, 12–23.
- Bianchi, T. S., Engelhaupt, E., Westman, P., Andr'en, T., Rolff, C. and Elmgren, R., 2000. Cyanobacterial blooms in the Baltic Sea: Natural or human induced?, *Limnology and Oceanography* 45, 716–726.
- Bidigare, R.R., Ondrusek, M.E. & Brooks, J.M., 1993. Influence of the Orinoco River outflow on distributions of algal pigments in the Caribbean Sea, *Journal of Geophysical Research* 98, 2259–2269.
- Bierman, P., Lewis, M., Ostendorf, B., Tanner, J., 2011. A review of methods for analysis spatial and temporal patterns in coastal water quality, *Ecological Indicators* 11, 103–114.
- Blough, N. V. and Del Vecchio, R., 2002. Chromophoric DOM in the coastal environment. In: *Biochemistry of Marine Dissolved organic Matter*, eds. D. A. Hansell and C. A. Carlson, Academic Press, Cambridge, MA, 509-546.
- Blough, N.V. and Green, S.A., 1995. Spectroscopic characterization and remote sensing of non-living organic matter. In: *Zepp, R.G. and*

Sonntag, C. (Eds.) The role of non-living organic matter in the earth's carbon cycle. John Wiley and Sons, 23–45.

Bowman, M. J. and Iverson, R. L., 1987. Estuarine and plume fronts. In: *Oceanic Fronts in Coastal Processes*, M. Bowman and W. Esaias (Eds.), New Yourk, Springer-Verlag, 87–104.

Bresciani, M., Giardino, C., Stroppiana, D., Pilkaitytė, R., Žilius, M., Bartoli, M., Razinkovas, A., 2012. Retrospective analysis of spatial and temporal variability of chlorophyll-a in the Curonian Lagoon. *Journal of coastal conservation* DOI 10.1007/s11852-012-0192-5, 1–9.

Bresciani, M., Stroppiana, D., Odermatt, D., Morabito, G., Giardino, C., 2011. Assessing remotely sensed chlorophyll-a for the implementation of the Water Framework Directive in European perialpine lakes, *Science of the Total Environment* 409, 3083–3091.

Brockmann, C., 2006. Limitations of the application of the MERIS atmospheric correction, *Proceedings of the Second Working Meeting on MERIS and AATSR Calibration and Geophysical validation (MAVT-2006)*, 20-24 March, Frascati, Italy, ESA SP-615.

Bučas, M., 2009. Distribution patterns and ecological role of the red alga *Furcellaria lumbricalis* (Hudson) J.V. Lamouroux off the exposed Baltic Sea coast of Lithuania. Doctoral Dissertation, Klaipėda, 124 pp.

Bukata, R.P., Jerome, J.H., Kondratyev, K.Y., Pozdnyakov, D.V., 1991. Satellite monitoring of optically active components of inland waters: an essential input to regional climate change impact studies. *J Great Lakes Res* 17(4), 470–478.

Bushaw, K.L., Zepp, R.G., Tarr, M.A., Schulz-Jander, D., Bourbonniere, R.A., Hodson, R.E., Miller W.L., Bronk D.A. and Moran, M.A., 1996. Photochemical release of biologically available nitrogen from aquatic dissolved organic matter, *Nature* 381, 404–407.

Buszewski, B., Buszewska, T., Chmarzyński, A., Kowalkowski, T., Kowalska, J., Kosobucki, P., Zbytniewski, R., Namieśnik, J., Kot-

- Wasik, A., Pacyna, J., Panasiuk, D., 2005. The present condition of the Vistula river catchment area and its impact on the Baltic Sea coastal zone. *Reg Environ Change* 5, 97–110.
- Caddy, J.F. 2000. Marine catchment basin effects versus impacts of fisheries on semi-enclosed seas. *ICES J.Mar.Sci.*, 57, 628–640.
- Capone, D.G. and Subramaniam, A., 2007. Seeing Microbes from Space, *ASM News* 71(4), 179–186.
- Carlson, R.E., 1977. A trophic state index for lakes. *Limnol. Oceanogr.* 22, 361–369.
- Červinskas, E., 1959. Characteristics of hydrological regime. The Curonian Lagoon, Vilnius, 47–68. [in Russian]
- Chao, S.-Y., 1988. Wind-driven motion of estuarine plumes. *Journal of Physical Oceanography* 18, 1144–1166.
- Chesney, E.J., Baltz, D.M., Thomas, R.G., 1998. Louisiana estuarine and coastal fisheries and habitats: perspectives from a fish's eye view. *Ecological Applications*.
- Clark, R.B., 1986. *Marine Pollution*. Clarendon Press, Oxford, 215 pp.
- COAST, 2002. Guidance on typology, reference conditions and classification systems for transitional and coastal waters. CIS working group 2.4, 121 pp.
- Coble, P., Hu, Ch., Gould Jr., R.W., Chang, G. and Wood, A.M., 2004. Colored Dissolved Organic Matter in the Coastal Ocean. An optical tool for coastal zone environmental assessment and management, *Oceanography* 17(2), 51–59.
- Connolly, R.M., Schlacher, T.A., Gaston, T.F., 2009. Stable isotope evidence for trophic subsidy of coastal benthic fisheries by river discharge plumes off small estuaries. *Marine Biology Research* 5, 164–171.
- Dagg, M., Benner, R., Lohrenz, S., Lawrence, D., 2004. Transformation of dissolved and particulate materials on continental

shelves influenced by large rivers: plume processes. *Continental Shelf Research* 24, 833–858.

Dagg, M.J., Ortner, P.B., 1995. Zooplankton grazing and the fate of phytoplankton in the northern Gulf of Mexico. In: *Nutrient-enhanced Coastal Ocean Productivity, Proceedings of the April 1994 Synthesis Workshop*, Baton Rouge, Louisiana. Louisiana Sea Grant College Program, Baton Rouge, Louisiana, 21–27.

Dailidienė I., Davulienė L., 2008. Salinity trend and variation in the Baltic Sea near the Lithuanian coast and in the Curonian Lagoon in 1984–2005, *Journal of Marine Systems* 74, S20–S29.

Dailidienė, I., Davulienė L., 2007. Long-term mean salinity in the Curonian Lagoon in 1993–2005. *Acta Zoologica Lituanica*, 17(2), 172–181.

Dailidienė, I., Davulienė, L., Kelpšaitė, L. and Razinkovas, A., 2012. Analysis of the Climate Change in Lithuanian Coastal Areas of the Baltic Sea, *Journal of Coastal Research* 28(3), 557–569.

Dailidienė, I., Davulienė, L., Tilickis, B., Stankevičius, A. and Myrberg, K., 2006. Sea level variability at the Lithuanian coast of the Baltic Sea, *Boreal Environmental Research* 11, 109–121.

Dailidienė. I., Baudler H., Chubarenko B., Navarotskaya S., 2011. Long term water level and surface temperature changes in the lagoons of the southern and eastern Baltic. *Oceanologia* 53(1-TI), 293–308.

Darecki, M., Kaczmarek, S., Olszewski, J., 2005. SeaWiFS ocean colour chlorophyll algorithms for the southern Baltic Sea. *Int. J. Remote Sensing* 26(2), 247–260.

Daunys, D., Olenin, S., Paškauskas, R., Zemlys, P., Olenina, I., Bučas, M., 2007. Typology and classification of ecological status of Lithuanian coastal and transitional waters: an update of existing system, procurement of services for the institutional building for the Nemunas River basin management, Tech. Rep. Transit. Fac. Proj. No. 2004/016-925-04-06.

Dekker, A.G., Peters, S.W.M., Vos, R.J., Rijkeboer, M., 2001. Remote sensing for inland water quality detection and monitoring: state-of-the-art application in Friesland waters. In: Van Dijk, A., Bos, M.G. (Eds.) GIS and Remote Sensing Technology in Land and Water Management. Kluwer Academic Publishers, Netherlands, 17-38.

DeMaster, D.J., Pope, R., 1996. Nutrient dynamics in amazon shelf waters: results from AMASSEDS. *Continental Shelf Research* 16, 263–289.

Devlin, M.J., McKinna, L.W., Álvarez-Romero, J.G., Petus, C., Abott, B., Harkness, P., Brodie, J., 2012. Mapping the pollutants in surface riverine flood plume waters in the Great Barrier Reef, Australia. *Marine Pollution Bulletin*, 65(4–9), 224–235.

Directive, 2000. Directive 2000/60/EC of the European Parliament and of the council of 23 October 2000 establishing a framework for community action in the field of water policy. *Off J Eur. Communities*, L327, 1–72.

Directive, 2008. Directive 2008/56/EC of the European Parliament and of the council of 17 June 2008 establishing a framework for community action in the field of marine environmental policy (Marine Strategy Framework Directive). *Official Journal of the European Union*, L164, 19–40.

Doerffer, R. and Schiller, H., 2000. Neural Network for Retrieval of Concentrations of Water Constituents with the Possibility to Detecting Exceptionall out of Scope Spectra, *IEEE 2000 International Geoscience and Remote Sensing Symposium*, 24-28 July, Honolulu Hawaii USA, Vol. II, ISBN 0-7803-6359-0, 714–717.

Doerffer, R. and Schiller, H., 2008a. MERIS lake water algorithm for BEAM ATBD, GKSS Research Center, Geesthacht, Germany, Version 1.0, 10 June.

Doerffer, R. and Schiller, H., 2008b. MERIS Regional Coastal and Lake Case 2 Water Project - Atmospheric Correction ATBD, GKSS Research Center 21502 Geesthacht Version 1.0 18. May.

- Doerffer, R., 2002. Protocols for the validation of MERIS water products, European Space Agency Doc. No. PO-TN-MEL-GS-0043.
- Doerffer, R., 2006. MERIS Case I validation, *Proceedings of the Second Working Meeting on MERIS and AATSR Calibration and Geophysical Validation*, CD SP-615.
- Doerffer, R., 2008. Atmosphere and Glint Correction Project, Algorithm Theoretical Basis Document (ATBD), Version 1.0, 1 September 2008, 45 pp.
- Doerffer, R., Sørensen, K. & Aiken, J., 1999. MERIS potential for coastal zone application, *International Journal of Remote Sensing* 20(9), 1809–1818.
- Dubra, J., 1970. Sea level changes in the Curonian Lagoon. *Articles of Hydrometeorology* 3, 99–106.
- Dubra, J., Červinskis, E., 1968. The balance of fresh water of the Curonian Lagoon. *The works of Academies of Lithuanian TSR. Geography and geology*, 5, 19–26. [in Lithuanian].
- Erm, A., Alari, V., Lips, I., Kask, J., 2011. Resuspension of sediment in a semi-sheltered bay due to wind waves and fast ferry wakes. *Boreal Environment Research* 16 (suppl.A), 149–163.
- ESA, 2006. MERIS Product Handbook, Issue 2.1, 24th October, Available at:
http://earth.esa.int/pub/ESA_DOC/ENVISAT/MERIS/meris.ProductHandbook.2_1.pdf.
- Ferrarin C., Razinkovas A., Gulbinskas S., Umgiesser G. and Bliūdžiūtė L., 2008. Hydraulic regime-based zonation scheme of the Curonian Lagoon. *Hydrobiologia* 611 (1), 133–146.
- Filardo, M.J., Dunstan, W.N., 1985. Hydrodynamic control of phytoplankton in low salinity waters of the James River estuary, Virginia, USA. *Estuarine Coastal Shelf Science* 21, 653–667.

- Fisher, T.R., Peele, E.R., Ammerman, J.W., Harding, L.W.J., 1992. Nutrient limitation of phytoplankton in Chesapeake Bay. *Marine Ecology Progress Series* 82, 51–63.
- Flint, R.W., Powell, G.L., Kalke, R.D., 1986. Ecological effects from the balance between new and recycled nitrogen in Texas coastal waters. *Estuaries* 9, 284–294.
- Fomferra, N. and Brockmann C., 2006. The BEAM project web page, Brockmann Consult, Hamburg, Germany Available from: <http://www.brockmann-consult.de/beam/>.
- Franks, P.J.S. and Anderson, D. M., 1992. Alongshore transport of a toxic phytoplankton bloom in a buoyancy current: *Alexandrium tamarense* in the Gulf of Maine. *Marine Biology* 112, 153–164.
- Franks, P.J.S., 1992. Phytoplankton Blooms at Fronts: Patterns, Scales, and Physical Forcing Mechanisms. *Reviews in Aquatic Science*, 6(2), 121–137.
- Gailiušis B., Kovalenkoviene M., Kriauciuniene. 2005. Hydrological and hydraulic investigations in the Curonian Lagoon territory between Kiaules nugara and Alksnyne. *Energetika* 4, 34–41. [in Lithuanian]
- Gailiušis B., Kriauciūnienė J., Kriauciūnas R. 2004. Changes of the hydrodynamical regime of Klaipėda Strait due to reconstruction of piers. *Energetika* 1, 57–61. [in Lithuanian].
- Gailiušis, B., Jablonskis, J. and Kovalenkoviene, M., 2001. Lithuanian rivers: hydrography and runoff, Lithuanian Energy Institute, Kaunas. [in Lithuanian with English summary].
- Gailiušis, B., Kriauciūnienė, J., Jakimavičius, D., Šarauskiene, D., 2011. The variability of long-term runoff series in the Baltic Sea drainage basin. *Baltica* 24(1), 45–54.
- Galkus, A., 2003. Summer water circulation and spatial turbidity dynamics in the Lithuanian waters of Curonian Lagoon and Baltic Sea, *Chronics of Geography* 36(2), Vilnius ISSN 0132-3156, 48–60. [in Lithuanian with English summary].

- Galkus, A., 2007. Specific fresh and saline water circulation patterns in the Klaipėda Strait and northern part of Curonian Lagoon. *Annales Geographicae* 40(1), 3–19.
- Galkus, A., Jokšas, K., 1997. Sedimentary material in the transitional aquasystem. Institute of Geography. Vilnius. 198 pp.
- Garvine, R.W., Monk, J.D., 1974. Frontal structure of a river plume. *Journal of Geophysical Research* 79, 2251–2259.
- Gasiūnaitė, Z. R., Cardoso, A. C., Heiskanen, A.-S., Henriksen, P., Kauppila, P., Olenina, I., Pilkaitytė, R., Purina, I., Razinkovas, A., Sagert, S., Schubert, H., Wasmund, N., 2005. Seasonality of coastal phytoplankton in the Baltic Sea: influence of salinity and eutrophication, *Estuarine, Coastal and Shelf Science* 65, 239–252.
- Gasiūnaitė, Z.R., Daunys, D., Omenin, S., Razinkovas, A., 2008. The Curonian Lagoon, In: U. Schiewer (ed.) *Ecology of Baltic coastal waters*, *Ecol. Stud.* 197, 197–216.
- Gelfenbaum, G., Stumpf, R. P., 1993. Observations of currents and density structure across a buoyant plume front. *Estuaries*, *Estuaries* 16(1), 40–52.
- Gelumbauskaitė, L.Z., Grigelis, A., Cato, I., Repečka, M., Kjellin, B., 1999. Bottom topography and sediment maps of the Central Baltic Sea. LGT series of marine geological maps No. 1, SGU series of geological maps Ba No. 54, Scale 1:500000, Vilnius, Uppsala, Lithuanian-Swedish project GEOBALT.
- Geyer, W.R., 1986. Modeling the motion of an estuarine front. *Eos, Trans. American Geophysical Union*, 67(16), 295 pp.
- Geyer, W.R., Beardsley, R.C., Candela, J., Castro, B.M., Legeckis, R.V., Lentz, S.J., Limeburner, R., Miranda, L.B. and Trowbridge, J.H., 1991. The physical oceanography of the Amazon outflow. *Oceanography* 4, 8–14.
- Giardino, C., Bresciani, M., Pilkaitytė, R., Bartoli, M., Razinkovas, A., 2010a. *In situ* measurements and satellite remote sensing of case 2

waters: first results from the Curonian Lagoon, *Oceanologia* 52(2), 197–210.

Giardino, C., Bresciani, M., Villa, P., Martinelli, A., 2010b. Application of Remote Sensing in Water Resource Management: The Case Study of Lake Trasimeno, Italy, *Water Resources Management* 24(14), 3885–3899.

Glasby, G.P., Szefer, P., 1998. Marine pollution in Gdansk Bay, Puck Bay and the Vistula Lagoon, Poland: An overview. *Science of the Total Environment* 212, 49–57.

Gower, J.F.R., Hu, C., Borstad, G.A., King, S., 2006. Ocean color satellites show extensive lines of floating *Sargassum* in the Gulf of Mexico, *IEEE T. Geosci. Remote* 44(12), 3619–3625.

Gower, J.F.R., King, S. and Goncalves, P. 2008. Global monitoring of plankton blooms using MERIS MCI. *International Journal of Remote Sensing* 29(21), 6209–6216.

Gower, J.F.R., King, S., 2007. An Antarctic ice-related ‘superbloom’ observed with the MERIS satellite imager, *Geophysical Research Letter*, 34, L15501, doi:10.1029/2007GL029638.

Graham, L.E., Wilcox, L.W., 2000. *Algae*. Upper Saddle River, NJ 07458.

Grimes, C.B., Finucane, J.H., 1991. Spatial distribution and abundance of larval and juvenile fish, chlorophyll and macrozooplankton around the Mississippi River discharge plume, and the role of the plume in fish recruitment. *Marine Ecology Progress Series* 75, 109–119.

Guillard, R. R. L., 1962. Salt and osmotic balance. In: R.A. Lewin (ed.), *Physiology and Biochemistry of Algae*. Academic Press, New York and London, 929 pp.

Guiry, M.D. and Guiry, G.M., 2012. *AlgaeBase*. World-wide electronic publication, National University of Ireland, Galway. <http://www.algaebase.org>; searched on 17 September 2012.

Hajdu, S., Edler, L., Olenina, I., Witek, B., 2000. The alien species *Prorocentrum minimum* in the Baltic Sea: its occurrence, distribution, and environmental requirements, J Internat Rev Hydrobiol 85, 557–571.

Håkanson, L., 1999. Water Pollution – Methods and Criteria to Rank, Model and Remediate Chemical Threats to Aquatic Ecosystems. Backhuys Publishers, Leiden, 299 pp.

Håkanson, L., Andersson, M. and Ryden, L., 2003. The Baltic Sea Basin - Nature, History and Economy. In: Ryden, L., Migula, P. and Andersson, M. (eds.), Environmental Science, The Baltic Univ. Press, Uppsala, 92–119.

Håkanson, L., Mikrenska, M., Petrov, K., Foster, I.D.L., 2005. Suspended particulate matter (SPM) in rivers—empirical data and models. Ecol Model 183, 251–267.

Hansson, M. and Öberg, J., 2010. Cyanobacterial blooms in the Baltic Sea. HELCOM Indicator Fact Sheets 2010. Online. [2012-09-07], http://www.helcom.fi/BSAP_assessment/ifs/ifs2010/en_GB/Cyanobacterial_blooms/.

Harvey, T., Kratzer, S., Andersson, A., Philipson, P., 2011. Bio-optical properties of the Baltic Sea -a comparison of coastal waters in the NW Baltic Proper and The Gulf of Bothnia. 3rd CoastColour User Consultation Meeting.

Haury, L.R., McGowan, J.A. and Wiebe, P.H., 1978. Patterns and processes in the time-space scales of plankton distribution. In: J.H. Steele (ed.) Spatial Patterns in Plankton Communities, Plenum Press, NY.

HELCOM, 1988. Guidelines for the Baltic Monitoring Programme for the third stage, Part D. Biological determinands. Baltic Sea Environment Proceedings No. 27 D. Baltic Marine Environment Protection Commission, Helsinki Commission. 164 pp.

HELCOM, 1996. Third periodic assessment of the state of the marine environment of the Baltic Sea, 1989-1993, background document. Baltic Sea Environment Proceedings No. 64B, 1–252.

HELCOM, 2007. The HELCOM Baltic Sea action plan. Available from:

http://www.helcom.fi/press_office/news_helcom/en_GB/BSAP_full/.

Hindák, K., 2001. Fotografický atlas mikroskopických sinic, Bratislava, 340 p.

Hochberg, E. J., Andrefouet, S. & Tyler, M. R., 2003. Sea surface correction of high spatial resolution IKONOS images to improve bottom mapping in near-shore environments, IEEE Transactions on Geoscience and Remote Sensing 41, 1724–1729.

Horstmann, U., 1983. Distribution patterns of temperature and water colour in the Baltic Sea as recorded in satellite images: Indicators for phytoplankton growth. Berichte Institut für Meereskunde Kiel 106, 145 pp.

Hulatt, Ch.J., Thomas, D.N., Bowers, D.G., Norman, L., Zhang, Ch., 2009. Exudation and decomposition of chromophoric dissolved organic matter (CDOM) from some temperate macroalgae, Estuarine, Coastal and Shelf Science 84, 147–153.

Ianora A., Bentley, M., Caldwell, G., Casotti, R., Cembella, C., Engstrom-ost J., Halsbank-lenk, C., Sonnenschein E., Legrand, C., Llewellyn C., Paldaviciene, A., Pohnert G., Pilkaityte, R., Razinkovas, A., Romano, G., Tillmann, U., Vaičiūtė, D., 2011. The Relevance of Marine Chemical Ecology to Plankton and Ecosystem. Marine Drugs, 9, 1625–1648.

Implementation of the EU Water Framework Directive, 2004. Meeting 2006 deadlines. Danish Environmental Protection Agency, DANCEE and the Ministry of Environment of Lithuania. DEPA reference number 124/025-0225. 78 pp.

IOCCG Report Number 3, 2000. Remote Sensing of Ocean Colour in Coastal, and Other Optically-Complex, Waters. Eds. Shubha Sathyendranath, MacNab Print, Dartmouth, Canada, 140 pp..

Jakimavičius, D., Kovalenkoviėnė, M., 2010. Long-term water balance of the Curonian Lagoon in the context of anthropogenic factors and climate change. *Baltica* 23(1), 33–46.

Jeffrey, S. W., Humphrey, G. F., 1975. New spectrophotometric equation for determining chlorophyll a, b, c1 and c2, *Biochem. Physiol. Pfl.* 167, 194–204.

Jokšas, K., Galkus, A., Stakėnienė, R., 2005. Geoecological state of the Lithuanian offshore of the Baltic Sea, the lower reaches of Nemunas and the Curonian Lagoon. *Acta Zoologica Lituanica* 15(2), 119–123.

Jönsson, B.F., Döös, K., Myrberg, K., Lundberg, P.A., 2011. A Lagrangian-trajectory study of a gradually mixed estuary. *Continental Shelf Research* 31, 1811–1817.

Jurgensone, I., Carstensen, J., Ikauniece, A., Kalveka, B., 2011. Long-term changes and controlling factors of phytoplankton community in the Gulf of Riga (Baltic Sea). *Estuaries and Coasts* 34, 1205–1219.

Kahru, M., 1997. Using satellites to monitor large-scale environmental change: A case study of cyanobacteria blooms in the Baltic Sea. In: Kahru M, Brown CW (eds.) *Monitoring Algal Blooms*. Springer-Verlag, Berlin Heidelberg New York, 43–57.

Kahru, M., Elken, J., Kotta, I., Simm, M. and Vilbaste, K., 1984. Plankton distribution and processes across a front in the open Baltic Sea. *Marine Ecology Progress Series* 20, 101–111.

Kahru, M., Horstmann, U., Rud, O., 1994. Satellite detection of increased Cyanobacteria blooms in the Baltic Sea: Natural fluctuations or ecosystem change? *Ambio* 23(8), 469–472.

Karlsson, K.G., 1996. Cloud classifications with the SCANDIA model. SMHI reports meteorology and climatology, No. 67.

- Kelpšaitė, L., Dailidienė, I., Soomere, T., 2011. Changes in wave dynamics at the south-eastern coast of the Baltic Proper during 1993–2008. *Boreal Environment research* 16 (suppl.A), 220–223.
- Kemp, W.M., Boynton, W.R., 1984. Spatial and temporal coupling of nutrient inputs to estuarine primary production: the role of particulate transport and decomposition. *Bulletin of Marine Science* 35(3), 242–247.
- Kirk, J.T.O., 2011. *Light and Photosynthesis in Aquatic Ecosystems*, 3rd edition, Cambridge, Cambridge University Press, 662 pp.
- Klavins, M., Briede, A., Rodinovs, V., Kokorite, I. and Frisk, T., 2002. Long-term changes of the river runoff in Latvia. *Boreal Environment Research* 7, 447–456.
- Komárek J., Anagnostidis K., 1999. Cyanoprokaryota, 1. Teil: Chroococcales, Süßwasserflora von Mitteleuropa, Jena-Stuttgart-Lübeck-Ulm.
- Komárek J., Foot B., 1983. Chlorophyceae (Grünalgen) Ordnung: Chloococcales. *Das Phytoplankton des Süßwassers* 7(1) Stuttgart, 1–1044.
- Kononen, K., 1992. Dynamics of the toxic cyanobacteria blooms in the Baltic Sea, *Finnish Marine Research* 261, 3–36.
- Kononen, K., Kuparinen, J. and Mäkelä, K., Laanemets, J., Pavelson, J., Nõmmann, S., 1996. Initiation of cyanobacterial blooms in a frontal regions at the entrance to the Gulf of Finland, Baltic Sea. *Limnol. Oceanogr.* 41(1), 98–112.
- Kononen, K., Leppänen, J.M., 1997. Patchiness, scales and controlling mechanisms of cyanobacterial blooms in the Baltic Sea: Application of a multiscale research strategy. In: M., Kahru, C.W., Brown (eds.) *Monitoring Algal Blooms*. Springer-Verlag, Berlin Heidelberg New York, 43–57.
- Koponen, S., Kallio, K., Pulliainen, J., Vepsäläinen, J., Pyhälähti, T., Hallikainen, M., 2004. Water quality classification of lakes using 250-

m MODIS data MERIS data. IEEE Geoscience and Remote Sensing letters 1(4), 287–291.

Koponen, S., Ruiz-Verdu, A., Heege, T., Heblinski, J., Sørensen, K., Kallio, K., Pyhälähti, T., Doerffer, R., Brockmann, C. and Peters, M., 2008. Development of MERIS lake water algorithms, Validation Report. Available from: http://www.brockmann-consult.de/beam-wiki/download/attachments/8355860/MERIS_LAKES_Validation_report.pdf.

Korshenko, A.N., 1991. The heterogeneity of zooplankton distribution according to the hydrological water structure. Summary of doctoral dissertation. Sevastopol, 24 pp. [in Russian].

Kowalczyk, P., Zablocka, M., Sagan, S., Kuliński, K., 2010. Fluorescence measured in situ as a proxy of CDOM absorption and DOC concentration in the Baltic Sea. *Oceanologia*, 52 (3), 431–471.

Kramer K., Lange-Bertalot H., 1986. Süßwasserflora von Mitteleuropa. Bacillariophyceae. Teil 1: Naviculaceae, Stuttgart-New York.

Kramer K., Lange-Bertalot H., 1988. Süßwasserflora von Mitteleuropa. Bacillariophyceae. Teil 2: Bacillariaceae, Epithemiaceae, Surirellaceae, Stuttgart-New York.

Kramer K., Lange-Bertalot H., 1991a. Süßwasserflora von Mitteleuropa. Bacillariophyceae. Teil 3: Centraceae, Fragilariaceae, Eunotiaceae, Stuttgart-Jena.

Kramer K., Lange-Bertalot H., 1991b. Süßwasserflora von Mitteleuropa. Bacillariophyceae. Teil 4: Achnanthaceae, Kritische Ergänzungen zu Navicula (Lineolatae) und Gomphonema, Stuttgart-Jena.

Kratzer, S. and Tett, P., 2009. Using bio-optics to investigate the extent of coastal waters a Swedish case study, *Hydrobiologia* 629, 169–186.

Kratzer, S., Brockmann, C. & Moore, G., 2008. Using MERIS full resolution data to monitor coastal waters — A case study from Himmerfjärden, a fjord-like bay in the northwestern Baltic Sea, *Remote Sensing of Environment* 112(5), 2284–2300.

Kratzer, S., Ebert K. and Sørensen, K., 2011. Monitoring the Bio-optical State of the Baltic Sea Ecosystem with Remote Sensing and Autonomous In Situ Techniques. In: Harff, J., Björck, S., Hoth, P. (Eds.) *The Baltic Sea Basin*. Springer, 449 pp.

Kratzer, S., Håkansson, B., Sahlin, C., 2003. Assessing Secchi and photic zone depth in the Baltic Sea from space, *Ambio* 32(8), 577–585.

Kratzer, S., Vinterhav, C., 2010. Improvement of MERIS level 2 products in Baltic Sea coastal areas by applying the Improved Contrast between Ocean and Land processor (ICOL) – data analysis and validation, *Oceanologia* 52(2), 211–236.

Kruk, M., Mroz, M., Nawrocka, L., Parszuto, K., Mleczko, M., 2010. Uniseasonal dynamics of main water quality parameters in Vistula Lagoon extracted from Envisat/MERIS geophysical products and *in situ* measurements, “Proceedings “Hyperspectral 2010 Workshop”, Frascati, Italy, ESA publication SP-683.

Kutser, T., 2004. Quantitative detection of chlorophyll in cyanobacterial blooms by satellite remote sensing. *Limnology and Oceanography* 49, 2179–2189.

Kutser, T., 2009. Passive optical remote sensing of cyanobacteria and other intense phytoplankton blooms in coastal and inland waters. *International Journal of Remote Sensing* 30(17), 4401–4425.

Kutser, T., Metsamaa, L., Dekker, A.G., 2008. Influence of the vertical distribution of cyanobacteria in the water column on the remote sensing signal. *Estuarine, Coastal and Shelf Science* 78, 649–654.

Kutser, T., Metsamaa, L., Strombeck, N., Vahtmae, E., 2006. Monitoring cyanobacteria blooms by satellite remote sensing, *Estuarine, Coastal and Shelf Science* 67, 303–312.

Kutser, T., Metsamaa, L., Vahtmae, E. and Strombeck, N., 2006. On suitability of MODIS 250 m resolution band data for quantitative mapping cyanobacterial blooms. *Proceedings of the Estonian Academy of Sciences. Biology-Ecology* 55, 318–328.

Kutser, T., Vahtmäe, E., Praks, J., 2009. A sun glint correction method for hyperspectral imagery containing areas with non-negligible water leaving NIR signal, *Remote Sensing of Environment* 113, 2267–2274.

Lampe, R., 1993. Environmental state and material flux in the western part of the Oder river estuary: results and consequences. *Petermanns Geographische Mitteilungen* 137, 275–282.

Langas, V., Daunys, D., Paškauskas, R., Zemlys, P., Pilkaitytė, R., Razinkovas, A., Gulbinukas, S., 2009. Status of transitional and costal waters, environmental factors and measures to improve environmental status. Part II, 136 pp. [in Lithuanian].

Largier, J.L., 1993. Estuarine fronts: How Important Are They? *Estuaries* 16(1), 1–11.

Leppäranta, M. and Myrberg, K. 2009. Water, salt and heat budget, [In:] *Physical oceanography of the Baltic Sea*, P. Blondel (ed.), Springer-Praxis, Heidelberg, Germany, 378 pp.

Liu, H., Dagg, M., 2003. Interactions between nutrients, phytoplankton growth, and micro- and mesozooplankton grazing in the plume of the Mississippi River. *Marine Ecology Progress Series* 258, 31–42.

Loder, J. and Platt, T., 1985. Physical controls on phytoplankton production at tidal fronts. [In:] *Proceedings of the 19th European Marine Biology Symposium*, P.E. Gibbs (eds.) Cambridge, Cambridge University Press, 3–22.

Lohrenz, S.E., Fahnenstiel, G.L., Redalje, D.G., Lang, G.A., Chen, X., Dagg, M.J., 1997. Variations in primary production of northern Gulf of Mexico continental shelf waters linked to nutrient inputs from the Mississippi River. *Marine Ecology Progress Series* 155, 45–54.

Malone, C., Crocker, L.H., Pike, S.E., Wendler, B.W., 1988. Influences of river flow on the dynamics of phytoplankton production in a partially stratified estuary. *Marine Ecology- Progress Series* 48, 235–249.

Management plan of Nemunas River basin region, 2010. Environmental Protection Agency, Vilnius, 333 pp. [in Lithuanian].

Mann, K.H. and Lazier, J.R.N., 1991. *Dynamics of Marine Ecosystems: Biological-Physical Interactions in the Ocean*. Blackwell Scientific Publications, Cambridge, 466 pp.

Mayer, L.M., Keil, R.G., Macko, S.A., Joye, S.B., Ruttenger, K.C., Aller, R.C., 1998. Importance of suspended particulates in riverine delivery of bioavailable nitrogen to coastal zones. *Global Biogeochemical Cycles* 12, 573–579.

Metsamaa, L., Kutser, T., Strömbeck, N., 2006. Recognising cyanobacterial blooms based on their optical signature: a modelling study. *Boreal Environment Research* 11, 493–506.

Mobley, C. D., 1994. *Light and Water – Radiative Transfer in Natural Waters*, San Diego, Academic Press, 529 pp.

Moisander, P.H., Rantajärvi, E., Huttunen, M. and Kononen, K., 1997. Phytoplankton community in relation to salinity fronts at the entrance to the Gulf of Finland, Baltic Sea. *Ophelia* 46(3), 187–203.

Moran M.A. and Zepp R.G., 1997. Role of photoreactions in the formation of biologically labile compounds from dissolved organic matter, *Limnology and Oceanography* 42, 1307–1316.

Morel A. and Prieur L., 1977. Analysis of variations of ocean colour, *Limnology and Oceanography* 22, 709–722.

MSFD 3rd intermediary report, 2012. Preparation of the documents for the management of the environmental protection of the Baltic Sea of Lithuania. (Lietuvos Baltijos jūros aplinkos apsaugos valdymo stiprinimo dokumentų parengimas). 3rd intermediate report, Consortium of marine research, Klaipėda, 497 pp. (in Lithuanian).

Muylaert, K., Sabbe, K., Vyverman, W., 2009. Changes in phytoplankton diversity and community composition along the salinity gradient of the Schelde estuary (Belgium/The Netherlands). *Estuarine, Coastal and Shelf Science* 82, 335–340.

Neumann, A., Krawczyk, H., Borg, E. and Fichtelmann, B., 2002. Towards Operational Monitoring of the Baltic Sea by Remote Sensing, [In:] G. Schernewski & N. Löser (eds.): *Managing the Baltic Sea*. *Coastline Reports* 2, ISSN 0928-2734, 211–218.

Ohde, T., Siegel, H. and Gerth, M., 2007. Validation of MERIS Level-2 products in the Baltic Sea, the Namibian coast and the Atlantic Ocean, *International Journal of Remote Sensing* 28(3-4), 609–624.

Olenin, S. and Daunys, D., 2004. Coastal typology based on benthic biotope and community data: the Lithuanian case study, In: *Baltic Sea Typology*, eds. G. Schernewski & M. Wielgat, *Coastline Reports* 4, 65–83.

Olenin, S., 2005. *Invasive Aquatic Species in the Baltic States*. Klaipėda, 42 pp.

Olenin, S., Daunys, D. and Leinikki, J., 2003. Biodiversity study and mapping of marine habitats in the vicinity of the Būtingė Oil Terminal, Lithuanian coastal zone, Baltic Sea, Joint Finnish – Lithuanian project report, pp. 30, Coastal Research and Planning Institute, Klaipėda University, Klaipėda.

Olenina, I. 2004. Technical Note X: Phytoplankton of the Curonian Lagoon and the Lithuanian coastal waters of the Baltic Sea. Danish Environmental Protection Agency, DANCEE and the Ministry of Environment of Lithuania. DEPA reference number 124/025-0225. 78 pp.

Olenina, I. and Kavolytė, R., 1996. Phytoplankton, chlorophyll *a* and environmental conditions in the southeastern coastal zone of the Baltic Sea, Proceedings of the 13th Symposium of the Baltic Marine Biologists, 53-61, Jūrmala, Latvia.

Olenina, I. and Olenin, S., 2002. Environmental problems of the South-Eastern Coast and the Curonian Lagoon, In: Baltic coastal ecosystems. Structure, Function and Coastal Management, eds. E. Schernewski & U. Schiewer, Berlin, Heidelberg, New York, Springer-Verlag, 149–156.

Olenina, I., 1997. Phytoplankton of the Kursiu marios lagoon and the south-eastern Baltic coastal zone. Doctoral Dissertation, Vilnius, 159 pp. [in Russian].

Olenina, I., Hajdu, S., Edler, L., Andersson, A., Wasmund, N., Busch, S., Göbel, J., Gromisz, S., Huseby, S., Huttunen, M., Jaanus, A., Kokkonen, P., Ledaine, I. and Niemkiewicz, E. 2006. Biovolumes and size-classes of phytoplankton in the Baltic Sea. HELCOM Baltic Sea Environmental Proceedings, No. 106, 144 pp.

Olenina, I., Wasmund, N., Hajdu, S., Jurgensone, I., Gromisz, S., Kownacka, J., Toming, K., Vaičiūtė, D., Olenin, S. 2010. Assessing impacts of invasive phytoplankton: The Baltic Sea case. Marine Pollution Bulletin 60, 1691–1700.

Öström, B., 1976. Fertilization of the Baltic by nitrogen fixation in the blue-green algae *Nodularia spumigena*. Remote Sensing of the Environment 4, 305–310.

Ou, H. W., 1984. Wind-driven motion near shelf-slope front. Journal of Physical Oceanography 14, 985–993.

Pastuszak, M., Nagel, K., Grelowski, A., Mohrholz, V., Zalewski, M., 2003. Nutrient dynamics in the Pomeranian Bay (southern Baltic): Impact of the Oder River outflow. Estuaries 26(5), 1238–1254.

Patt, F. S., 2002. Navigation algorithms for the SeaWiFS mission, NASA Tech. Memo. 206892, Greenbelt, MD: National Aeronautics and Space Administration, Goddard Space Flight Center.

- Pegau, W.S., Gray, D. and Zaneveld, J.R.V., 1997. Absorption and attenuation of visible and near-infrared light in water: dependence on temperature and salinity, *Applied Optics* 36, 6035–6046.
- Pepe, M., Brivio, P. A., Rampini, A., Rota Nodari, F. and Boschetti, M., 2005. Snow cover monitoring in Alpine regions using ENVISAT optical data, *International Journal of Remote Sensing* 26(21), 4661–4667.
- Pilkaitytė, R., Razinkovas, A., 2007. Seasonal changes in phytoplankton composition and nutrient limitation in a shallow Baltic lagoon, *Boreal Environmental Research* 12(5), 551–559.
- Pilkaitytė, R., Schoor, A. and Schubert, H., 2004. Response of phytoplankton communities to salinity changes – a mesocosm approach. *Hydrobiologia* 513, 27–38.
- Pöder, T., Maestrini, S.Y., Balode, M., Lips, U., Béchemin, Ch., Andriushaitis, A. and Purina, I., 2003. The role of inorganic and organic nutrients on the development of phytoplankton along a transect from Daugava River mouth to the Open Baltic, in spring and summer 1999. *ICES Journal of Marine Science*, 60, 827–835.
- Premazzi, G., Borsani, G., Cardoso, A.C., Chiaudani, G., Defreancesco, C., Kallio, K., Petterson, K., Pierson, D., Rodari, E., 1999. Methods in Limnology. In: Lindell, T., Pierson, D., Premazzi, G., Zilioli, E. (Eds.) *Manual for monitoring European lakes using remote sensing techniques*. Luxembourg, Office for Official Publications of the European Communities, 164 pp.
- Pustelnikovas, O., 1998. *Geochemistry of sediments of the Curonian Lagoon (Baltic Sea)*, Vilnius.
- Reimers, N.F., 1990. *Nature Management. Glossary*. Moscow. [in Russian].
- Reinart, A., Kutser, T., 2006. Comparison of different satellite sensors in detecting cyanobacterial bloom events in the Baltic Sea, *Remote Sensing of Environment* 102, 74–85.

- Remane, A., 1934. Die Brackwasserfauna, *Zool Anz* 7 (Suppl), 34–74.
- Rempel, R.S., Kaukinen, D. and Carr, A.P., 2012. Patch Analyst and Patch Grid. Ontario Ministry of Natural Resources. Centre for Northern Forest Ecosystem Research, Thunder Bay, Ontario.
- Reynolds, C.S., 1989. Physical determinants of phytoplankton succession. In: U. Sommer (ed.), *Plankton ecology*. Springer, 9–56.
- Richardson, K., 1985. Plankton distribution and activity in the North Sea/Skeggerak-Kattegat frontal area in April 1984. *Mar. Ecol. Prog. Ser.* 26, 233–244.
- Rönnerberg, C. and Bonsdorff, E., 2004. Baltic Sea eutrophication: area-specific ecological consequences, *Hydrobiologia* 514, 227–241.
- Ruiz-Verdú, A., Simis, S.G.H., de Hoyos, C., Gons, H.J., Peña-Martínez, R., 2008. An evaluation of algorithms for the remote sensing of cyanobacterial biomass. *Remote Sensing of Environment*, 112(11), 3996–4008.
- Rundquist, D.C., Han, L., Schalles, J.F., Peake, J. S., 1996. Remote measurement of algal chlorophyll in surface waters: The case for the first derivative of reflectance near 690 nm, *Photogrammetric Engineering & Remote Sensing*, 62(2), 195–200.
- Salmaso, N., 1996. Seasonal variation in the composition and rate of change of the phytoplankton community in a deep subalpine lake (Lake Garda, northern Italy). An application of nonmetric multidimensional scaling and cluster analysis. *Hydrobiologia* 337, 49–68.
- Sathyendranath, S., Cota, G., Stuart, V., Maass, H. and Platt, T., 2001. Remote sensing of phytoplankton pigments: a comparison of empirical and theoretical approaches. *International Journal of Remote Sensing*, 22, 249–273.
- Schiller H. and Doerffer R., 1999. Neural Network for emulation of an inverse model operational derivation of Case II water properties from MERIS data, *International Journal of Remote Sensing* 26, 123–137.

- Schroeder, T., Behnert, I., Schaale, M., Fischer, J., Doerffer, R., 2007a. Atmospheric correction for MERIS above Case-2 waters. *International Journal of Remote Sensing* 28(7), 1469–1486.
- Schroeder, T., Schaale, M., Fischer, J., 2007b. Retrieval of atmospheric and oceanic properties from MERIS measurements: A new Case-2 water processor for BEAM, *International Journal of Remote Sensing* 28(24), 5627–5632.
- Schubert, H., Fulda, S., and Hagemann M., 1993. Effects of adaptation to different salt concentrations on photosynthesis and pigmentation of the cyanobacterium *Synechocystis* sp. PCC 6803. *Journal of Plant Physiology* 142, 291–295.
- Seisuma, Z., Kulikova, I., 2007. Behaviour of heavy metals in the Daugava plume zone (1999–2003, Gulf of Riga, the Baltic Sea). *Geologija* 58, 10–15.
- Seppälä, J., Ylöstalo, P., Kuosa, H., 2005. Spectral absorption and fluorescence characteristics of phytoplankton in different size fractions across a salinity gradient in the Baltic Sea. *Int. J. Remote Sensing* 26(2), 387–414.
- Siegel, D.A., Maritorena, S., Nelson, N.B., Hansell, D.A., Lorenzi-Kayser, M., 2002. Global distribution and dynamics of colored dissolved and detrital organic materials. *Journal of Geophysical Research* 107 (C12), 3228.
- Siegel, H., Gerth, M., Mutzke, A., 1999. Dynamics of the Oder River Plume in the Southern Baltic Sea - Satellite data and Numerical Modelling. *Continental Shelf Research* 18, 1143–1159.
- Siegel, H., Gerth, M., Schmidt, T., 1996. Water exchange in the Pomeranian Bight investigated by satellite data and ship-borne measurements. *Continental Shelf Research* 16 (14), 1793–1817.
- Siegel, H., Ohde, T., Gerth, M., 2003. Preliminary MERIS-Validation Results for the Baltic Sea, *Proceedings of Envisat – Validation Workshop*, 8-13 December 2002, Frascati, Italy.

Simis, S.G.H., Peters, S.W.M., Gons, H.J., 2005. Remote sensing of the cyanobacterial pigment phycocyanin in turbid water, *Limnology and Oceanography* 50, 237–245.

Sokal, R.R. and Rohlf, F.J., 1995. *Biometry*. 3rd edn. New York: WH Freeman and Company.

Sørensen, K., Aas, E. and Høkedal, J., 2007. Validation of MERIS water products and bio-optical relations in the Skagerrak, *International Journal of Remote Sensing* 28(3-4), 555–568.

Sørensen, K., Høkedal, J., Aas, E., Doerffer, R. and Dahl, E., 2002. Early results for validation of MERIS water products in the Skagerrak, *Proceedings, MAVT Validation Workshop*, ESA publication SP-531.

Stelzer, K., Geißler, J., Brockmann, C., Klein, H., Göbel, J., Reinart, A., Sørensen, K., 2008. MERIS validation with respect to operational monitoring needs in the North and Baltic Sea, *Proceedings of the 2nd MERIS/(A)ATSR User Workshop*, Frascati, Italy, ESA SP-666.

Storch, H., Omstedt, A., 2008. Introduction and Summary. In: Bolle, H.-J., Menenti, M., Rasool, I. (Eds.) *Assessment of Climate Change for the Baltic Sea Basin*. Springer-Verlag Berlin Heidelberg, 473 pp.

Strickland, J. H. D. and Parsons, T. R., 1972. A practical handbook of sea water analysis, *Bulletin Journal of the Fisheries Research Board of Canada* 167, 185–203.

Telesh I.V., Khlebovich V.V., 2010. Principal processes within the estuarine salinity gradient: A review. *Marine Pollution Bulletin* 61, 149–155.

Telesh, I.V., 2004. Plankton of the Baltic estuarine ecosystems with emphasis on Neva Estuary: a review of present knowledge and research perspectives. *Marine Pollution Bulletin* 49 (3), 206–219.

Telesh, I.V., 2006. Impact of biological invasions on the diversity and functioning of zooplankton communities in the Baltic estuarine ecosystems (a review). *Izvestiya Samarskiy Scientific Center RAS* 8, 220–232. [in Russian].

- Tyler, J.E., 1968: The Secchi disc. *Limnology and Oceanography* 13, 1–6.
- Ulbricht, K.A., Schmidt, D., 1977. Massenaufreten mariner Blaualgen in der Ostsee auf Satellitenaufnahmen erkannt. *DFVLR-Nachrichten*, No. 22, 913–915.
- Utermöhl H 1958 Zur Vervollkommnung der quantitativen Phytoplankton-Methodik. *Int Ass Theor Appl Limnol Commun* 9, 1–38.
- Vaičiūtė, D., 2012. Using MERIS/Envisat data to assess the Secchi depth – A case study from Lithuanian Baltic Sea waters. *Baltic International Symposium (BALTIC), 2012 IEEE/OES*, 1–5.
- Vaičiūtė, D., Bresciani, M., Bučas, M., 2012. Validation of MERIS bio-optical products with in situ data in the turbid Lithuanian Baltic Sea coastal waters. *Journal of Applied Remote Sensing* 6(1), 063568-1–063568-20.
- Van den Hoek, C., Mann, D.G., Jahns, H.M., 1995. *Algae. An Introduction to Phycology*. Cambridge.
- Wallentinus, I., 1991. The Baltic Sea gradient. *Ecosystems of the world*, v. 24, Intertidal and littoral ecosystems, 83–108.
- Wasmund, N. and Uhlig, S., 2003. Phytoplankton trends in the Baltic Sea, *ICES Journal of Marine Science* 60, 177–186.
- Wasmund, N., Andrushaitis, A., Łysiak-Pastuszek, E., Müller-Karulis, B., Nausch, G., Neumann, T., Ojaveer, H., Olenina, I., Postel, L., Witek, Z., 2001. Trophic Status of the South-Eastern Baltic Sea: A Comparison of Coastal and Open Areas, *Estuarine, Coastal and Shelf Science* 53(6) 849–864.
- Wasmund, N., Tuimala, J., Suikkanen, S., Vandepitte, L., Kraberg, A., 2011. Long-term trends in phytoplankton composition in the western and central Baltic Sea, *Journal of Marine Systems* 87, 145–159.

Webster, I.T., Hutchinson, P.A., 1994. Effect of the wind on the distribution of phytoplankton cells in lakes revisited, *Limnol. Oceanogr.*, 39(2), 365–373.

Wetzel, R.G., 1983. *Limnology*. Saunders College Publishers, 767 pp.

Wieland, E., Santschi, P.H., Beer, J., 1991. Scavenging of Chernobyl $^{137}\text{Cesium}$ and natural ^{210}Pb in Lake Sempach, Switzerland. *Geochim. Cosmochim. Acta* 57, 259–2979.

Wynne, T.T., Stumpf, R.P., Tomlinson, M.C. and Dyble, J., 2010. Characterizing a cyanobacterial bloom in western Lake Erie using satellite imagery and meteorological data, *Limnology Oceanography*, 55(5), 2025–2036.

Žaromskis, R., 1996. *Oceans, Seas and Estuaries*, Vilnius, 293 pp. [in Lithuanian].

Zibordi, G., Berthon, J.-F., Mélin, F., D'Alimonte, D., 2011. Cross-site consistent in situ measurements for satellite ocean color applications: The BiOMaP radiometric dataset. *Remote Sensing of Environment* 115, 2104–2115.

Žilinskas, G., 2005. Trends in dynamic processes along the Lithuanian Baltic Sea coast. *Acta Zoologica Lithuanica* 15, 2004–2007.

Zuur, A. F., Ieno, E. N. & Smith, G. M., 2007. *Analysing ecological data*, Springer, New York, 672 pp.

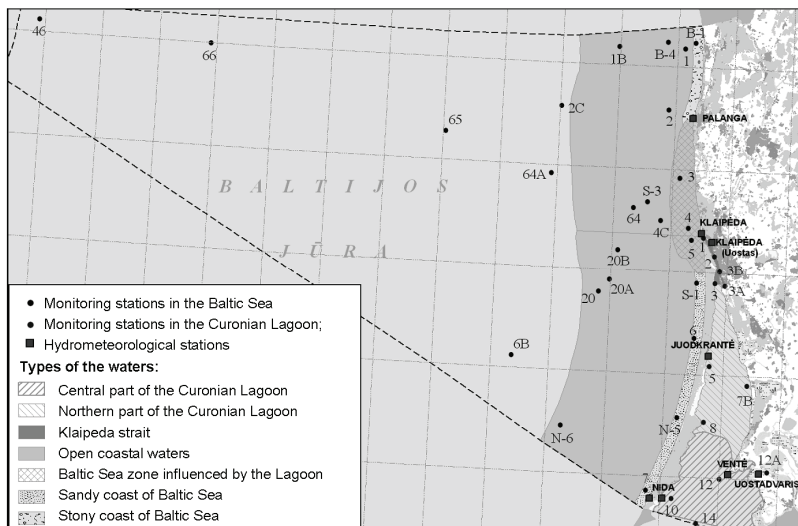
Давыдова Н. Н., 1985. Диатомовые водоросли – индикаторы природных условий водоемов в голоцене. Наука, Ленинград.

Царенко П. М., 1990., *Краткий определитель хлорококковых водорослей Украинской ССР*. Киев.

Appendix 1. The summary of samples and MERIS images used during this study.

	Date/Period	<i>In situ data</i>						<i>MERIS images</i>		
		Chl a	CDOM	TSM	Phyto	Secchi	Sal	Chl a	CDOM	TSM
Validation of satellite data	2010 05 20	8	8	8	-	8	-	1	1	1
	2010 06 05	8	8	8	-	8	-	1	1	1
	2010 07 04	7	7	7	-	7	-	1	1	1
	2010 07 21	16	16	16	-	16	-	1	1	1
	2010 08 11	7	7	7	-	7	-	1	1	1
	2010 08 30	8	8	8	-	8	-	1	1	1
	2010 08 31	6	6	6	-	6	-	1	1	1
	2010 09 06	17	17	17	-	17	-	1	1	1
Plume investigation	Long-term salinity 1992-2010 08						276			
	Relationship between Chl a and salinity 2010 07 04	3	3	3	-	-	3			
	2010 07 21	10	10	10	-	-	10			
	2010 08 11	7	7	7	-	-	7			
	2010 09 06	11	11	11	-	-	11			
	2011 08 04	12	12	12	-	-	12			
	2005 06-09							19	19	19
	2006 06-09							23	23	23
	2007 06-09							16	16	16
	Spatial distribution of the plume 2008 06-09							17	17	17
2009 06-09							18	18	18	
2010 06-09							29	29	29	
2011 06-09							25	25	25	
Phytoplankton communities	2010 07 04				3		3			
	2010 07 21				10		10			
	2010 08 11				7		7			
	2010 09 06				11		11			
	2011 08 04				12		12			

Appendix 2. The scheme of monitoring stations in the Lithuanian Baltic Sea waters and Curonian Lagoon (originated by Department of Marine Research, Environmental Protection Agency).



Appendix 3. MERIS image (left) showing algal blooms in the SE Baltic Sea and the Curonian Lagoon on 21st July 2010. Two different species causing bloom can be detected by the different remote sensing signature: *Nodularia spumigena* in the central part of the Baltic Sea, *Aphanizomenon flos-aquae* and other microalgae – in the plume area. Image (right) showing the beach in Klaipėda caused by the outflow of blooming waters of the Curonian Lagoon (foto: D. Vaičiūtė).



Appendix 4. RGB image (left) and maximum chlorophyll index - MCI (right) in the Baltic Sea from MERIS/Envisat image from 4th of July, 2005.

